

Materials Science at Large Scale Facilities

Diffraction

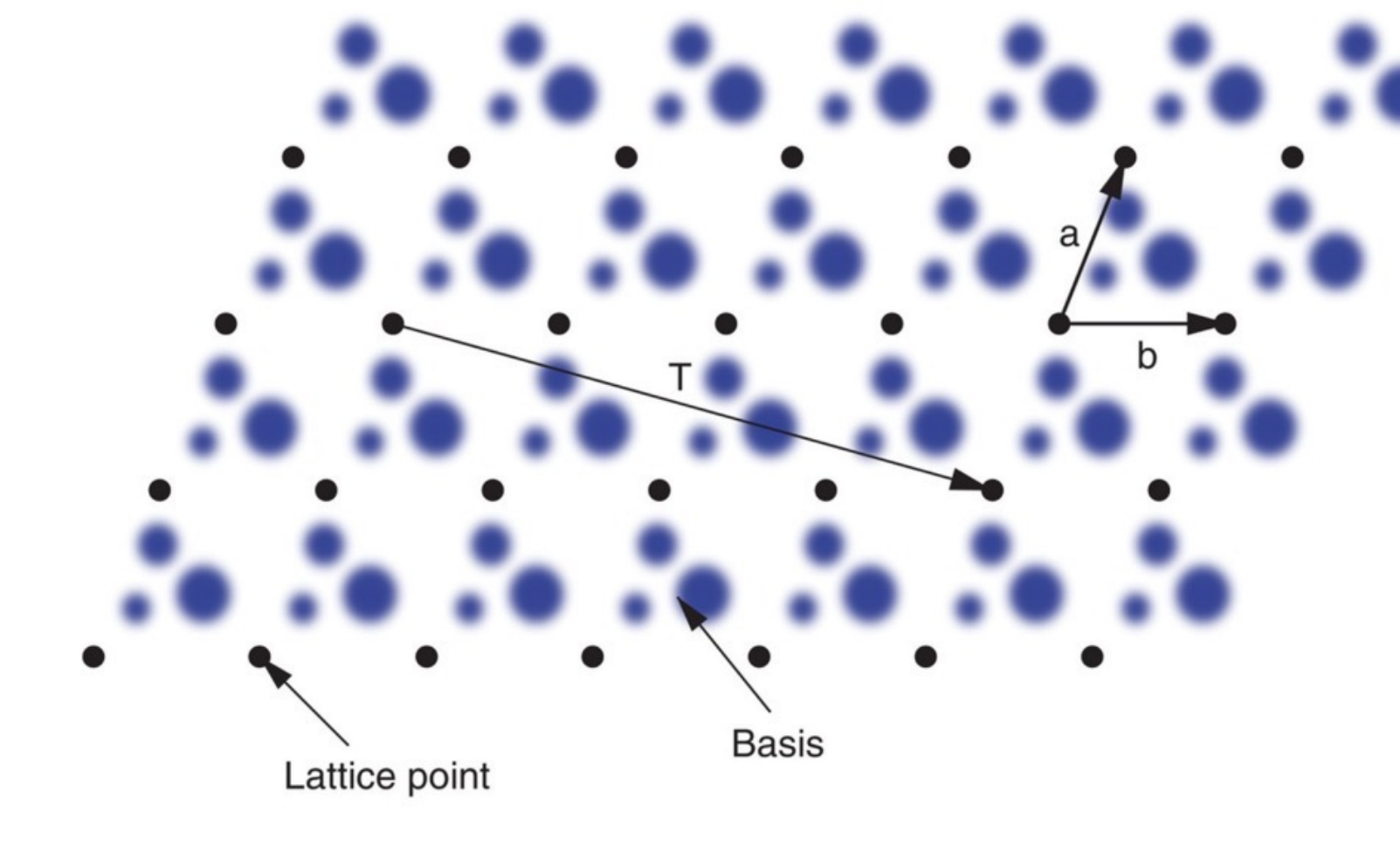


X-ray and neutron diffraction

- A bit of crystallography
- Diffraction basics
- Diffraction methods + applications
 - Laue / rotating crystal
 - Powder
 - Pair distribution function
 - Energy dispersive
 - Neutron time-of-flight
 - Surface x-ray diffraction

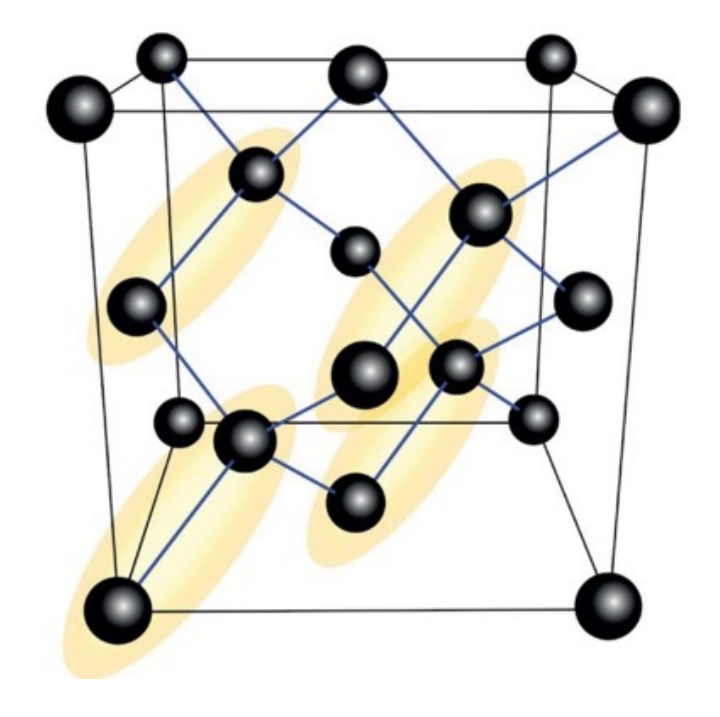


Crystal structure

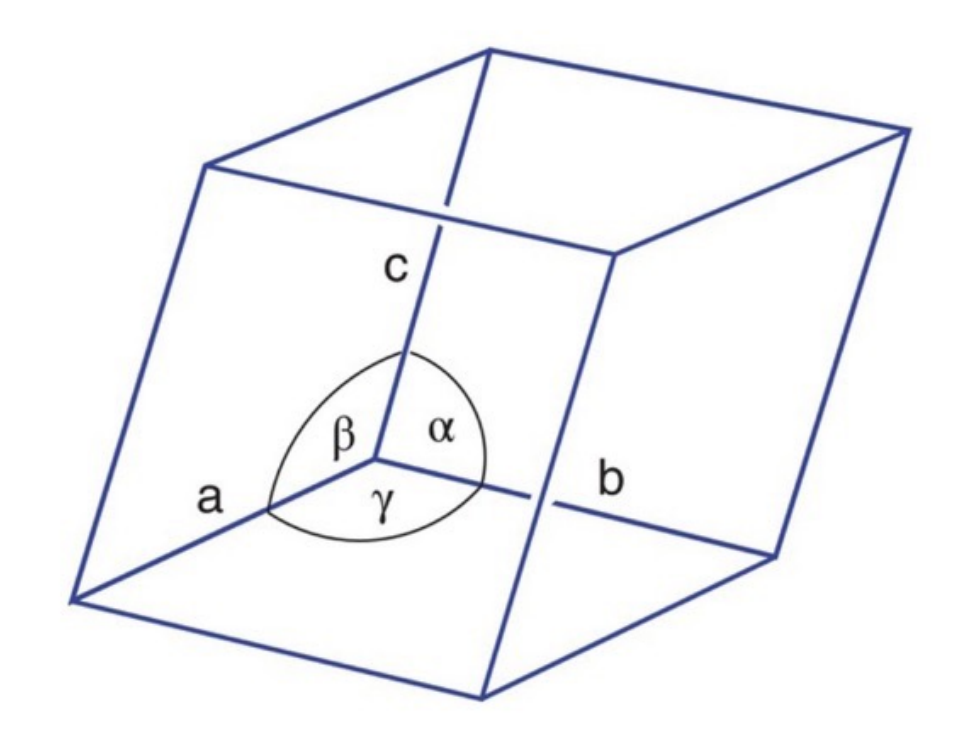




Crystal structure



The crystal structure of diamond



Crystal unit cell



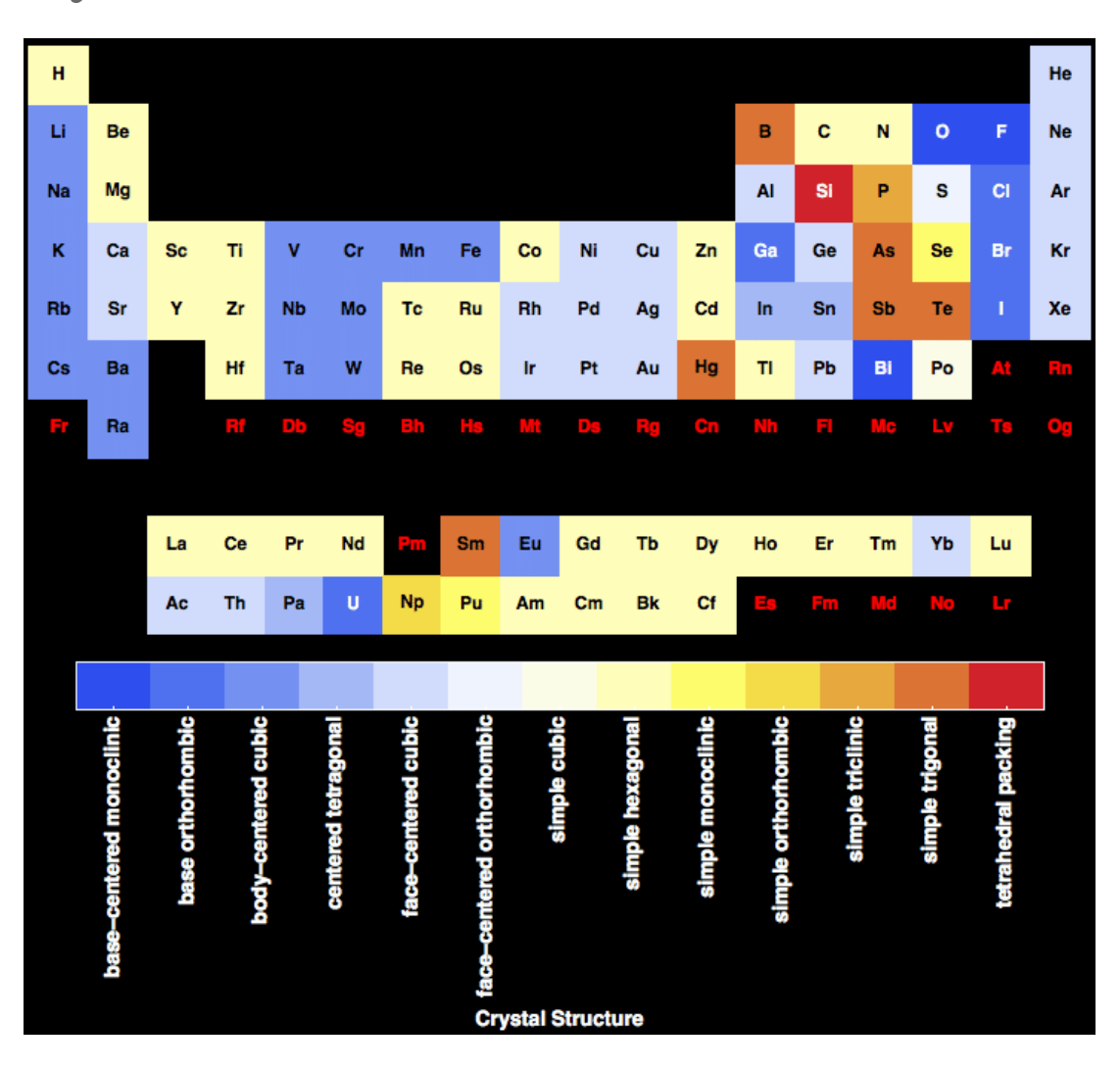
EPFL Crystal structure – Bravais lattices

Crystal system	The 14 Bravais	The 14 Bravais lattices			Defining symmetry	
Triclinic						Rhombohedral (trigonal)
a≠b≠c						(trigonal)
α≠β≠γ≠90°					1-fold axis	a= b = c
	Triclinic				1-10ld axis	α=β=γ≠90°
Monoclinic	,	,	β ≥ 90°			
a≠b≠c;			α,γ = 90°		2-fold axis	Hexagonal
$\alpha = \gamma = 90^\circ; \beta \neq 90$	Simple Monoclinic	Base-centered monoclinic	a Bab			a= b ≠ c
Orthorhombic						 α=β=90, γ=120°
a≠b≠c					3 x 2 fold axis	
α=β=γ=90°						Cubic
α-ρ-γ-90	Simple orthorhombic	Body-centered orthorhombic	Base-centered orthorhombic	Face-centered orthorhombic		a= b = c
	orthornomble		o. c.io.i.io.ii.b.ic			α=β=γ=90°
Tetragonal						
a= b ≠ c			ĺ			
α=β=γ=90°					4 fold ovic	
- F 7 5 5	Simple	Body-cente			4-fold axis	
	tetragonal	tetragona	il			

Rhombohedral (trigonal) a= b = c α=β=γ≠90°	Rhombohedral	P Tridonal R	Press, Indiga, core	3-fold axis
Hexagonal a= b ≠ c α=β=90, γ=120°	Hexagonal			6-fold axis
Cubic a= b = c α=β=γ=90°	Simple cubic	Face-centered cubic	Body-centered cubic	4 x 3-fold axis



Crystal structure – Bravais lattices



Crystal structure

• Volume unit cell:

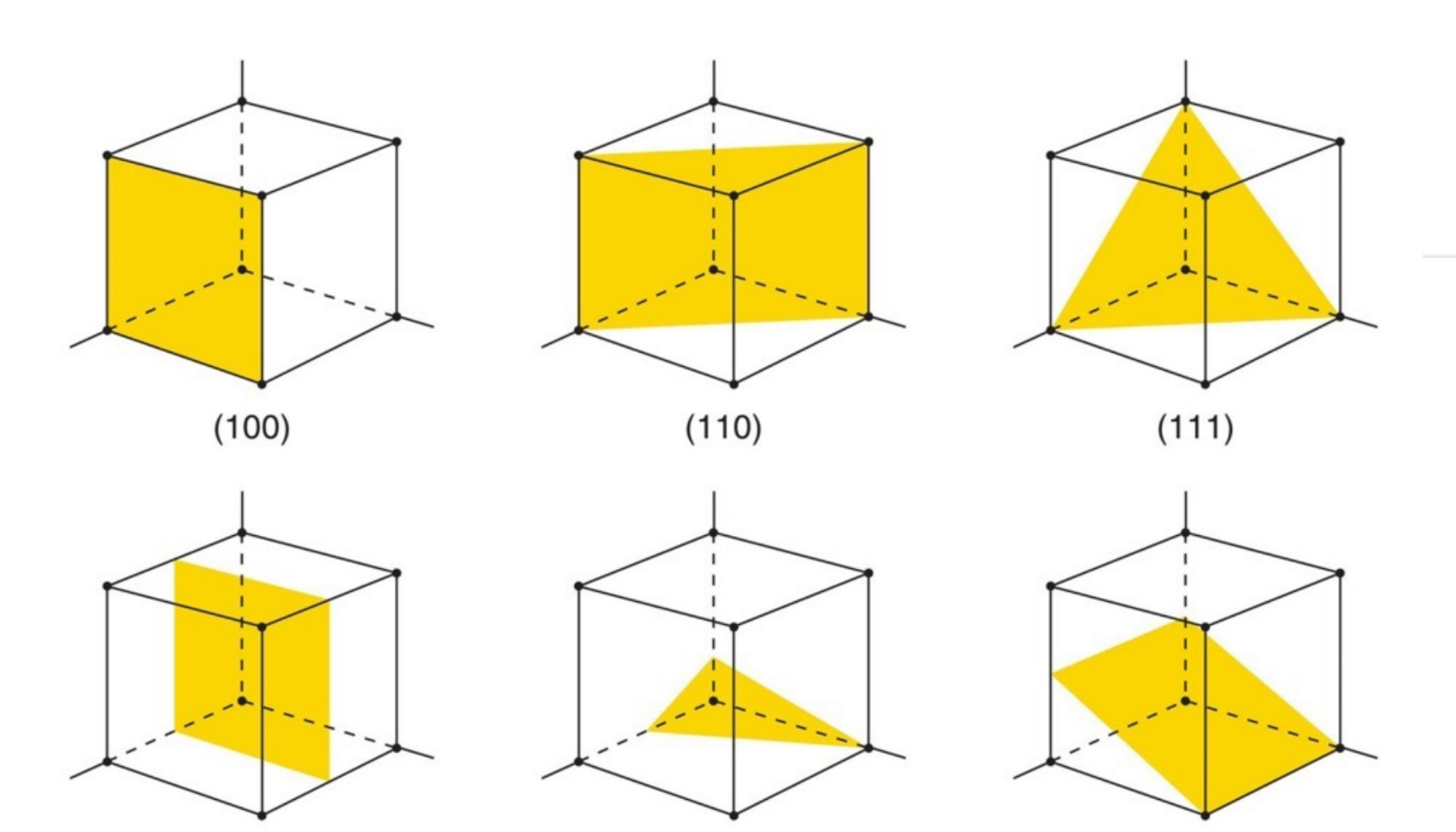
$$V_c = |\mathbf{a} \cdot \mathbf{b} \times \mathbf{c}|.$$

$$V_c = abc(1 + 2\cos\alpha\cos\beta\cos\gamma - \cos^2\alpha - \cos^2\beta - \cos^2\gamma)^{1/2}.$$



(200)

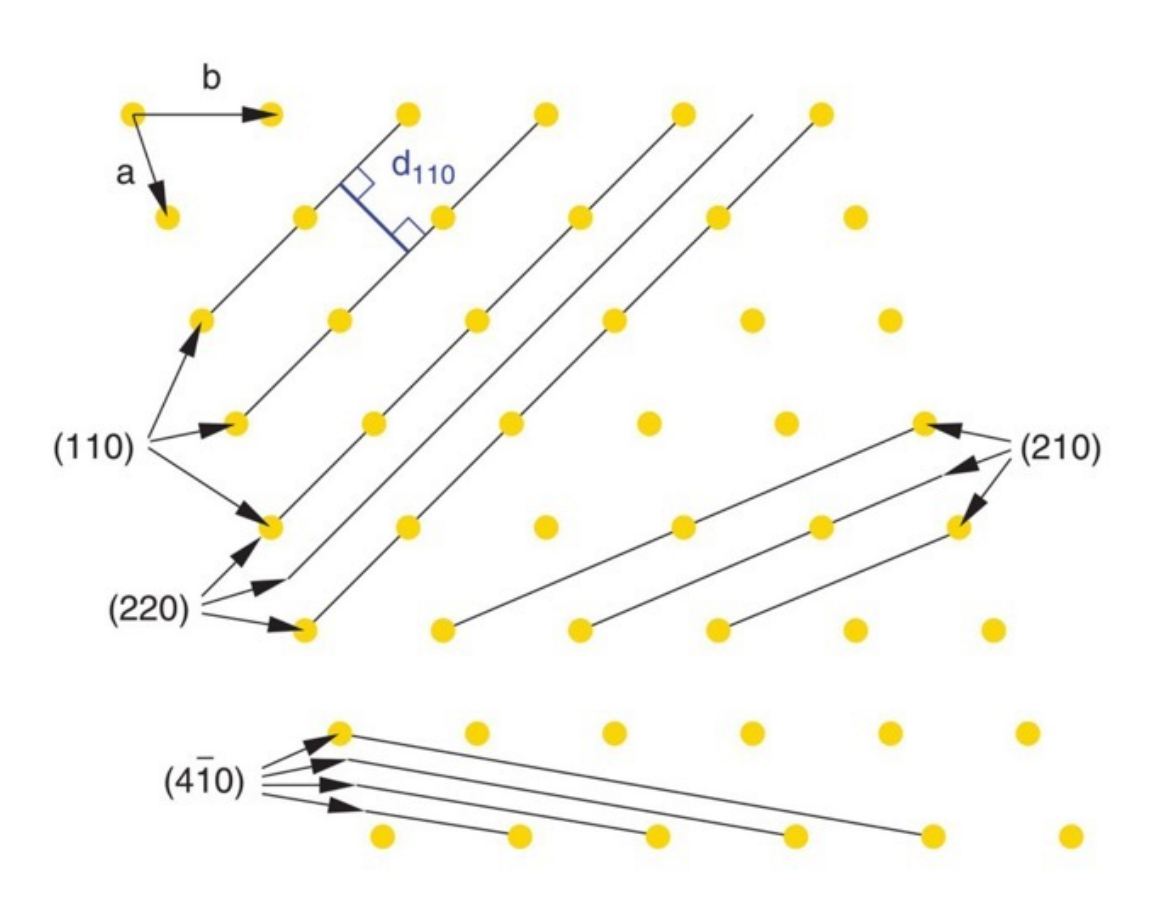
Miller indices - planes



$$\frac{h}{a}x + \frac{k}{b}y + \frac{l}{c}z = C$$



Miller indices - planes



General case

$$d_{hkl} = \frac{X}{Y},$$

$$X = [1 - \cos^2 \alpha - \cos^2 \beta - \cos^2 \gamma + 2\cos \alpha \cos \beta \cos \gamma]^{1/2}$$

$$Y = \left[\left(\frac{h}{a} \right)^2 \sin^2 \alpha + \left(\frac{k}{b} \right)^2 \sin^2 \beta + \left(\frac{l}{c} \right)^2 \sin^2 \gamma \right.$$
$$\left. - \frac{2kl}{bc} \left(\cos \alpha - \cos \beta \, \cos \gamma \right) - \frac{2lh}{ca} \left(\cos \beta - \cos \gamma \, \cos \alpha \right) \right.$$
$$\left. - \frac{2hk}{ab} \left(\cos \gamma - \cos \alpha \, \cos \beta \right) \right]^{1/2}.$$

Cubic unit cell

$$d_{hkl} = \frac{a}{\sqrt{(h^2 + k^2 + l^2)}}$$



Miller indices - multiplicity

- Miller indices of the set of all planes that are equivalent by symmetry of the lattice: {hkl}
- Be careful! The multiplicity depends on the symmetry, so on the crystal system

• Example:

```
multiplicity of {100} plane in cubic system= 6(100), (010), 001), (-100), (0-10), (00-1)
```

- multiplicity of {001} plane in tetragonal system= 2 (001), (00-1)
- multiplicity of {100} plane in tetragonal system = 4 (100), (-100), (010), (0-10)



EPFL Miller indices - multiplicity

System	hkl	hhl	hh0	0kk	hhh	hk0	h0I	0kI	h00	0k0	001
Cubic	48	24	12	12	8	24	24	24	6	6	6
Tetragonal	16	8	4	8	8	8	8	8	4	4	2
Hexagonal	24	12	6	12	12	12	12	12	6	6	2
Orthorhombic	8	8	8	8	8	4	4	4	2	2	2
Monoclinic	4	4	4	4	4	4	2	4	2	2	2
Triclinic	2	2	2	2	2	2	2	2	2	2	2



Miller indices - directions

Direction OP:

Coordinates point P: $\frac{1}{2}$, 0, 1 Vector OP = $\frac{1}{2}$ **a** + **c** or $[\frac{1}{2}$ 0 1]

Coordinates point Q: $\frac{1}{2}$, 0, $\frac{1}{2}$ Vector OQ = $\frac{1}{4}$ **a** + $\frac{1}{2}$ **c** or [$\frac{1}{4}$ 0 $\frac{1}{2}$]

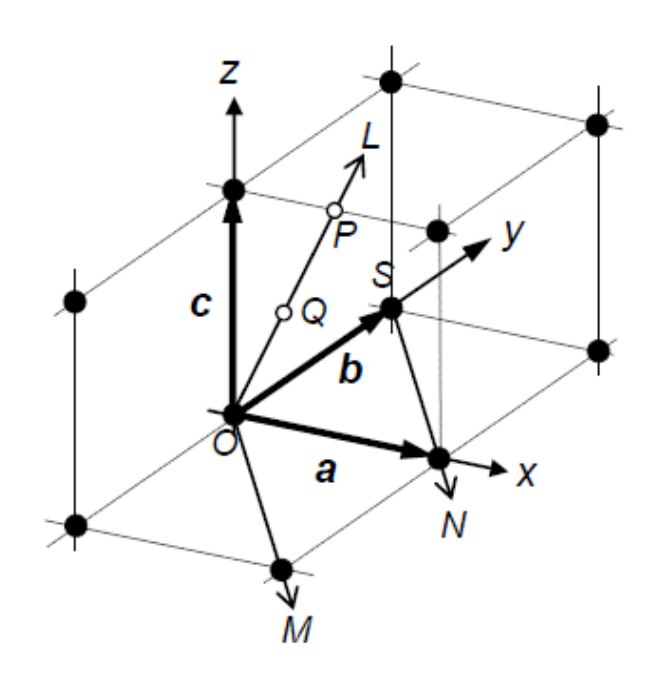
Direction SN

consider OM which is parallel to SN

Coordinates OM: 1, -1,0

Vector $OM = \mathbf{a} - \mathbf{b}$

Direction SN and OM: [1-10]



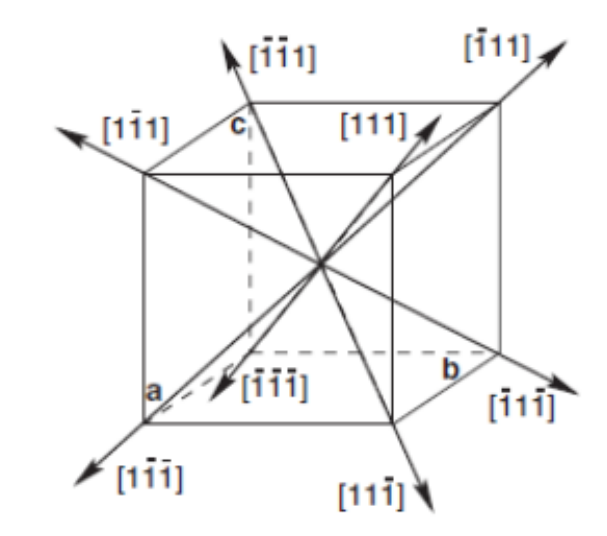
Miller indices - directions

Due to the symmetry of crystal systems, different directions can be equivalent. e.g. For cubic crystals, the directions $[1\ 0\ 0]$, $[-1\ 0\ 0]$, $[0\ 1\ 0]$, $[0\ -1\ 0]$, $[0\ 0\ 1]$, $[0\ 0\ -1\]$ are all equivalent by symmetry. There is a special notation for directions of the same form: <100>, which in this case means the family made of the three basis axis **a**,**b**,**c**

Similarly, there are 8 equivalent <111> directions in a cubic system. The number of equivalent directions is called the multiplicity of the direction.

The angle between the directions [u1 v1 w1] and [u2 v2 w2] is:

$$\cos \vartheta = \frac{u_1 u_2 + v_1 v_2 + w_1 w_2}{\sqrt{u_1^2 + v_1^2 + w_1^2} \cdot \sqrt{u_2^2 + v_2^2 + w_2^2}}$$





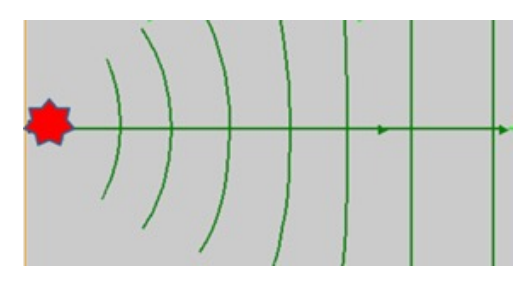
Miller indices – directions/planes

In the cubic system the (hkl) plane and the vector [hkl] are normal to one another but this characteristic is unique to the cubic crystal system and does not apply to crystal systems of lower symmetry.

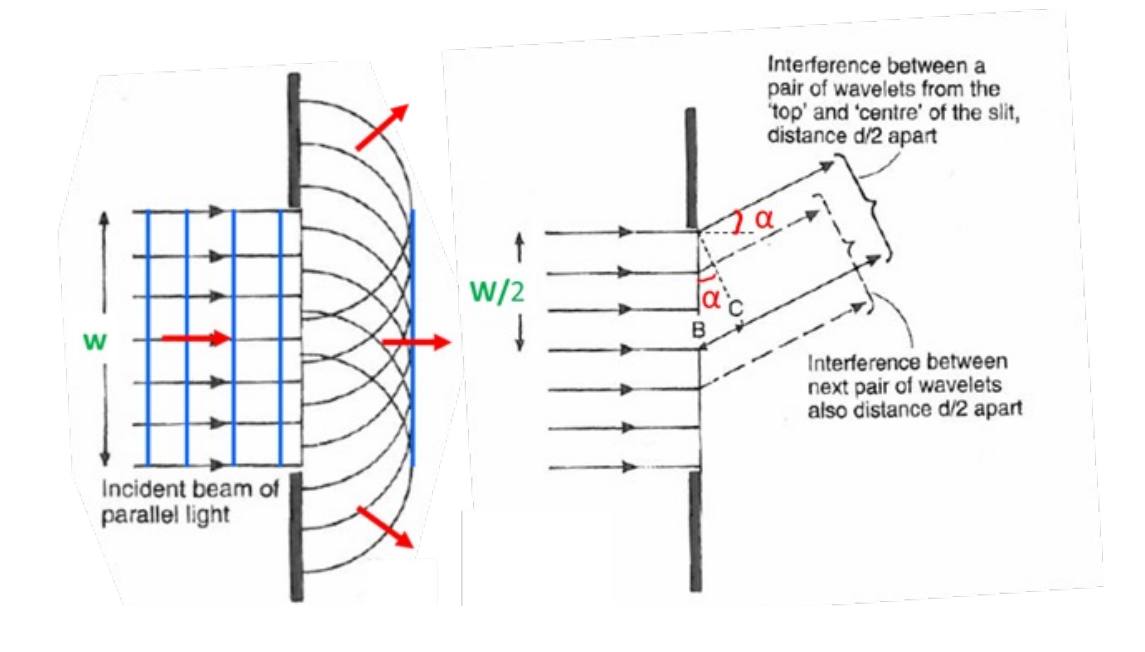
A zone is defined as "a set of planes in a crystal whose intersections are parallel". The common direction of the intersections is called the zone axis. Therefore one often has to calculate the intersection of two planes. For instance the [001] direction is the zone axis of the {100} and {110} family of planes.

Interference

• Electromagnetic wave far away from the source: flat wavefront



• Single slit (Huygens' Principle)



Destructive interference when:

BC =
$$\lambda/2 = (w/2) \sin \alpha$$

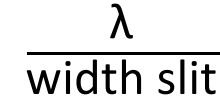
or

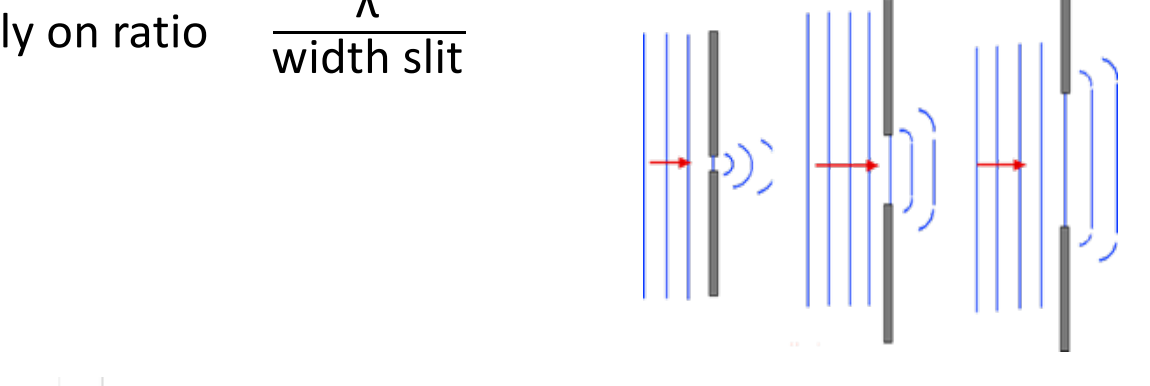
$$\sin \alpha = \lambda/w$$
, $2\lambda/w$, $3\lambda/w$, ...

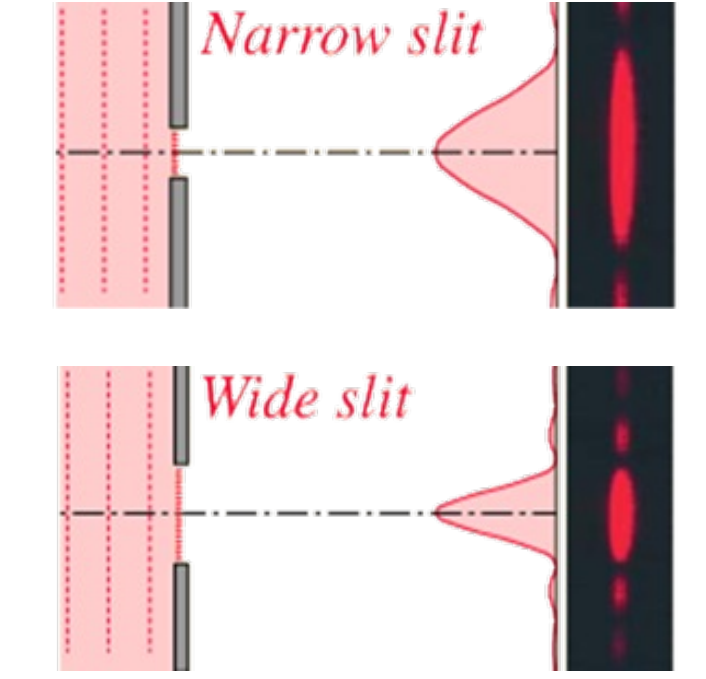


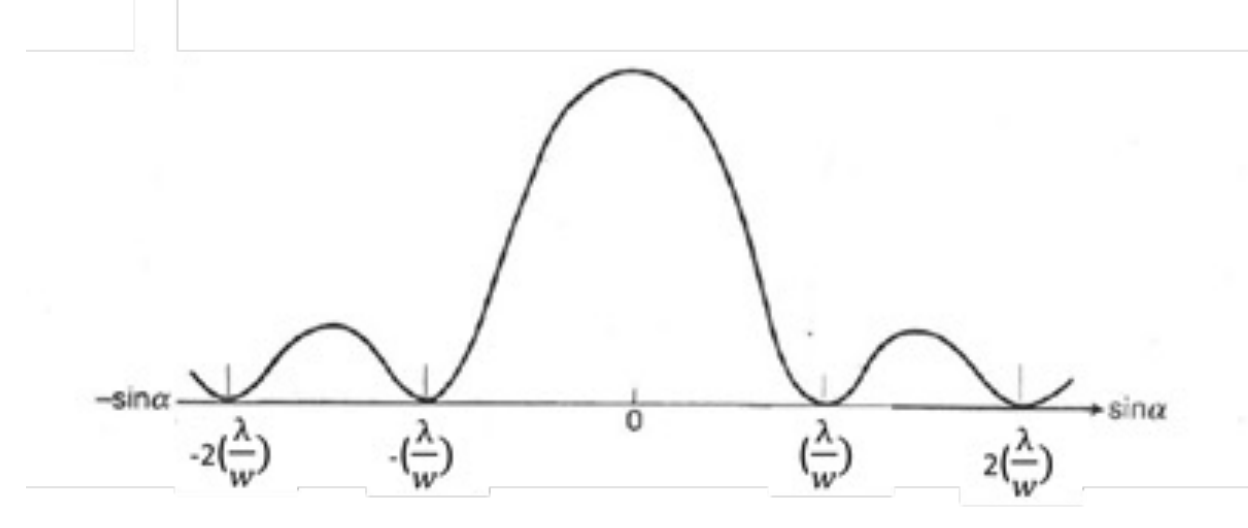
Interference











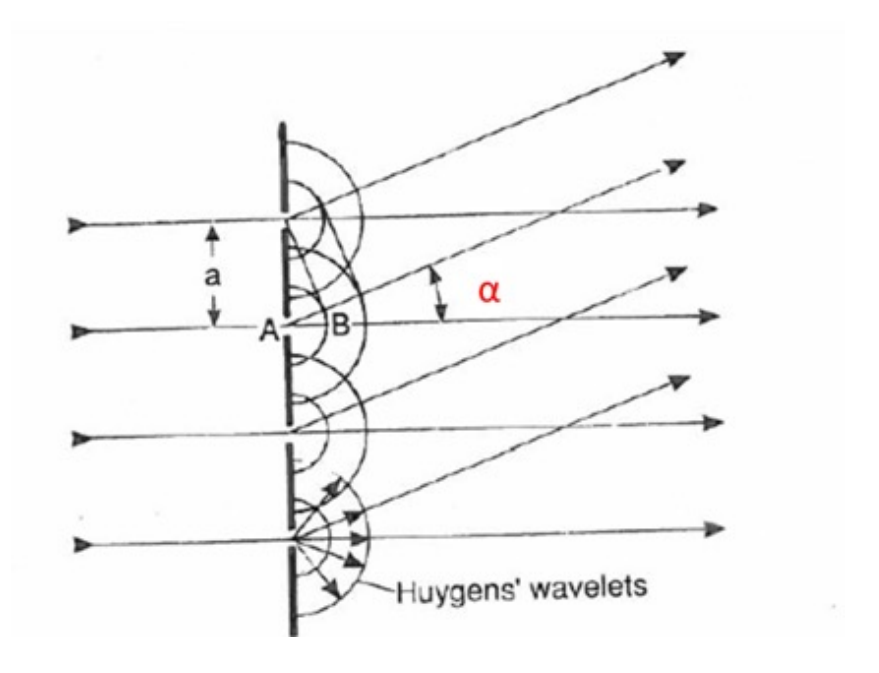


Diffraction from a grating

In 1803, Thomas Young showed in a two-slit experiment that the distance between the maximum of a detector and the center of the pattern was proportional to the reciprocal of the distance between the slits.

The conditions for constructive interference are very similar as for diffraction at one gap, but here the path difference is a function of the distance a between the openings in the diffraction grating:

 $asin\alpha = n\lambda$ where n is an integer





Diffraction from grating

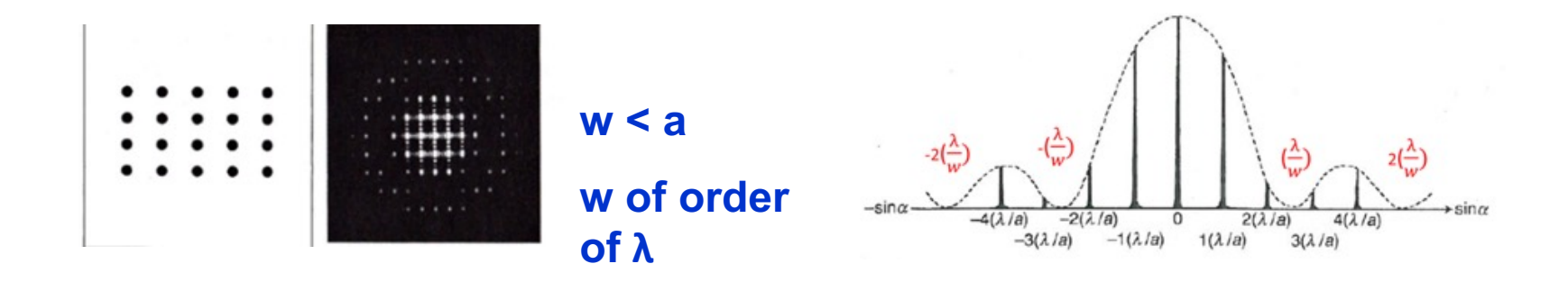
- To have constructive interference among slits nλ ≤ a (distance between slits). This means
 that we need a wavelength of the order of the distance between the slits. If the
 wavelength is much smaller, the maxima will be very close to the forward direction i.e.
 the interference fringes will be very close to each other.
- When the width w of the slit is only slightly larger than λ smaller and w<a, the envelope function becomes broader and the first min induced by the width of the slit might not be visible. The pattern will look like





Diffraction from grating

• When w is larger than λ but still w<a, the diffraction pattern will look like

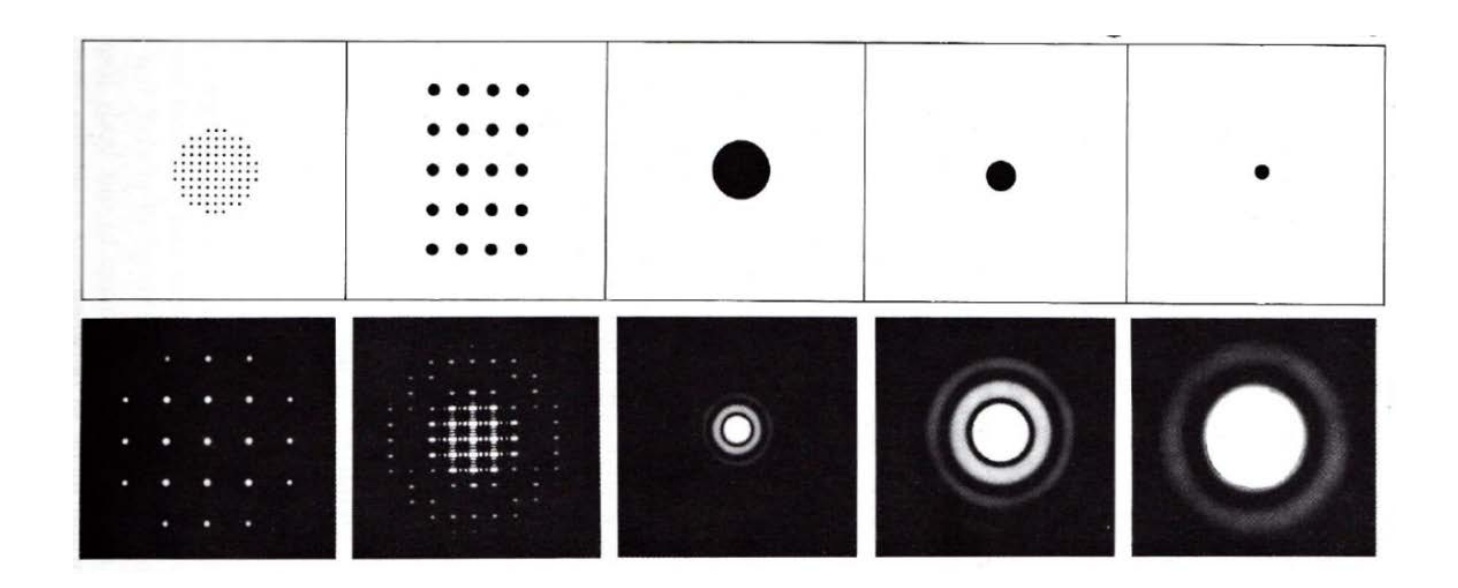


- The diffraction angles are invariant under scaling; that is, they depend only on the ratio of the wavelength to the size (w) of the diffracting object
- While diffraction occurs whenever propagating waves encounter slits, its effects are generally most pronounced for waves whose wavelength is roughly similar to the dimensions of the diffracting objects



Diffraction from grating

• The pictures below show the diffraction patterns for a planar diffracting grating consisting of circular openings.





Diffraction from crystal lattice

- Classical diffraction theory at a series of line slits (2D aperture grating) can be extended to diffraction at a 3D crystal lattice. That is in principle the contribution of Max von Laue and William Lawrence and William Henry Bragg (father and son). In 1912 Von Laue had the idea to send a beam of X-rays through a copper sulfate crystal and showed that there were diffraction spots surrounding the central spot of the primary beam. Around the same time, crystallographers were becoming convinced of the lattice-like construction of crystals.
- If one derives it from an analogy with the slits, the distance between the atoms is the grating distance and the size of the atoms is the width of the slit.
- Distance between atoms is of the order of 10⁻¹⁰m, size of the atoms is smaller ⇒This means that w<a, so one can have constructive interference.



Which radiation?

• X-rays, neutrons and electrons can be used. Typical wavelengths are:

	Energy	Wavelength
Neutrons	1 – 5 meV (cold) 25 – 50 meV (thermal)	9 – 4 Å 1.8 – 1.3 Å
X-rays	100 keV 40 keV 5 keV	0.12 Å (hard X-rays) 0.31 Å 2.48 Å (soft X-rays)
Electrons	200 keV	0.025 Å

• X-rays and electrons fulfill the conditions for the relations between a, w and λ , the diffraction patterns will however differ i.e. the relation between λ and θ will differ. For instance, when one uses hard X-rays, the angle at which one will see constructive interference will be smaller than when using soft X-rays. Cold neutrons have a too large wavelength for diffraction from typical metals.

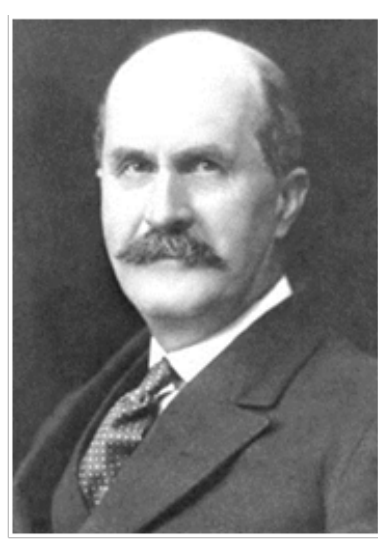


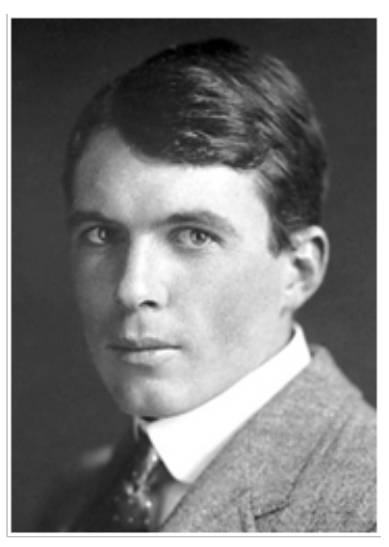
Historical figures

Max von Laue



William Lawrence Bragg William Henry Bragg





The discoveries of von Laue and Bragg gave birth to two new sciences, X-ray crystallography and X- ray spectroscopy, and two Nobel Prizes in physics: Max von Laue "for his discovery of the diffraction of X-rays by crystals" in 1914 and to Bragg and his father, Sir William Henry Bragg, "for their services in the analysis of crystal structure by means of X-rays" in 1915. William was then 25 years old! Max von Laue made already in 1912 the analogy between grating interference and diffraction at crystals but he took the 3D crystal as an ensemble of rows of atoms. His theory did not become immediately popular because it was rather complex. Father (W.H. Bragg) and son (W.L.) Bragg explained these patterns as layers of planes of atoms which behave as reflecting planes.



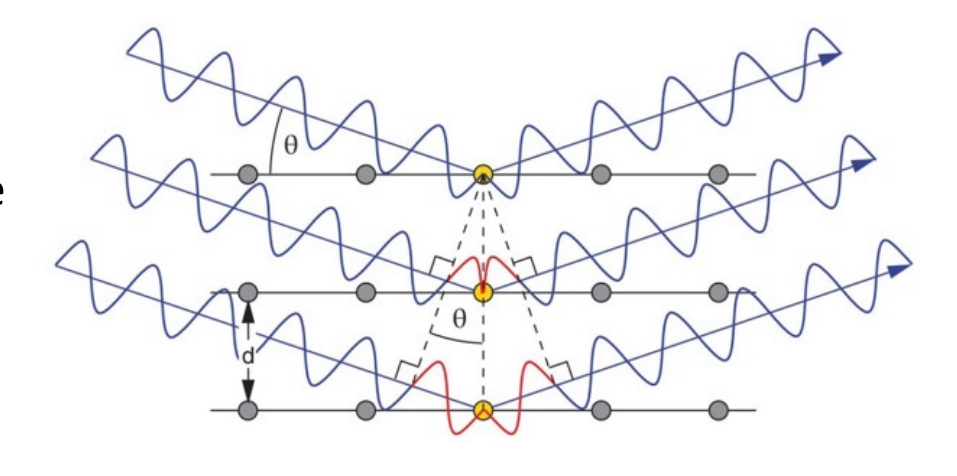
Bragg law

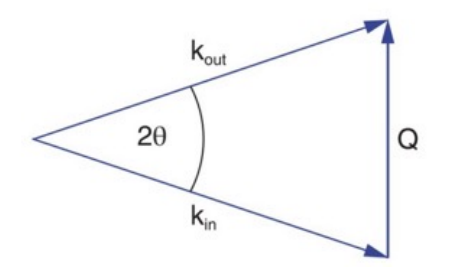
 Within a year of the discovery that X-rays diffract at crystals, father and son Bragg, have exploited the phenomenon to solve the first crystal structure and determined the rule governing a diffraction

$$m\lambda = 2d \sin \theta.$$

$$\sin \theta = \frac{6.1992}{d_{hkl} [\text{Å}] E[\text{keV}]}$$

• The scattering vector \mathbf{Q} always lies perpendicular to the scattering planes, or in other words, the angle subtended by $|\mathbf{k}_{in}| = \frac{2\pi}{\lambda}$ (or \mathbf{k}_{out}) and the scattering planes is θ .





Bragg law defines on a purely geometrical basis for which angles constructive interference <u>can</u> occur

Reciprocal lattice

Reciprocal lattice:

$$\mathbf{a}^* = 2\pi \frac{\mathbf{b} \times \mathbf{c}}{\mathbf{a} \cdot (\mathbf{b} \times \mathbf{c})}$$

$$\mathbf{b}^* = 2\pi \frac{\mathbf{c} \times \mathbf{a}}{\mathbf{b} \cdot (\mathbf{c} \times \mathbf{a})}$$

$$\mathbf{c}^* = 2\pi \frac{\mathbf{a} \times \mathbf{b}}{\mathbf{c} \cdot (\mathbf{a} \times \mathbf{b})}$$

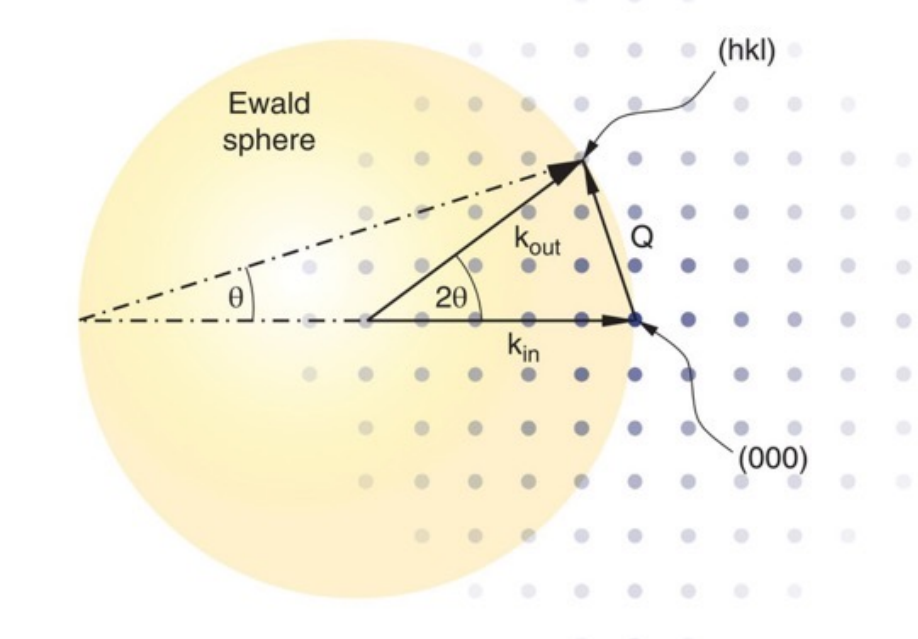
- A geometric lattice is an infinite, regular array of vertices (points) in space
- The reciprocal lattice represents the Fourier transform of this lattice
- It exists in the space of spatial frequencies, known as reciprocal space or k space, where k refers to the wave vector



Ewald sphere

The incident wavevector \mathbf{k}_{in} must end, and the scattering vector $\Delta k = \mathbf{Q}$, must begin at the (000) diffraction spot of the direct beam, while, for constructive interference to occur, \mathbf{Q} and \mathbf{k}_{out} must end at another diffraction maximum (a 'reciprocal-lattice point'). As x-ray diffraction is an elastic process, this means that these two points must lie on the surface of a sphere (the 'Ewald sphere') of radius $|\mathbf{k}|$ and whose centre lies at the base of the \mathbf{k}_{in} and \mathbf{k}_{out} vectors.

$$\mathbf{Q} = 2|k|\sin\theta = \frac{4\pi}{\lambda}\sin\theta \qquad |Q| = \frac{2\pi}{d_{hkl}}$$





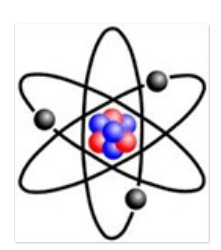
Structure factor

Elastic scattering of X-rays is due to the interaction with electrons in an atom.

To know what the scattering power is of a crystal:

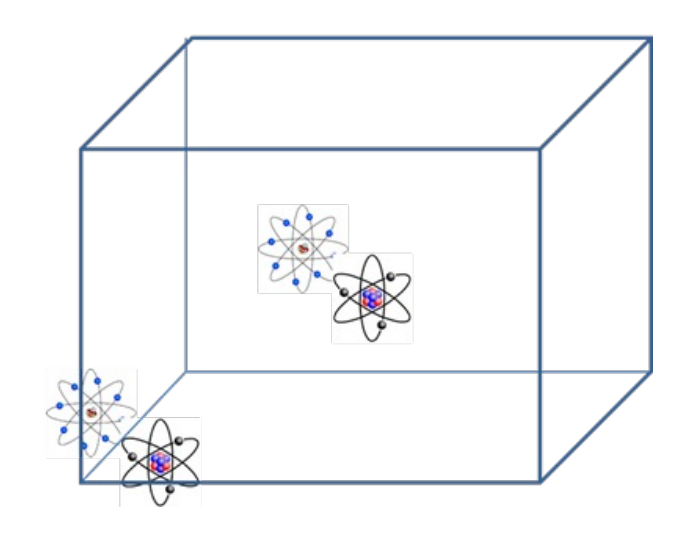
- ⇒ scattering from an electron,
- ⇒ scattering from an atom
- ⇒ scattering from the unit cell,

Interaction with electron (polarization factor) e^{-}



Scattering at an atom (atomic form factor f)

Scattering from unit cell (Structure factor F)

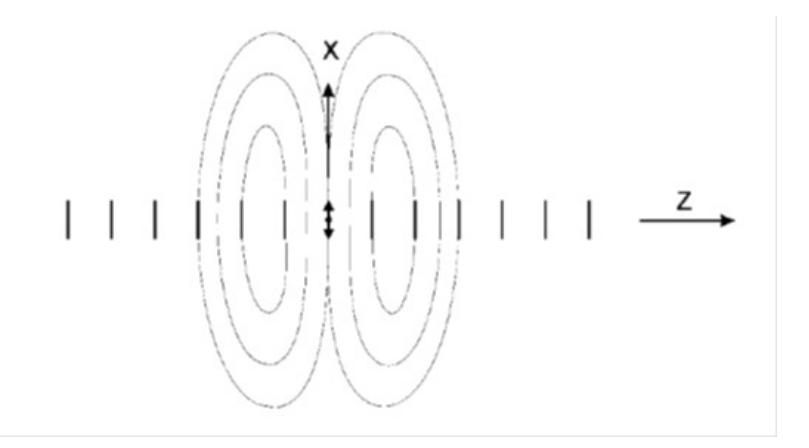




Interaction with electron

- Elastic scattering of an electromagnetic wave by electrons of the outer shell of an atom

 ⇒ Thompson scattering
- same wavelength as the incoming wave and there will be a defined phase relationship, i.e. the radiation is coherent.



Intensity scattered wave

$$\left(\frac{e^2}{c^2 m_e}\right)^2 \left(1 + \cos^2 2\theta\right)$$



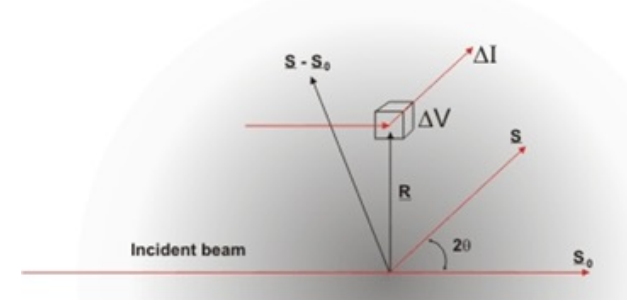
Interaction with an atom

The orbital electrons in an atom move very fast (of the order of 10^{-18} sec for one orbital) and therefore an impinging wave sees only an average electron cloud which is characterized by an electron density of charge $\rho(r')$.

Atomic scattering factor

$$f = \frac{amplitude\ scattered\ by\ one\ atom}{amplitude\ scattered\ by\ a\ single\ elect}$$

f(k) =
$$4\pi \int_0^\infty r^2 \rho(r) \frac{\sin(k-k_0).r}{(k-k_0).r}$$
 where $k-k_0 = (s-s_0)/\lambda$



Spherical ator

EPFL PAUL SCHERRER INSTITUT

Interaction with an atom

f(k) =
$$4\pi \int_0^\infty r^2 \rho(r) \frac{\sin(k-k_0).r}{(k-k_0).r}$$
 where $k-k_0 = (s-s_0)/\lambda$

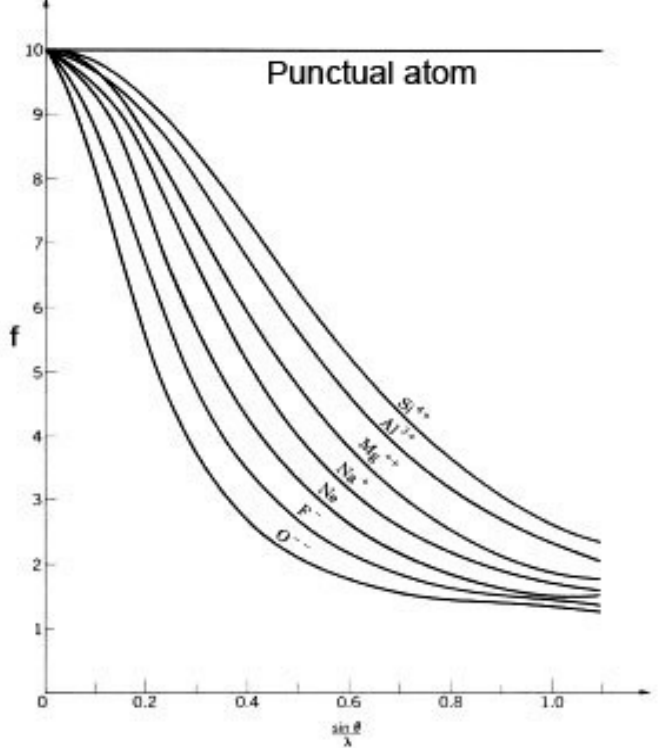
 $4\pi \int r^2 \rho(r) dr = Z$ i.e. # electrons in atom.

 \Rightarrow f = Z when θ =0 (forward direction),

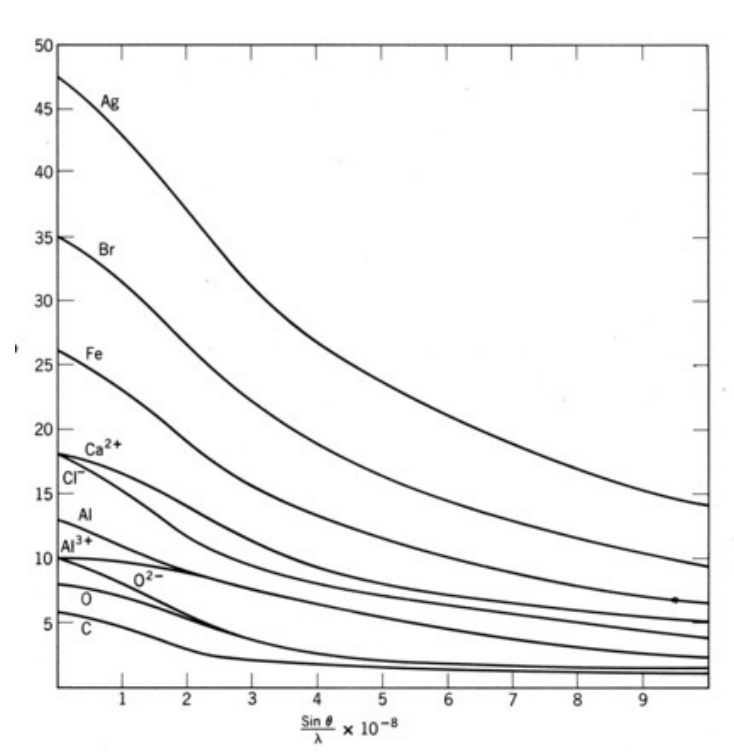
 \Rightarrow F< Z for all other angles of scattering. The form factor depends via $(s-s_0)$ on $sin\vartheta/\lambda$.



Interaction with an atom



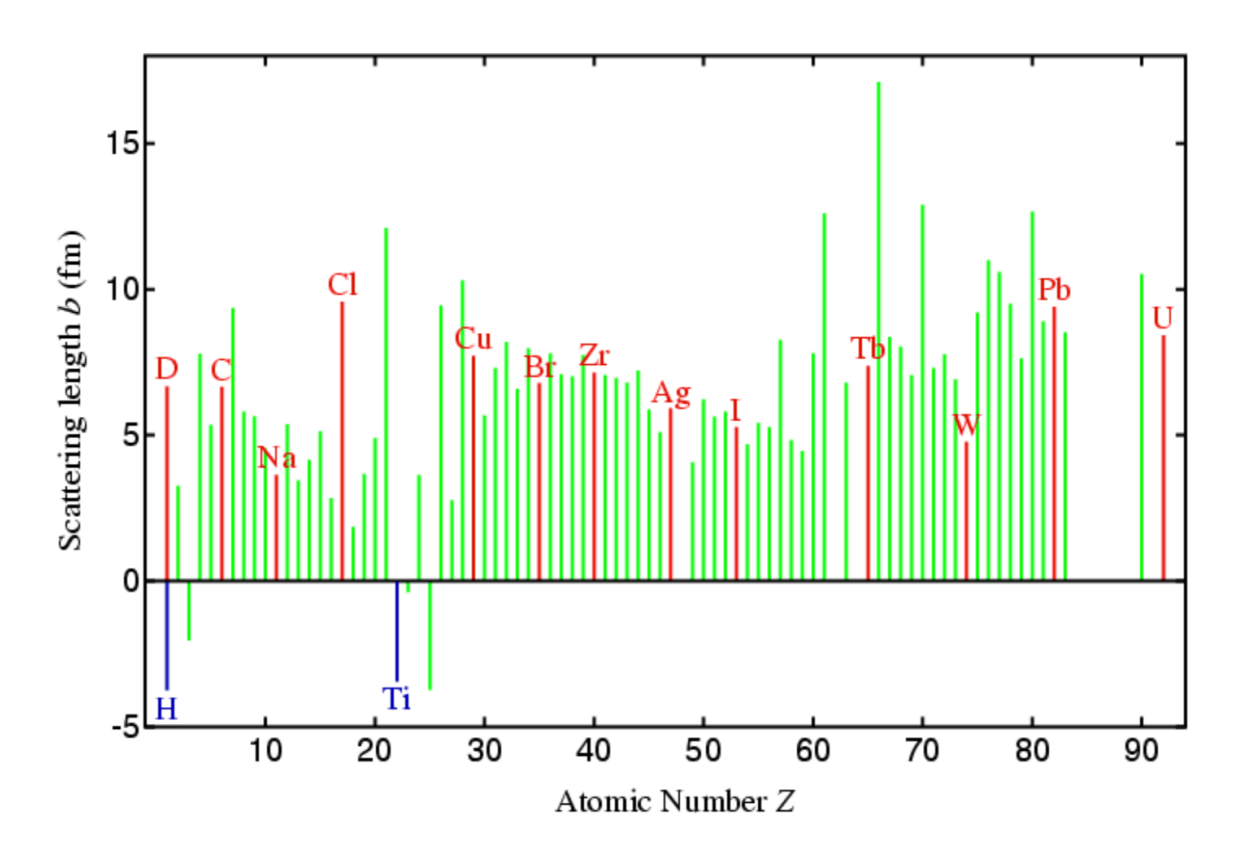
Atomic scattering factors for several ions with the same number of electrons. One can observe that the O⁻⁻ has a more diffuse electronic cloud than Si ⁴⁺ and shows a faster decay.



Atomic scattering factors calculated for atoms and ions with different numbers of electrons. Hydrogen (only one electron) scatters very little as compared with other elements.



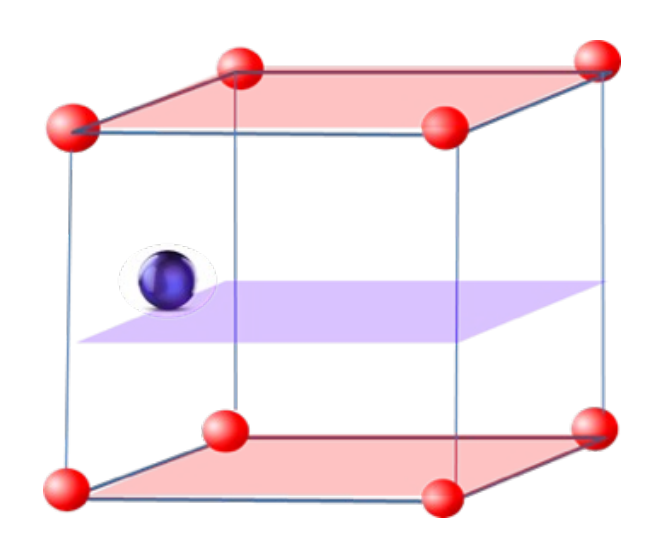
X-rays vs neutrons

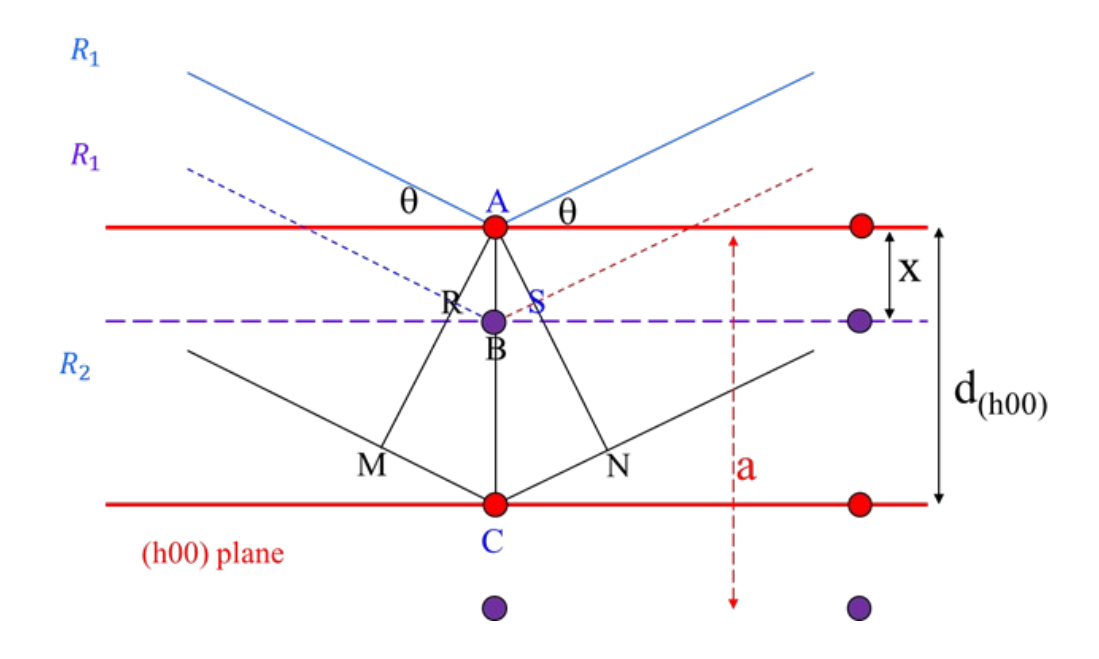


- For neutrons, the atomic nucleus acts a pin-point scatterer unlike the electron cloud, which is of finite size compared to the wavelengths used. The implication of this is that the scattering length b is independent of the scattering angle, 2θ, in contrast to the X-ray case.
- The neutron b values are a property of the nucleus and do not vary in the systematic way that the equivalent f values do in the X-ray case



Let's consider a simple cubic unit cell with a motif with one (red) atom at a lattice point and one (blue) atom in one of the faces at a position x from the top face. The atoms are different chemical species. The red planes are those that fulfill the Bragg equation. The purple plane is parallel to the Bragg planes but does not fulfill the Bragg equation.







The path difference between the rays (R1 and R2) impinging on the (h00) planes (Bragg fulfilled)

MCN= 2AC
$$\sin\vartheta = 2 \ d_{h00} \sin\vartheta = \lambda$$

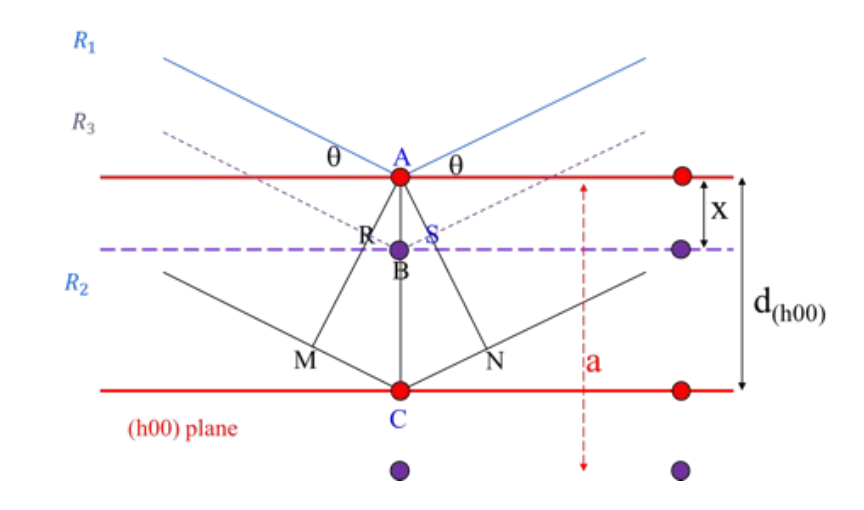
The path difference between R1 and R3

RBS=
$$2ABsin\vartheta = AB \lambda/d_{h00}$$

AC is the distance between the lattice planes (h00)

$$AC=d_{h00}=a/h$$
 and $\frac{AB}{AC}=\frac{x}{\frac{a}{h}}$

RBS=
$$\frac{x}{\frac{a}{h}}\lambda$$
 or a path difference RBS= $h\frac{x}{a}\lambda$



For an atom sitting halfway (x/a=1/2) there will be maximal reduction in intensity



Structure factor:

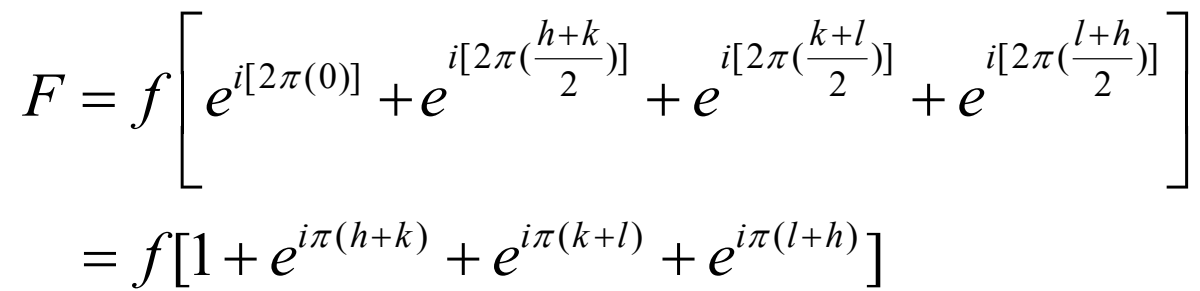
$$F_{hkl} = \sum_{j} f_j \exp[-i2\pi(hx_j + ky_j + kz_j)]$$

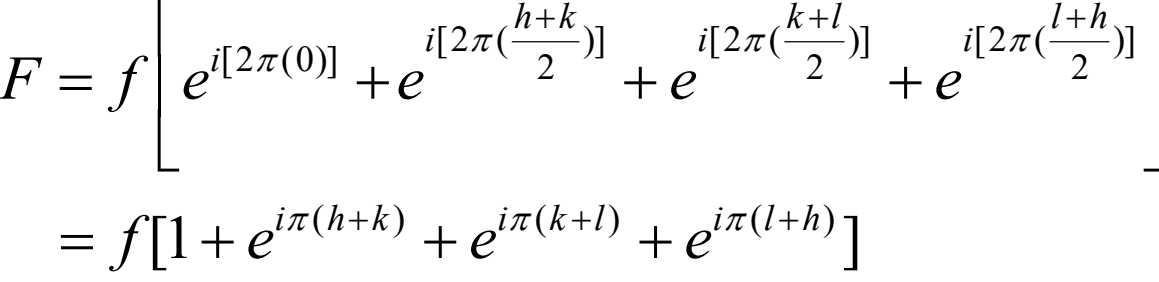
where f_j is the atomic form factor of the j^{th} atom, (x_j, y_j, z_j) is its position in the unit cell expressed in fractions of the unit-cell lattice vectors, and the summation is over the j atoms within the unit cell. The scattered intensity I_{hkl} is the absolute square of \mathbf{F}_{hkl} .





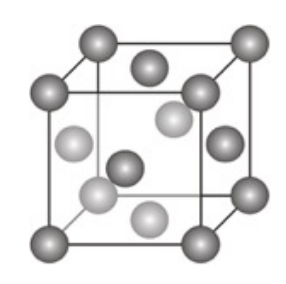
Positions of equivalent atoms: (0,0,0), $(\frac{1}{2},\frac{1}{2},0)$, $(\frac{1}{2},0,\frac{1}{2})$, $(0,\frac{1}{2},\frac{1}{2})$





hkl all even or odd: F=4f e.g. 111, 200, 220, 333, 420

hkl mixed: F=0 e.g. . 100, 211; 210, 032, 033

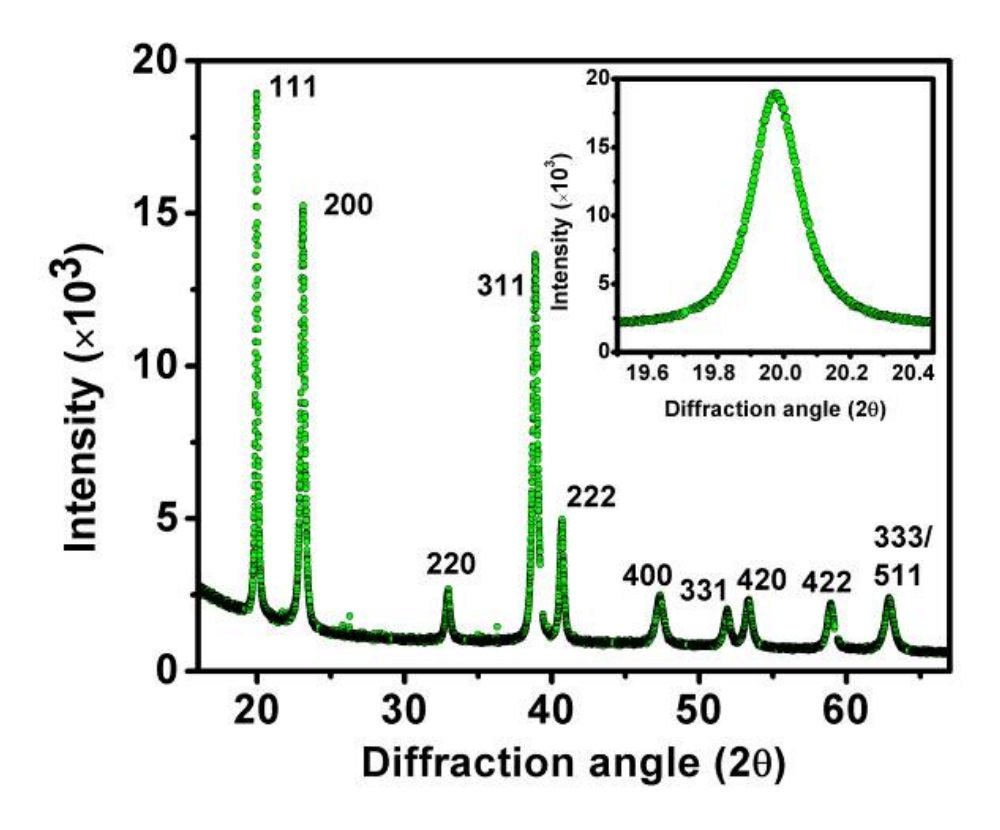


 $e^{i\pi n} = 1$ when n is even = -1 when n is odd



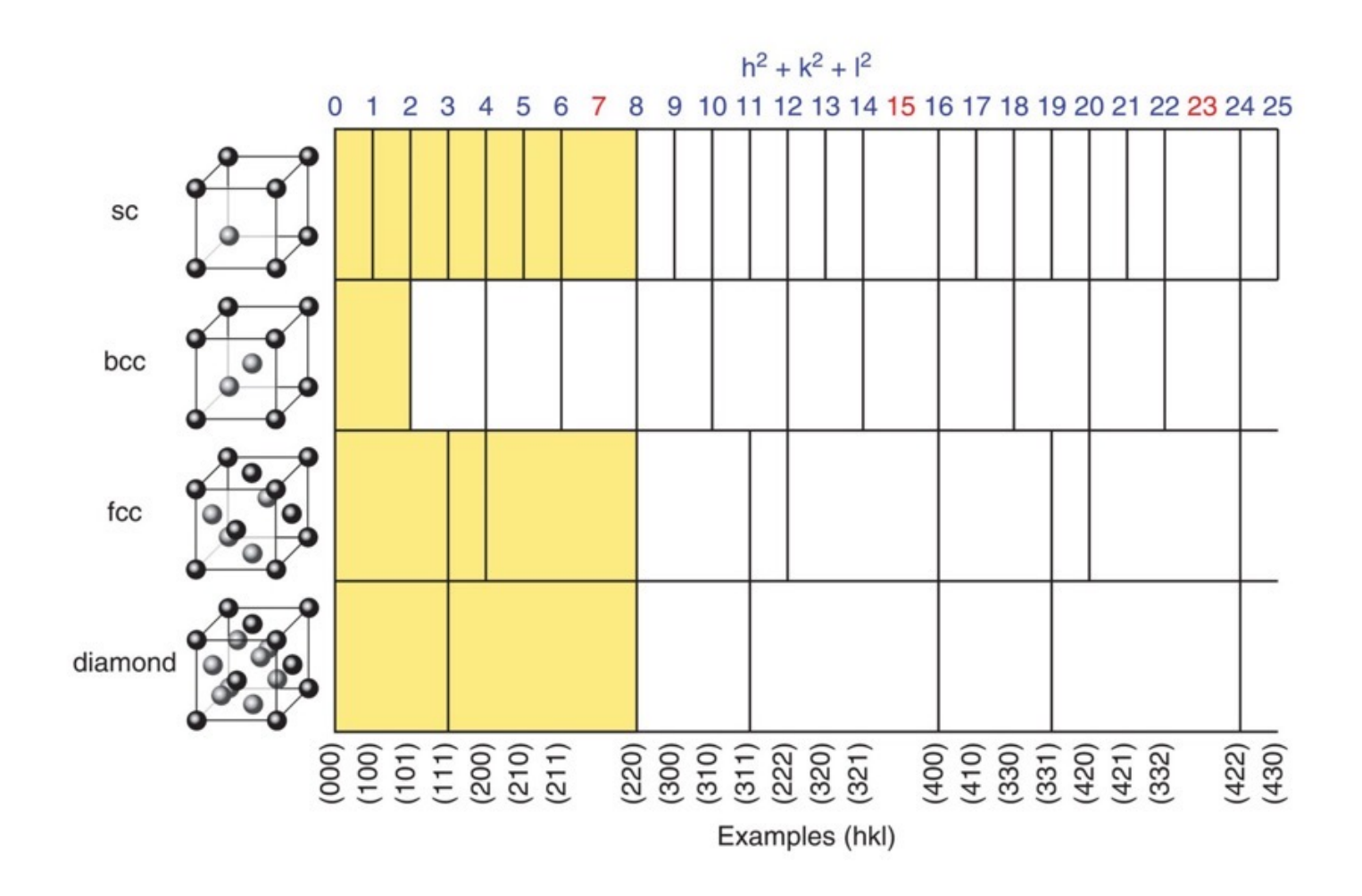
Interaction with a unit cell

• Example: nanocrystalline Ni





Interaction with a unit cell





Chemical ordering

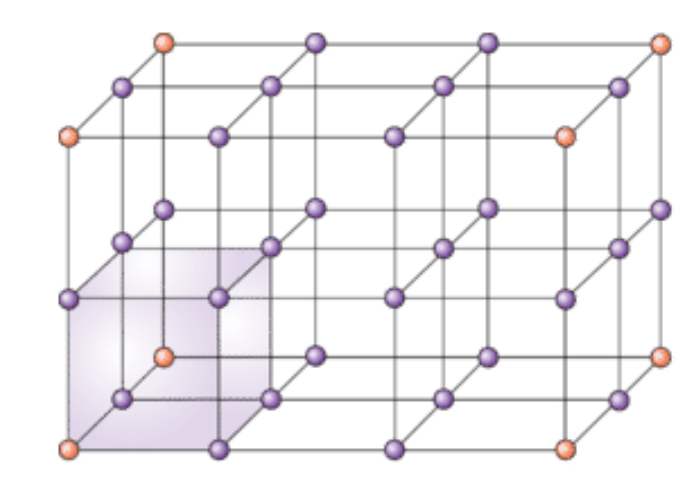


- Atomic fractions: x_A and x_B.
- y_{α} and y_{β} fractions of α and β -sites



- r_{α} : fraction of α -sites occupied by the right atom
- $-\mathbf{w}_{\alpha}$: fraction of α -sites occupied by the wrong atom
- r_{β} : fraction of β -sites occupied by the right atom
- w_{β} : fraction of β -sites occupied by the wrong atom

The long-range order parameters can be defined as: $S = (r_{\alpha} - x_{A})/y_{\beta} = (r_{\beta} - x_{B})/y_{\alpha}$



EPFL PAUL SCHERRER INSTITUT

Chemical ordering: CuAu

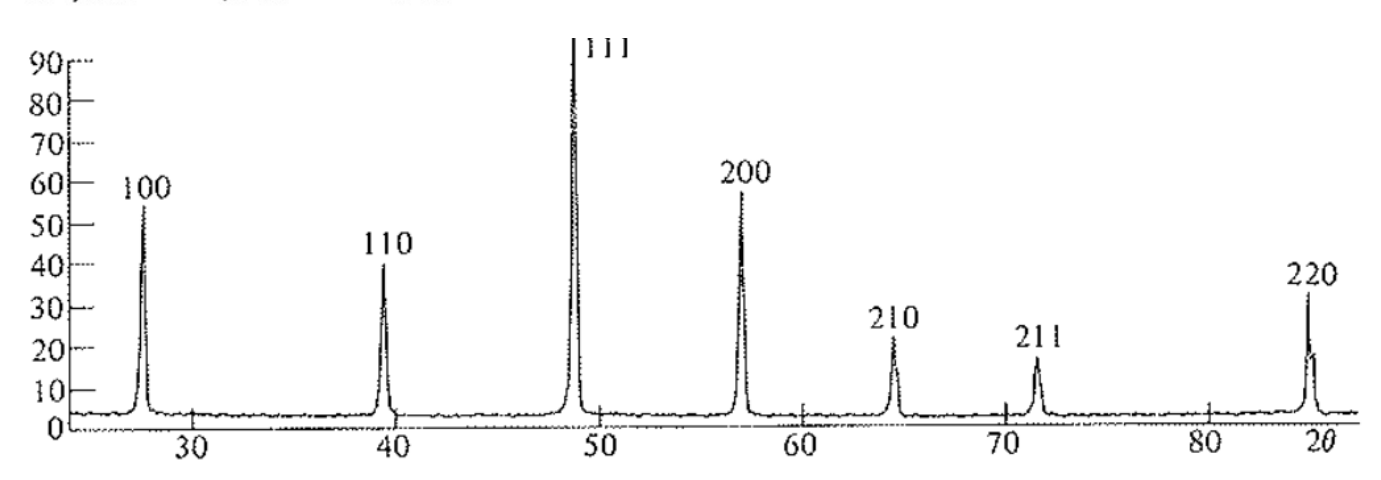
$$\beta = 000, \frac{1}{2}, \frac{1}{2}, 0; \alpha = \frac{1}{2}, 0, \frac{1}{2}; 0, \frac{1}{2}, y_{\alpha} = \frac{1}{2}; y_{\beta} = \frac{1}{2};$$

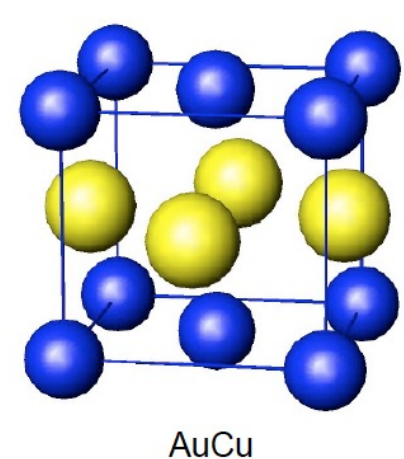
$$F = (r_{\alpha}f_{A} + w_{\alpha}f_{B})[e^{\pi i(h+l)} + e^{\pi i(k+l)}] + (r_{\beta}f_{B} + w_{\beta}f_{A})[1 + e^{\pi i(h+k)}],$$
(12.7)
hkl unmixed;

$$F = 2[(r_{\alpha}f_A + w_{\alpha}f_B) + (r_{\beta}f_B + w_{\beta}f_A)] = 4(x_Bf_B + x_Af_A)$$
 Fundamental,

$$h + k = \text{even}, k + l = \text{odd};$$

$$F = 2[(r_{\beta}f_B + w_{\beta}f_A) - (r_{\alpha}f_A + w_{\alpha}f_B)] = 2S(f_B - f_A)$$
 Superstructure.





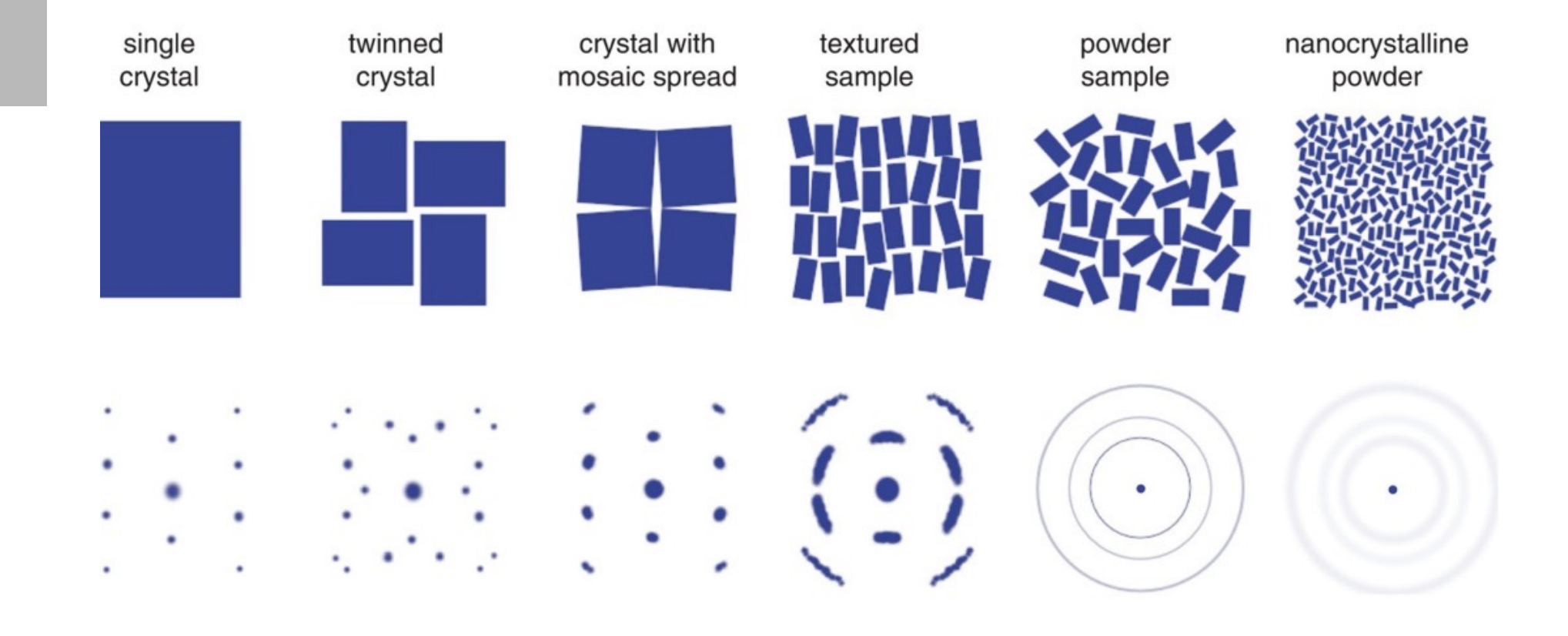
B.E. Warren X-ray diffraction, Dover publications, New York (1990)



Method	Wavelength	Sample angle	Detector angle	Measured
Laue	Variable	Fixed	Fixed	Intensity vs. angle
Rotating crystal	Fixed	Variable	Fixed	Intensity vs. angle
Powder	Fixed	Variable/fixed	Variable	Intensity vs. angle
Energy dispersive	Variable	Fixed	Fixed	Intensity vs. energy
Neutron time-of-flight	Variable	Fixed	Fixed	Intensity vs. time
Bragg coherent diffraction imaging	Fixed	Variable	Fixed	Intensity vs. angle



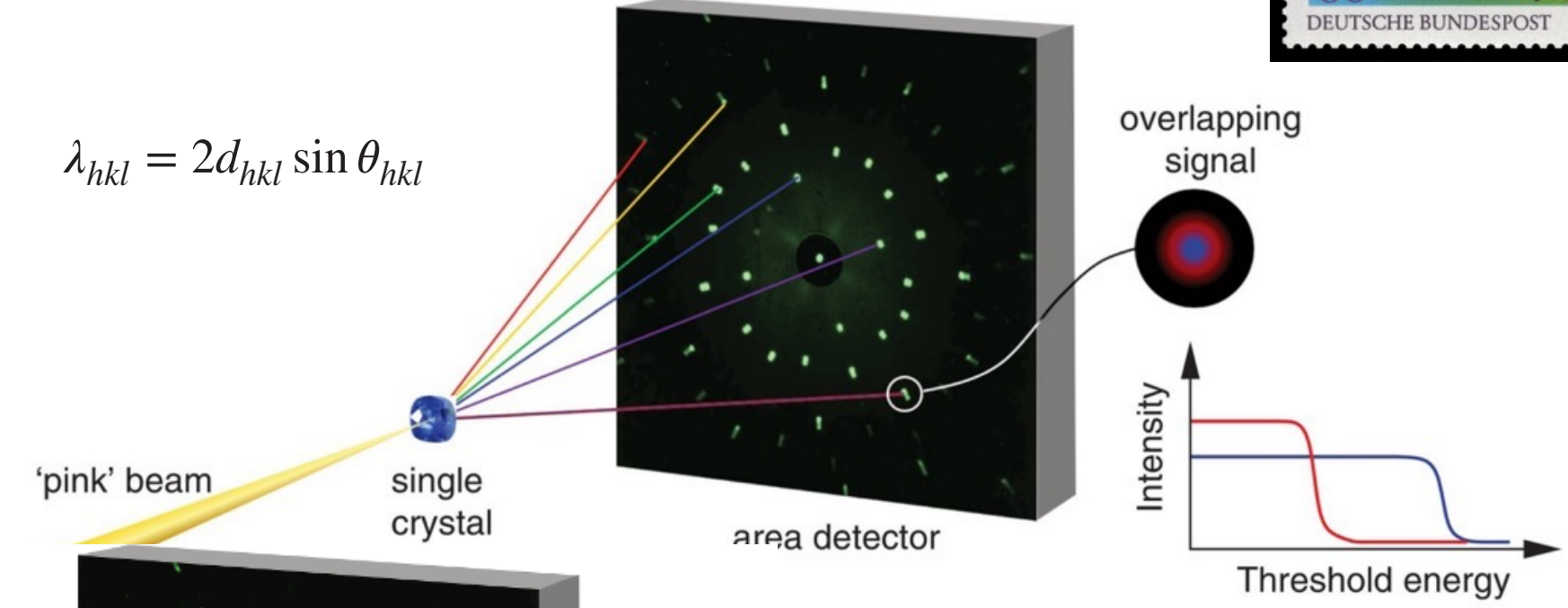
Sample types





Single crystal diffraction - Laue

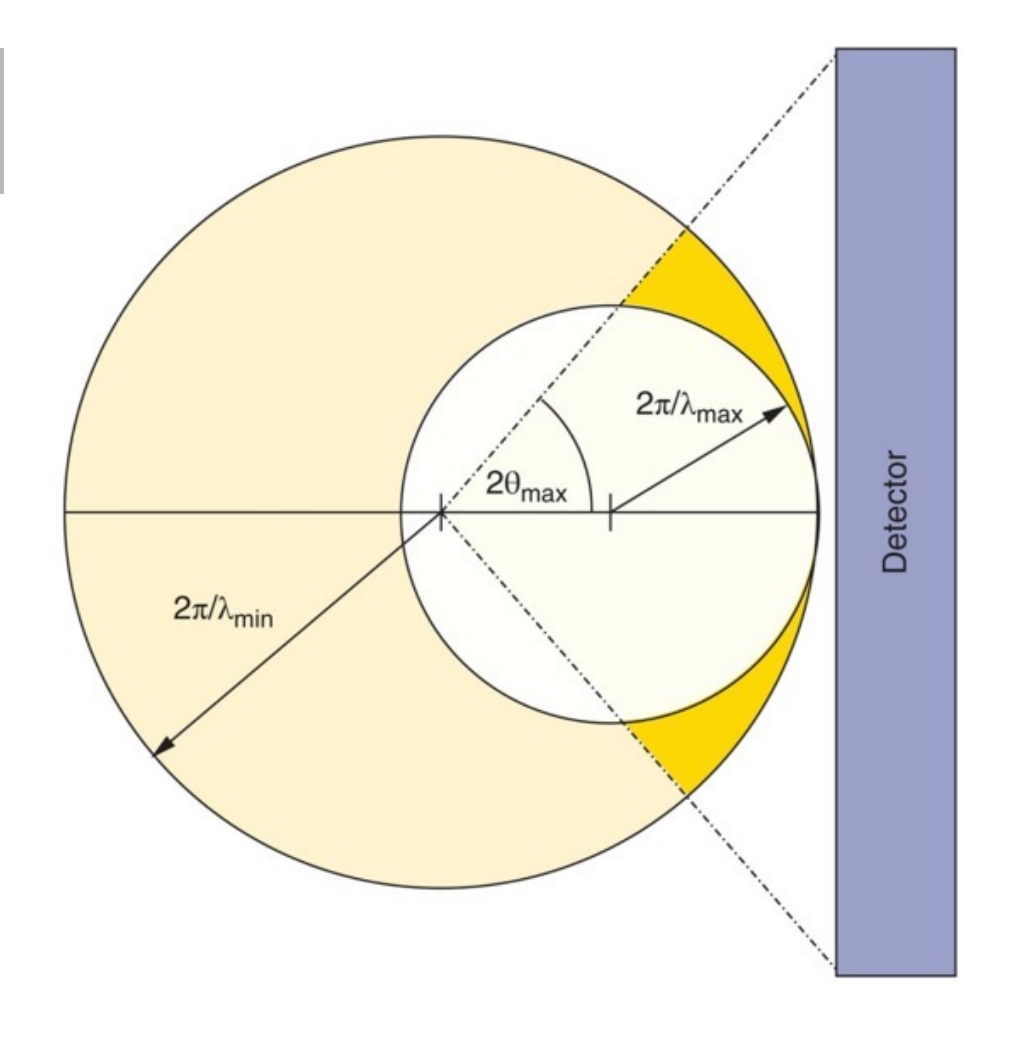




- Pink beam: many wavelengths
- Bragg equation fulfilled for multiple combinations of d and ϑ



Single crystal diffraction - Laue



Laue diffraction provides a lot of structural information in a very short time. However, it is not as well-suited as monochromatic scattering for determining the full atomic structure of a crystal, due on the one hand to the often complex and unknown intensity distribution of the 'pink' incident x-ray beam .

In addition, families of lattice planes that are parallel to one another, for example the (111), (222), (333) ... planes, have Laue diffraction maxima overlapping at the same position, resulting in a loss of information. This is called the 'energy overlapping problem'.

Application: stress in thin films

- -Position spots related to both orientation AND shape of the crystal unit cell
- Any rotation or distortion of the shape of the unit cell will result in offset peak positions
- Positions Laue spots ⇒ crystal orientation + deviatoric strain (stress) tensor
- -In praxis: the positions of the reflections \mathbf{q}_{hkl} with respect to the laboratory reference frame are calculated by:

$$\mathbf{q}_{hkl} = \mathbf{U} \, \mathbf{B} \, \mathbf{G}_{hkl}$$

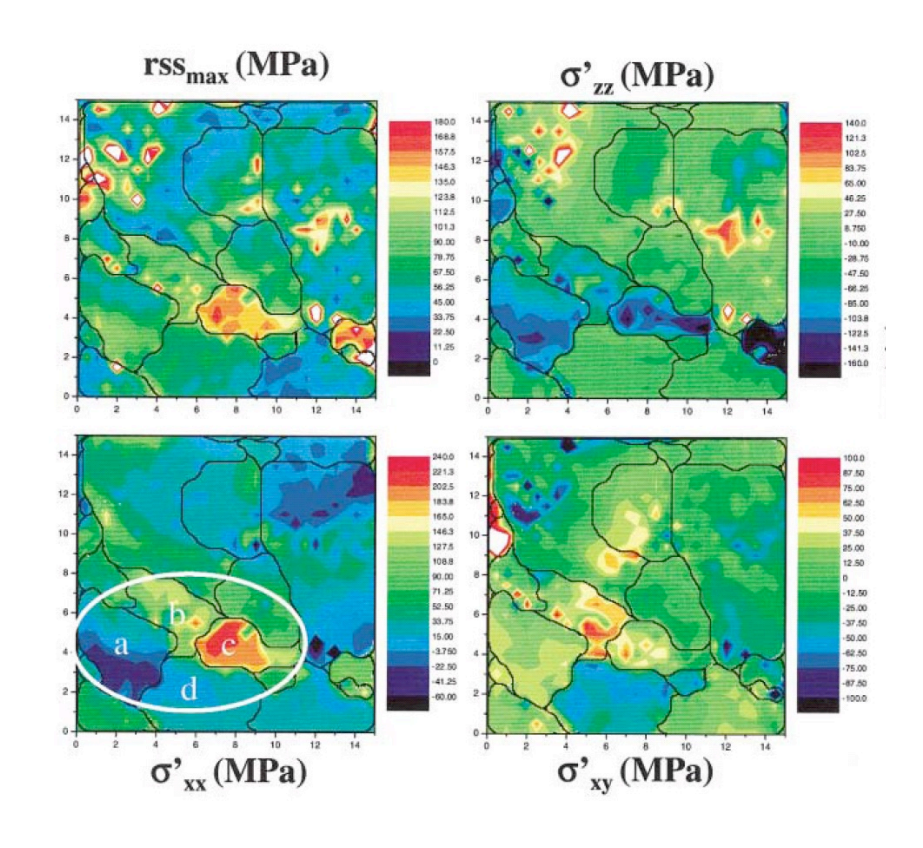
where G_{hkl} is the reciprocal-lattice vector for the hkl reflection, \mathbf{B} depends on elastic strain and \mathbf{U} is the rotation matrix between laboratory and crystal frame.

$$\begin{pmatrix}
\boldsymbol{\varepsilon}_{11} & \boldsymbol{\varepsilon}_{12} & \boldsymbol{\varepsilon}_{13} \\
\boldsymbol{\varepsilon}_{12} & \boldsymbol{\varepsilon}_{22} & \boldsymbol{\varepsilon}_{23} \\
\boldsymbol{\varepsilon}_{13} & \boldsymbol{\varepsilon}_{23} & \boldsymbol{\varepsilon}_{33}
\end{pmatrix} = \begin{pmatrix}
\boldsymbol{\varepsilon}_{11} - \frac{\Delta}{3} & \boldsymbol{\varepsilon}_{12} & \boldsymbol{\varepsilon}_{13} \\
\boldsymbol{\varepsilon}_{12} & \boldsymbol{\varepsilon}_{22} - \frac{\Delta}{3} & \boldsymbol{\varepsilon}_{23} \\
\boldsymbol{\varepsilon}_{13} & \boldsymbol{\varepsilon}_{23} & \boldsymbol{\varepsilon}_{33} - \frac{\Delta}{3}
\end{pmatrix} + \begin{pmatrix}
\frac{\Delta}{3} & 0 & 0 \\
0 & \frac{\Delta}{3} & 0 \\
0 & 0 & \frac{\Delta}{3}
\end{pmatrix}$$



Application: stress in thin films

- Crystal orientation and deviatoric strain tensor can be refined simultaneously when sufficient spots are present. The hydrostatic component can be determined by an energy scan of at least one spot.
- Example: Al 0.5 wt % Cu thin film with thickness of 0.5μm deposited at 400C on a SiN membrane on a Si frame.
 During cooling stresses arise in individual grains. X-ray beam spot size: 0.8μm.

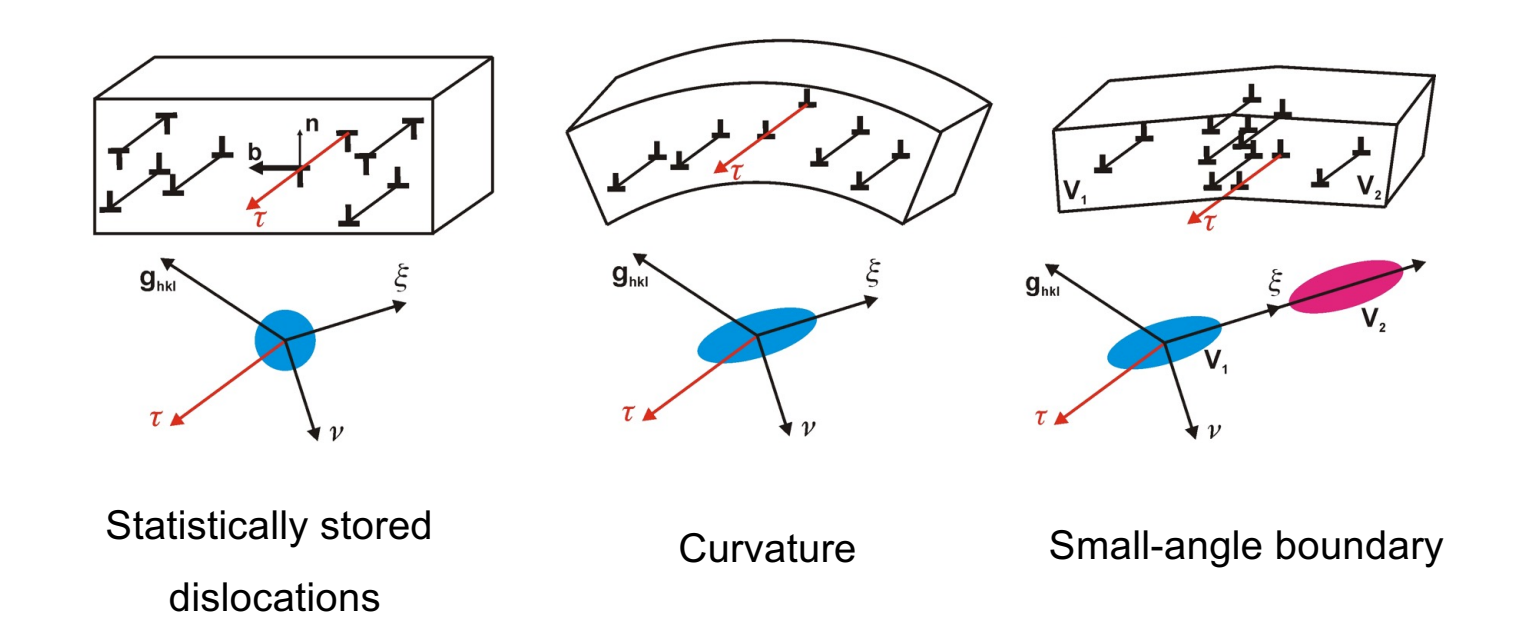


Spolenak et al, Phys. Rev. Lett 90, 096102 (2003)



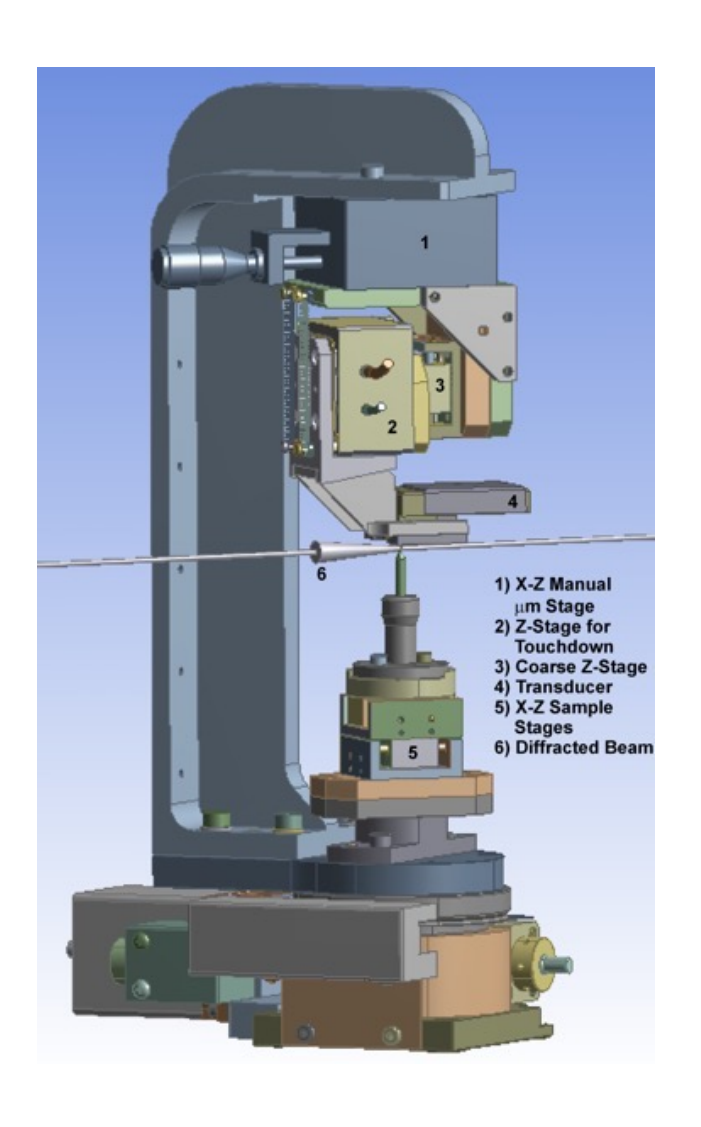
Application: microcompression of single crystals

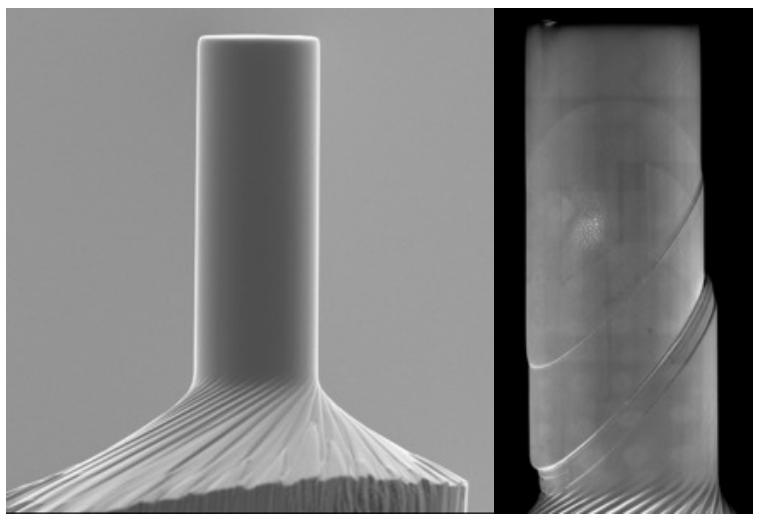
 Microstructural variations within the illuminated volume can lead to change in shape of spots

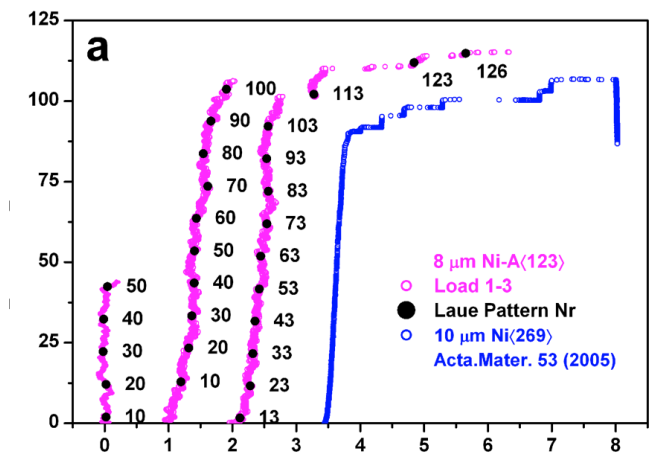




Application: microcompression of single crystals

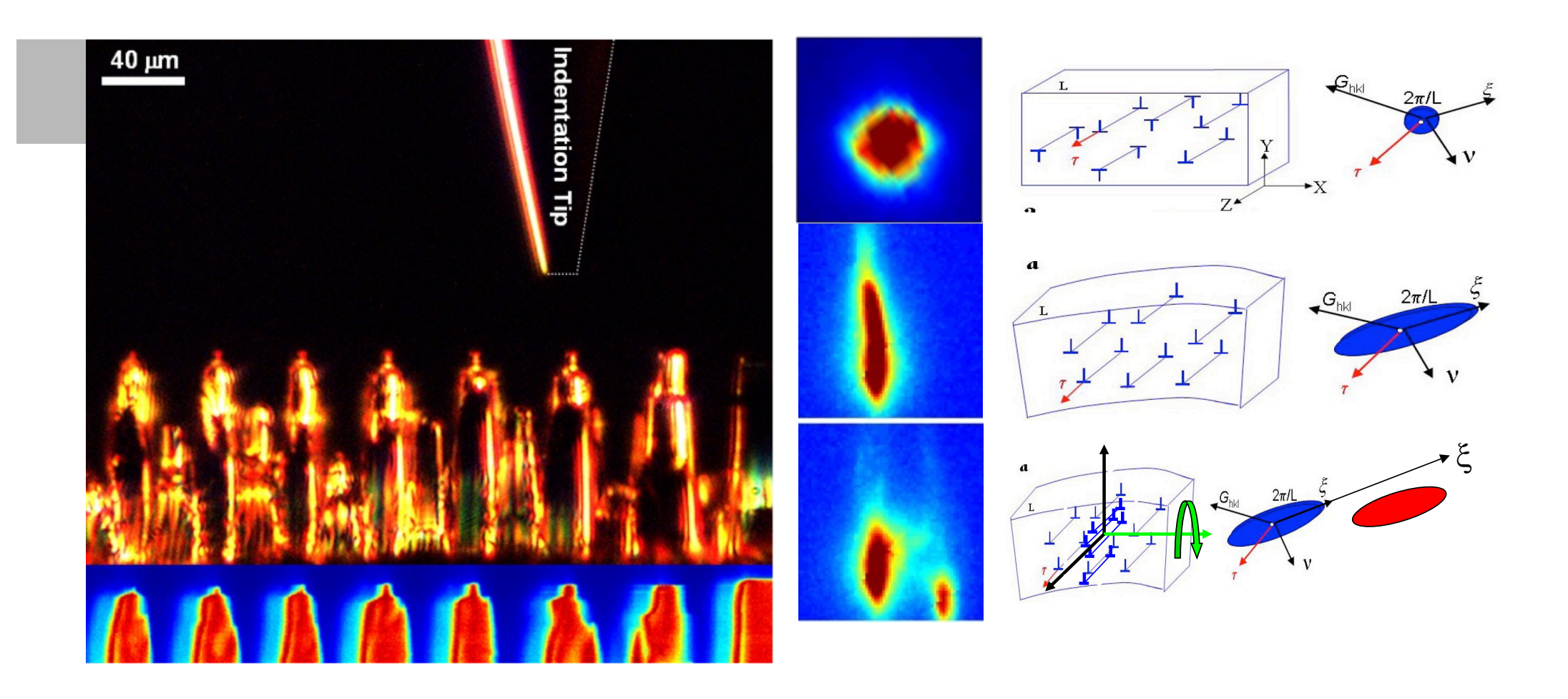








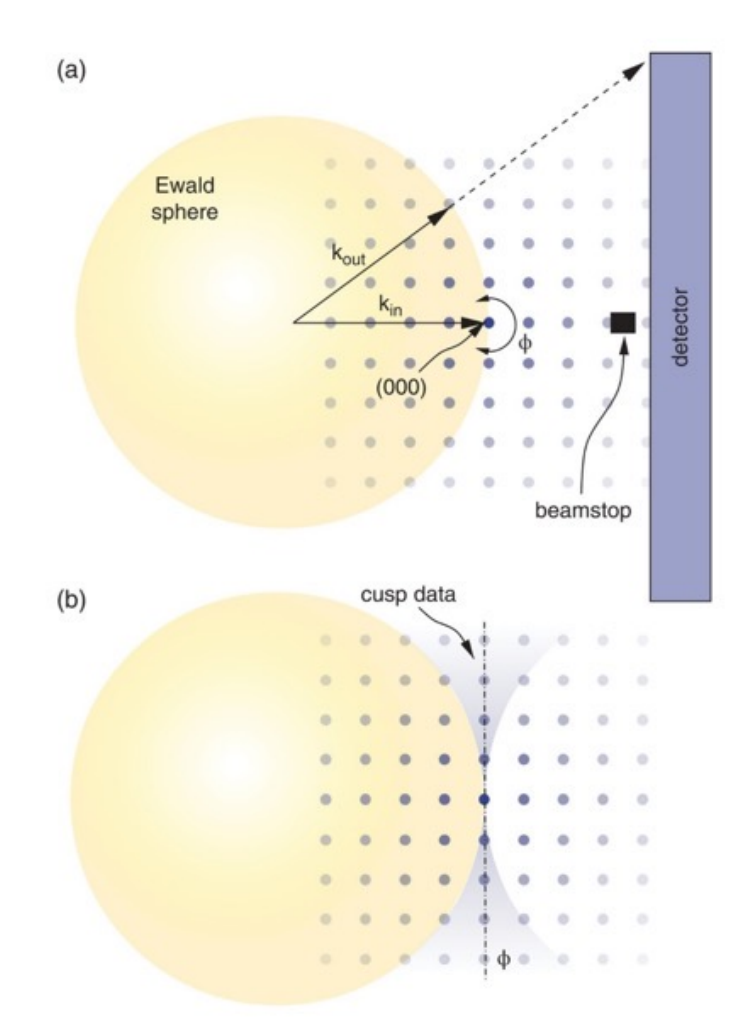
Application: microcompression of single crystals





Single crystal diffraction – rotation method

- In the large majority of single-crystal diffraction experiments, monochromatic radiation is used and the so-called 'rotation' or 'oscillation' method is applied.
- By rotating the crystal around an axis perpendicular to the incident beam (ϕ), diffraction maxima pass through the surface of the Ewald sphere and are registered on a 2D x-ray detector
- When viewed from above the plane containing the ϕ -axis, one sees that for a given crystal orientation relative to the axis, some data cannot be accessed (known as 'cusp' data and shaded blue here). However, by reorienting the crystal axis (typically by 90°), this data can also be recorded.





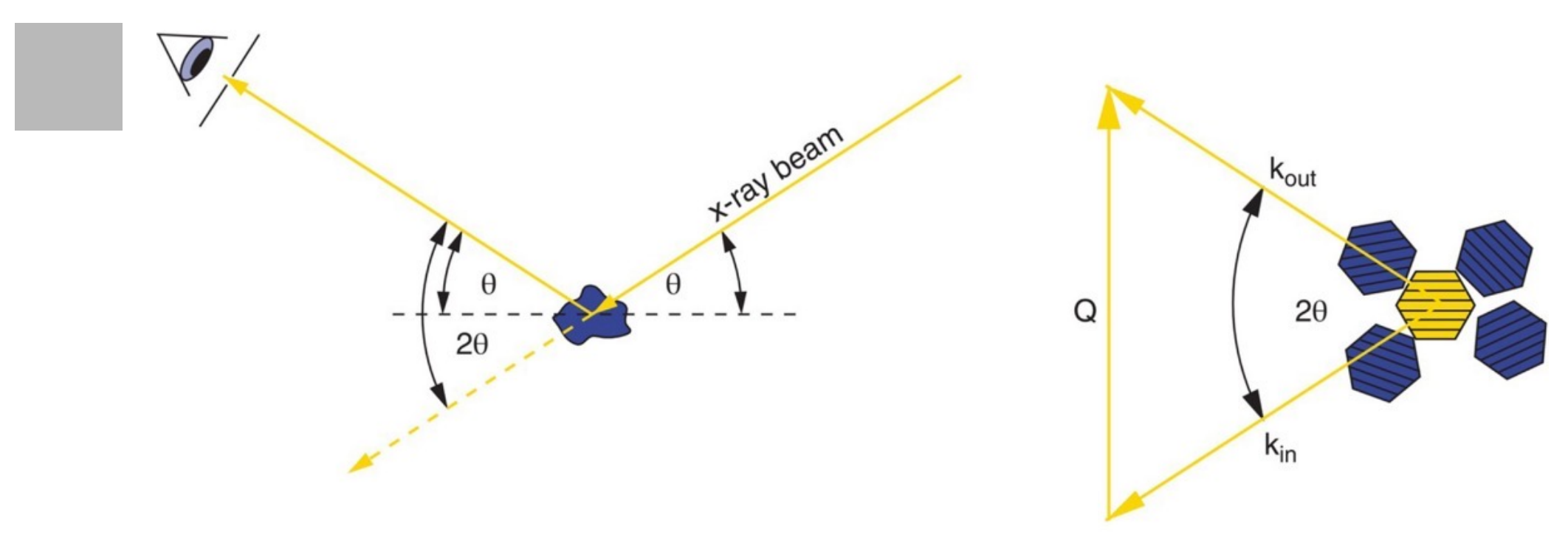
Application: protein crystallography

- Goal: to study the three-dimensional structure of biological macromolecules.
- Unfortunately, it is only possible to measure the amplitude of the diffraction pattern spots by experimental means; the phase information is missing
- Without phase information it is difficult to reconstruct the electron density in the unit cell. There exist various method to circumvent this: (https://www.ruppweb.org/Xray/101index.html)

Data collection: wave length = 0.097nm, Canadian Light Source - 1 second per frame, total of ~360 frames, step size 0.5 degrees

Courtesy: F. Van Petegem, UBC, Canada

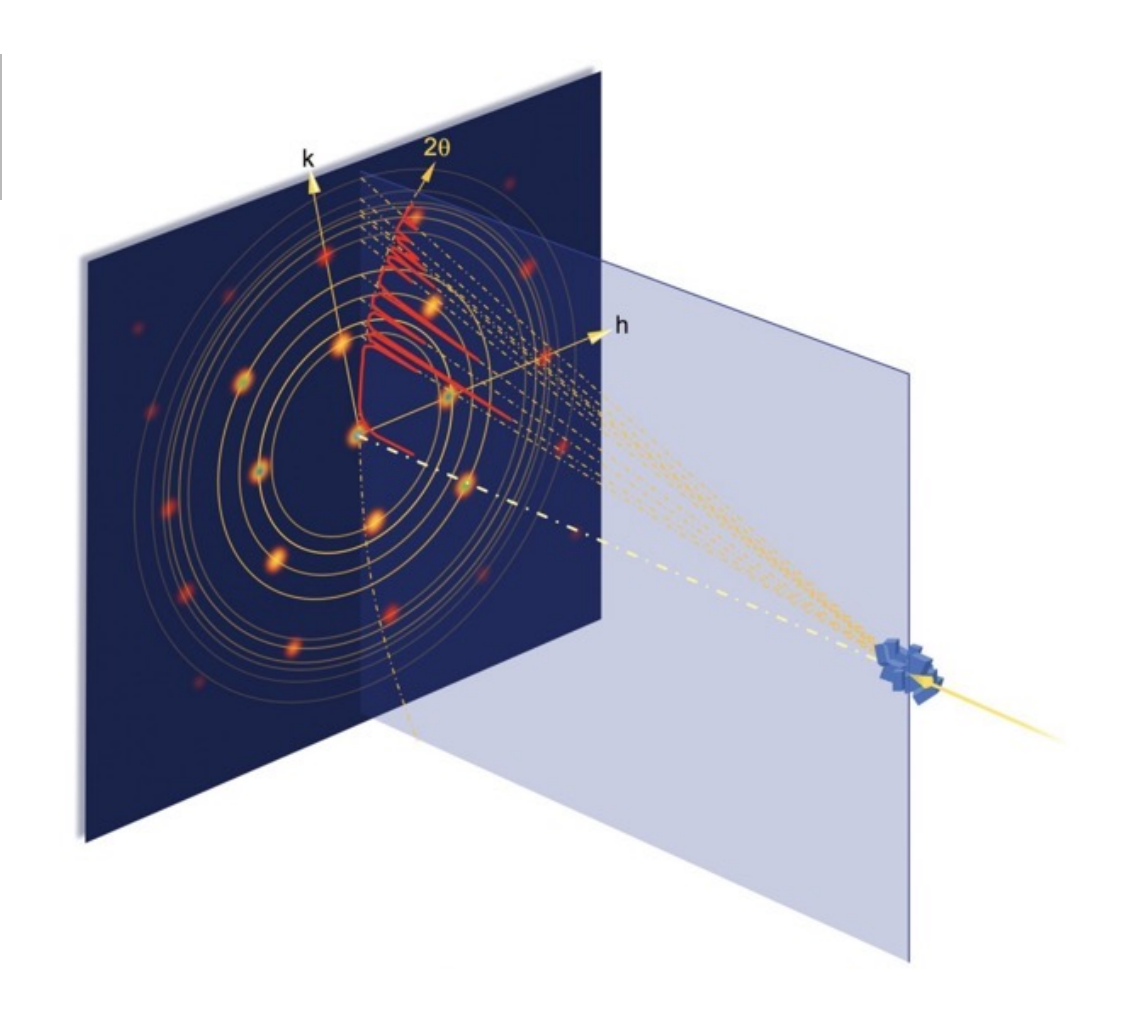
EPFL PAUL SCHERKER INSTITUTION Powder diffraction



Conditions for diffraction in a powder sample. A detector will only see a diffracted signal if the d_{hkl} spacing, the orientation of the crystallite, and the angle of the detector 2θ to the incident x-ray beam lead to the diffraction condition being satisfied. This is fulfilled by the yellowhighlighted crystallite.



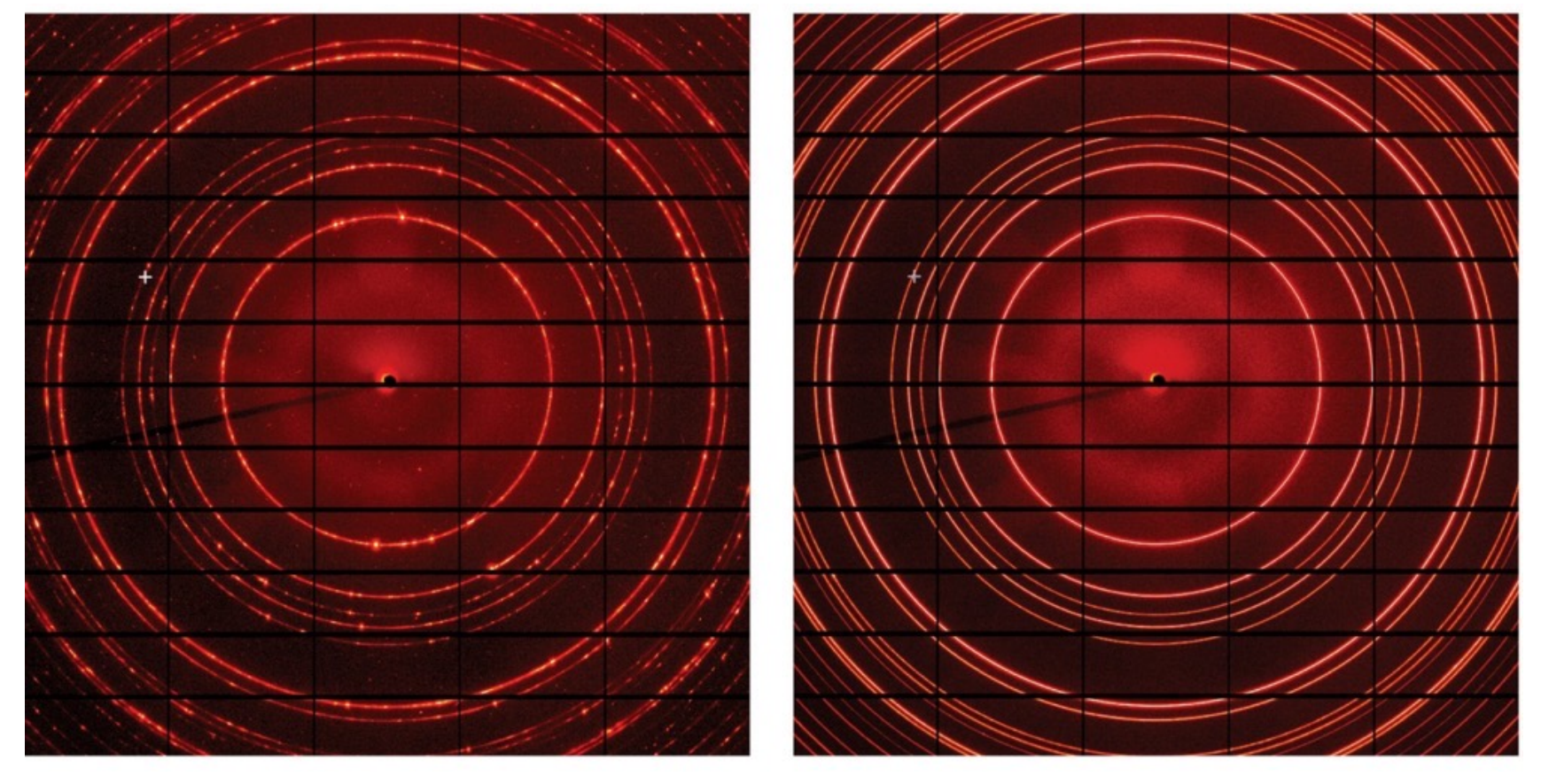
Powder diffraction



A schematic of a powder diffraction experiment. Those crystallites with crystal planes (hkl) at an angle θ given by the Bragg law to the incoming beam will diffract. The cylindrical symmetry of the experimental setup about the incident beam axis means cones of diffracted signal are produced. A diffraction pattern is obtained by scanning radially out from the beam axis with a detector in a plane that contains that axis.



Powder diffraction



The effect of spinning or shaking a powder sample during data acquisition



Rietveld refinement

- The collapse of three-dimensional reciprocal space onto one-dimensional data sets leads to a severe reduction of information, caused by an accidental and systematic peak overlap. This is known as the grave powder problem
- In 1969, Hugo Rietveld published the seminal article on what has become known as the Rietveld refinement method (cited over 18'000 times).
- The underlying idea relies on modeling a calculated powder diffraction pattern, described by a set of parameters.
- All of these parameters can be simultaneously refined by the least-squares method, until the calculated pattern matches the experimentally collected data.
- Since then, many 'whole powder pattern fitting' methods have been developed.



Rietveld refinement

The intensity $I(2\theta)$ at the angle 2θ can be written as:

$$I(2\theta) = \sum_{i=n}^{m} F_i^2 \chi_i (2\theta_i - 2\theta) C_i$$

 F_i is the structure factor for the i^{th} reflection χ_i the peak shape function C_i geometric factor including multiplicity and Lorentz factor

Refinement parameters may include: lattice constants, atomic positions, thermal parameters, site occupancy, peak asymmetry, Lorentz and polarization, axial divergence, background coefficients, strain and size broadening, ...

Lorentz factor

• Polarization correction: accounts for polarization state of incident beam (in most powder x-ray diffractometers, unpolarized)

$$P = 1 - \cos^2(2\theta)$$

• Lorentz correction: takes into account change in scattering volume size & scan rate as a function of angle for a particular diffraction geometry

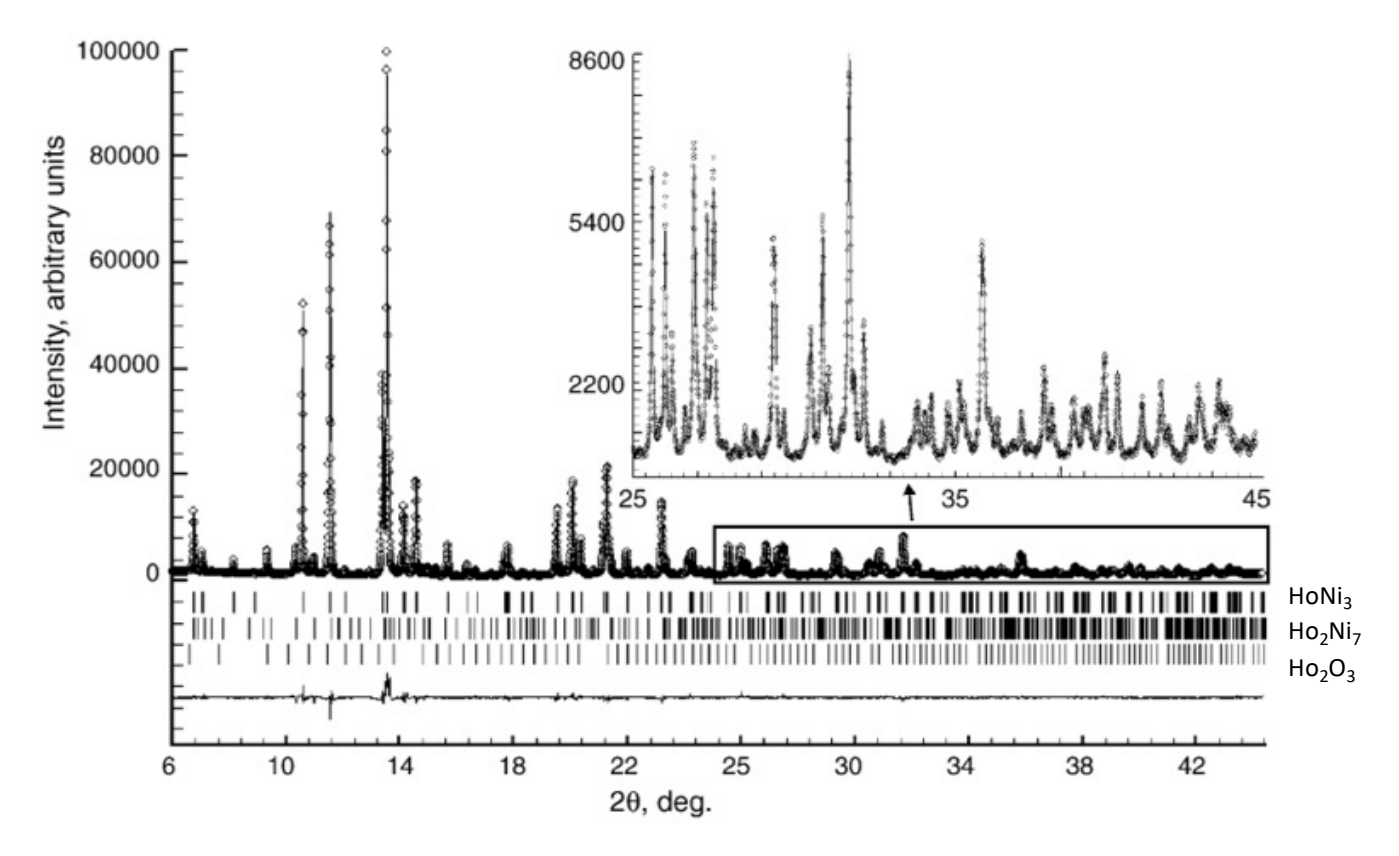
$$L = 1/(\sin^2\theta \cos\theta)$$

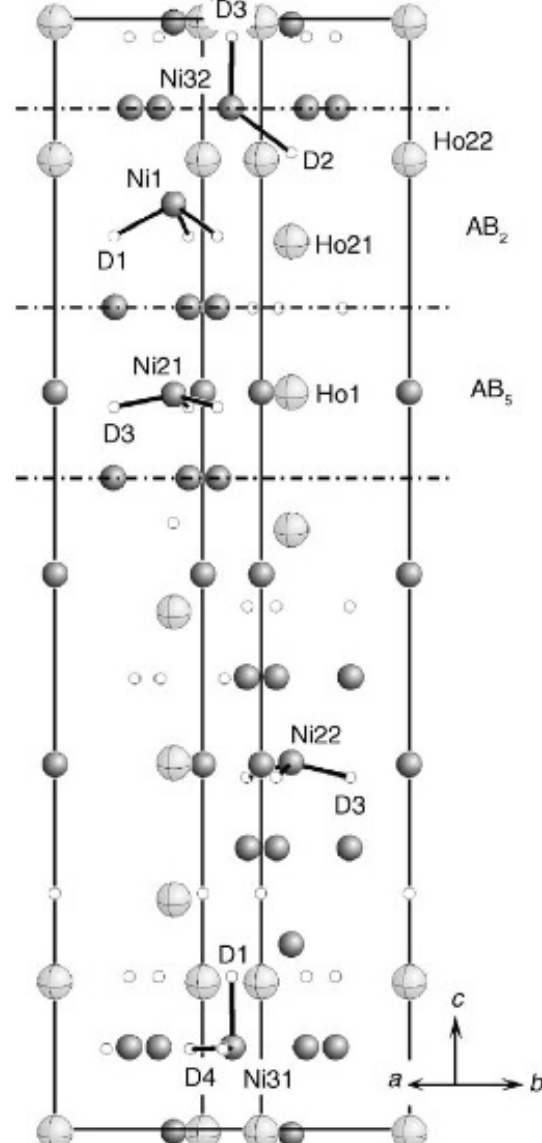
• Lorentz–polarization factor

$$LP = (1 - \cos^2(2\theta)) / (\sin^2 \theta \cos \theta)$$



Rietveld refinement





Y.E. Filinchuk et al J. of Alloys and Compounds 413 (2006) 106



There exist many data analysis routines that include Rietveld refinement, such as

Fullprof: http://www.ill.eu/sites/fullprof

GSAS: http://www.ncnr.nist.gov/xtal/software/gsas.html

MAUD: http://maud.radiographema.com

The International Centre for Diffraction Data: http://www.icdd.com

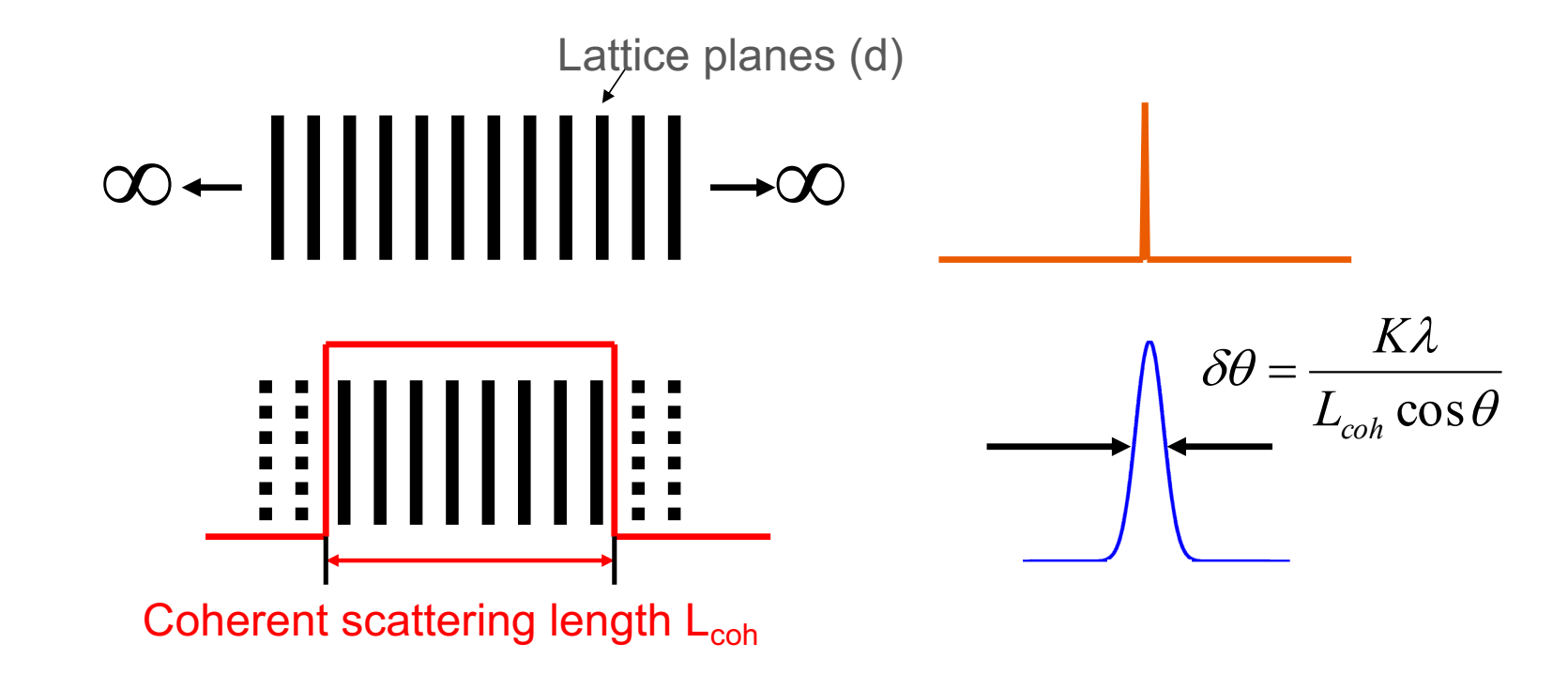


Peak profiles

- Peak profiles are determined by many factors. The most important ones include:
 - Resolution function
 - Coherent scattering length
 - Microstrain
 - Inhomogeneous elastic strain
 - Anti-phase boundaries
 - Faulting
 - Dislocations
 - Grain surface relaxation
 - Solid solution inhomogeneity
 - Temperature factors
- Peak profile is a convolution of the profiles from all of these contributions

EPFL PAUL SCHERRER INSTITUT

Grain size analysis



Size broadening due to incomplete 'canceling' of small deviations from the Bragg angle

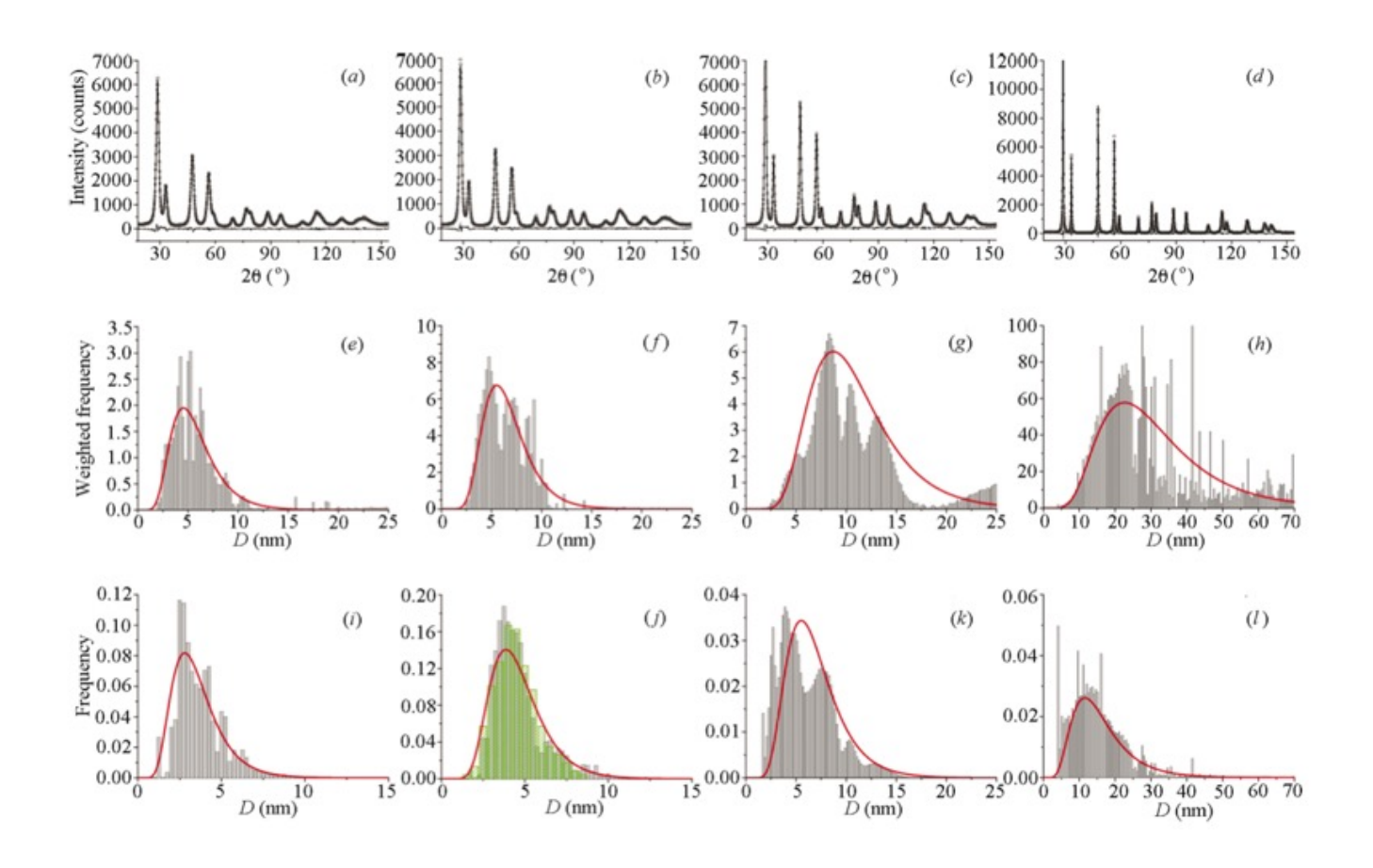


Grain size analysis

- Scherrer formula: $B(2\theta) = \frac{K\lambda}{L\cos\theta}$
- - the most common values for K are:
 - 0.94 for FWHM of spherical crystals with cubic symmetry
 - 0.89 for integral breadth of spherical crystals with cubic symmetry
 - 1, because 0.94 and 0.89 both round up to 1
- K actually varies from 0.62 to 2.08
- For an excellent discussion on K, refer to J.I. Langford and A.J.C. Wilson, J. Appl. Cryst. 11
 (1978) p102



Grain size analysis – example: CeO₂





Dislocation density

Elastic strain variations

 \downarrow

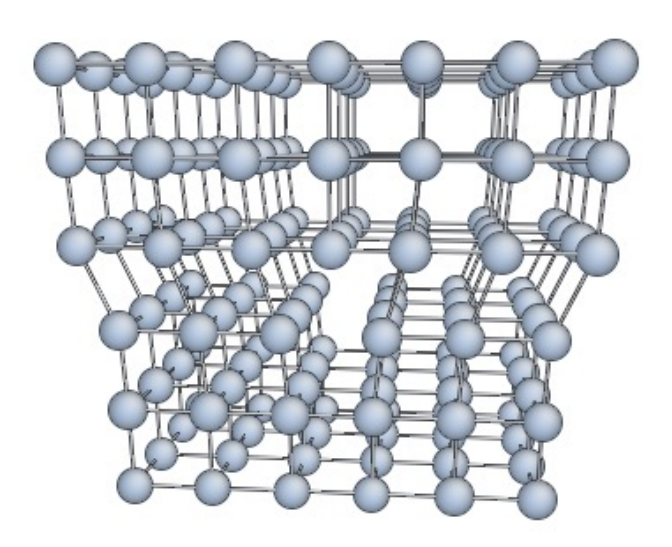
distribution of lattice distances

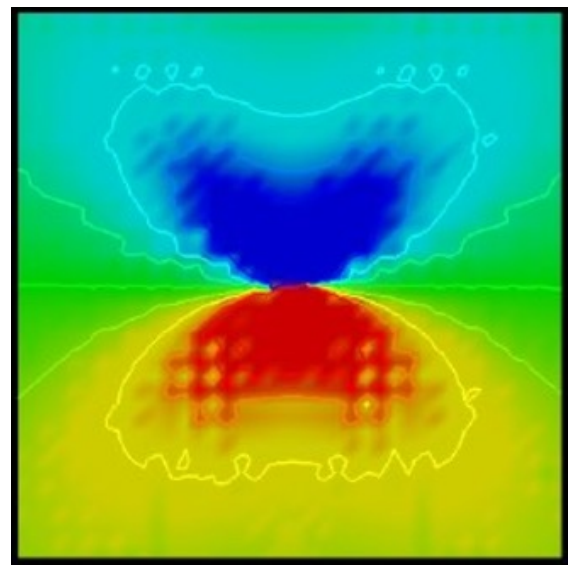
 \prod

peak broadening
Dislocations: anisotropic strain distribution

 \downarrow

Dislocation contrast factor C





EPFL PAUL SCHERRER INSTITUT

Dislocation density

- Modified Willamson-Hall method
 - T. Ungar et al. Appl. Phys. Lett. 69, 3173 (1996)
- Fourier analysis

$$A_{hkl}^D = \exp\left[-\frac{1}{2}\pi b^2 \bar{C}_{hkl} \rho \, d_{hkl}^* L^2 f^* \left(\frac{L}{R_e}\right)\right],$$

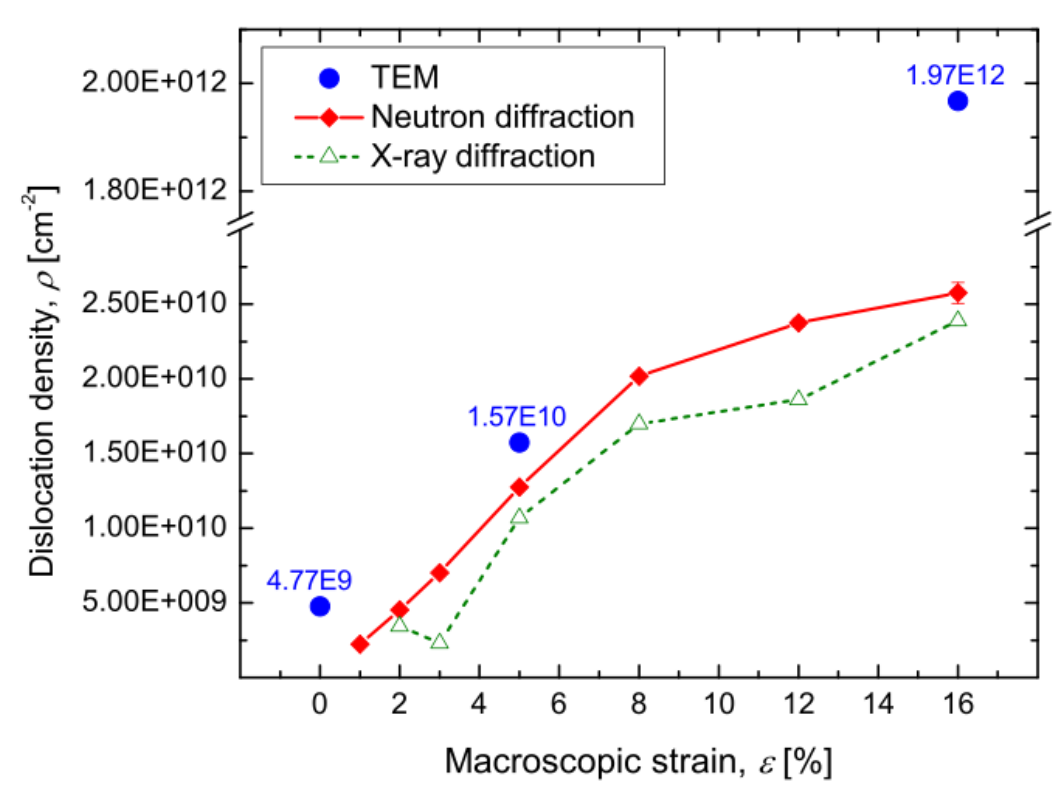
- X-ray Diffraction, B.E. Warren, Dover Publications, 1990
- Full pattern fitting (e.g. PM2K)
 - M. Leoni et al. J. Appl. Crystall. 40, 719 (2007)

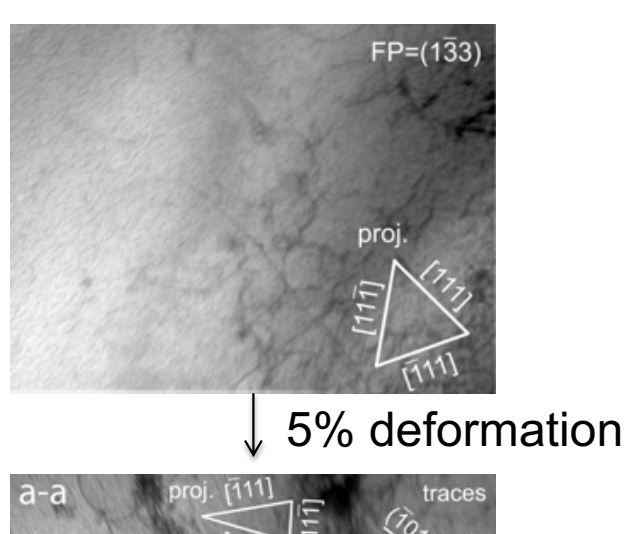
Parameters: dislocation density, cut-off radius and character

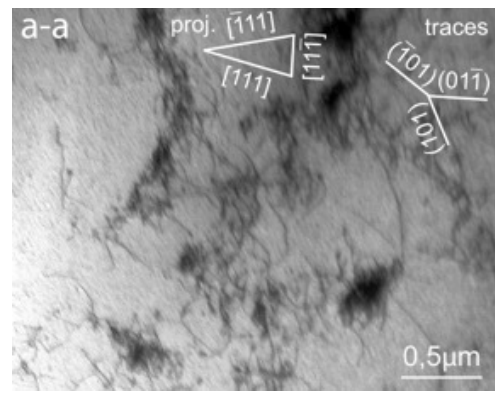


Dislocation density

• Example: deformation of a low carbon C10E steel.





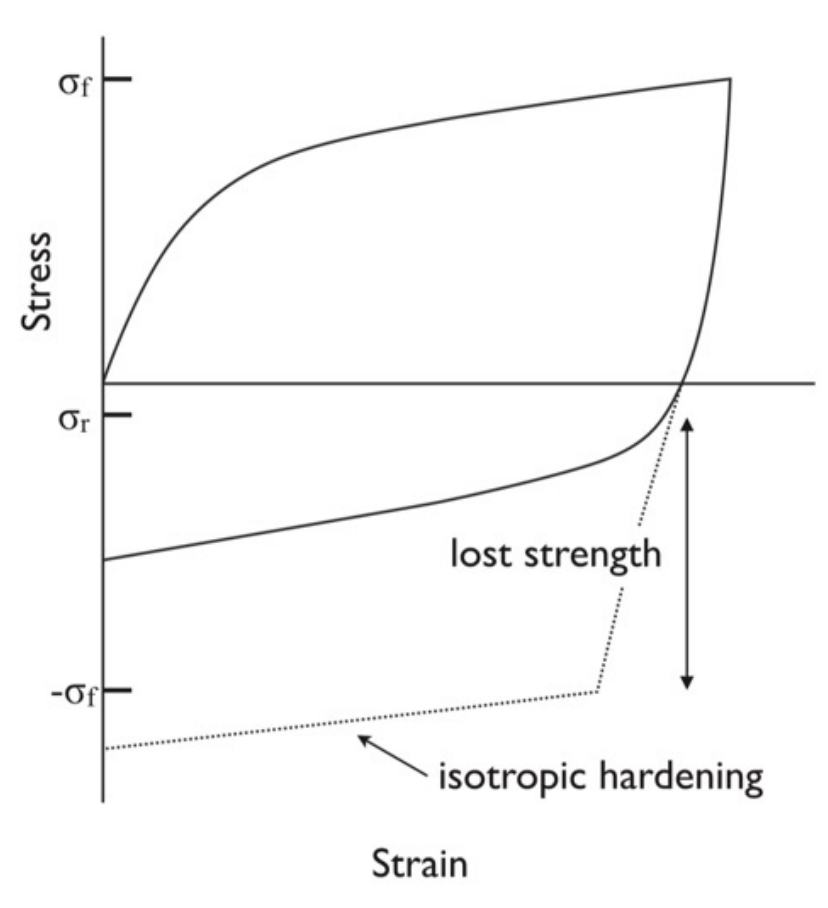


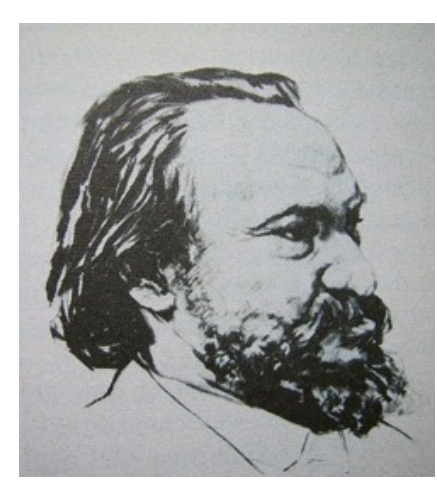
V. Davydov. PhD thesis (2010)





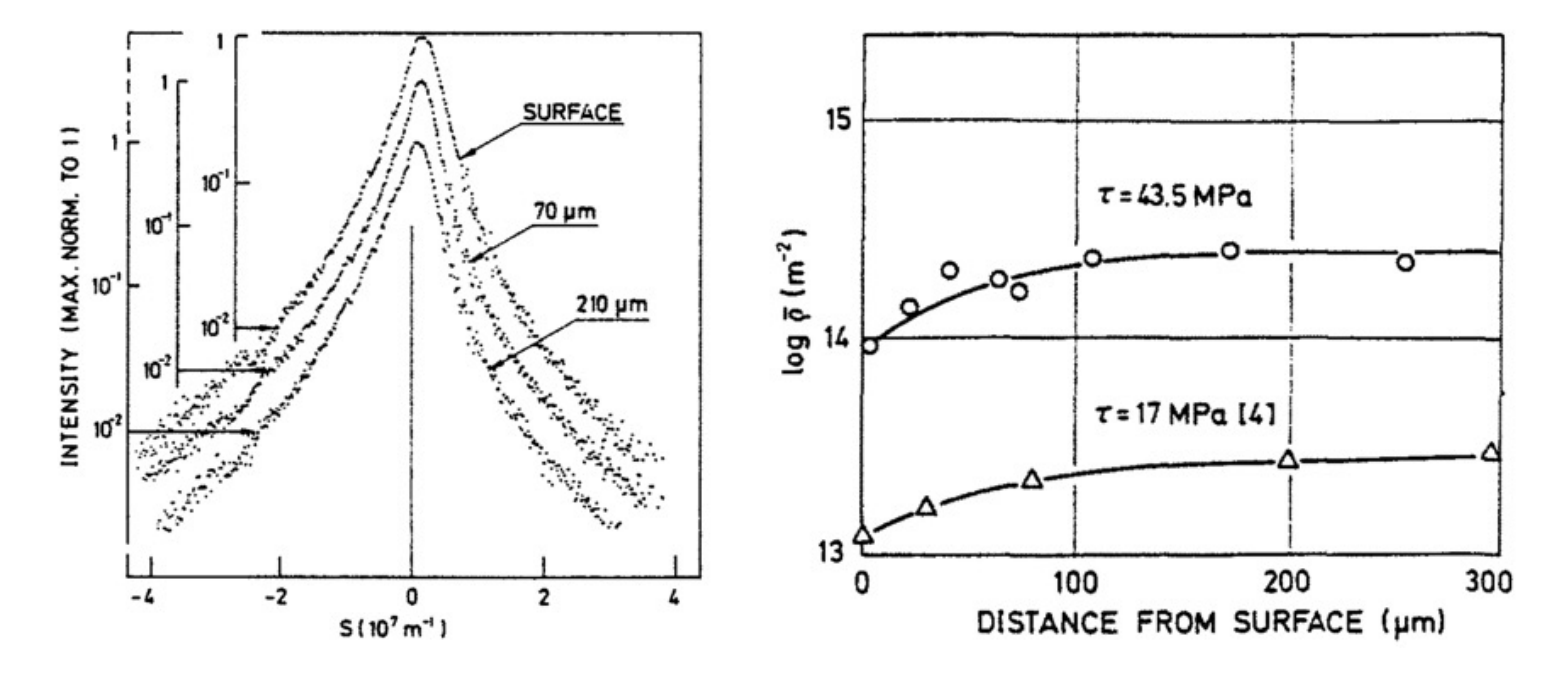
• Bauschinger effect (1881), Civiling. N.F., 27, 289.







Ungar et al. (1982) Acta. Metall. 30, 1861

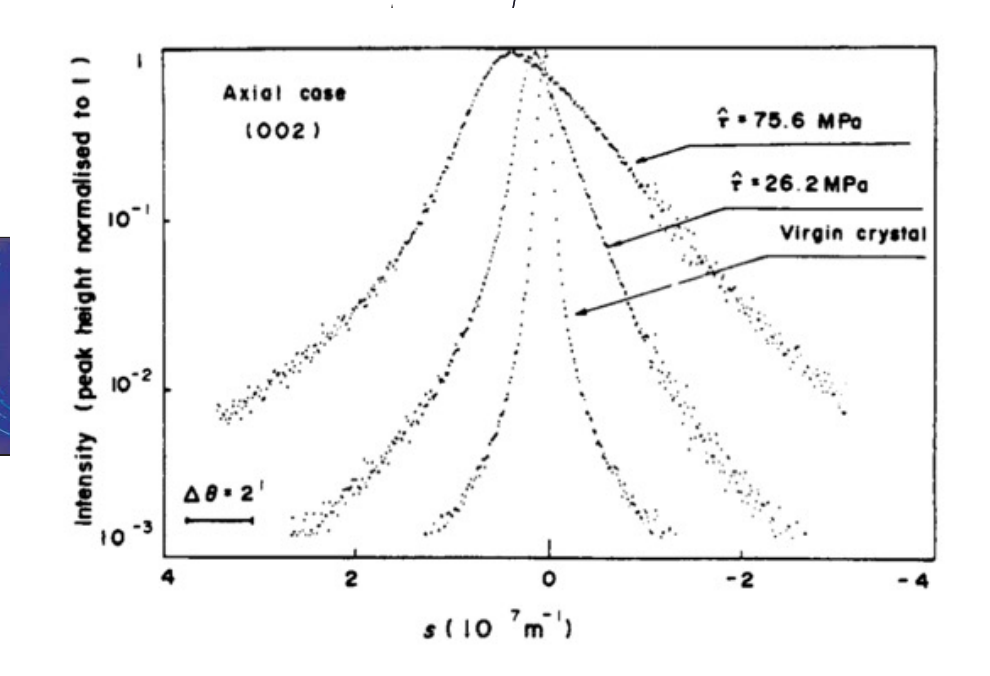


Dislocation density measurements based on approach Wilkens (physica status sol 2, 359 (1970).





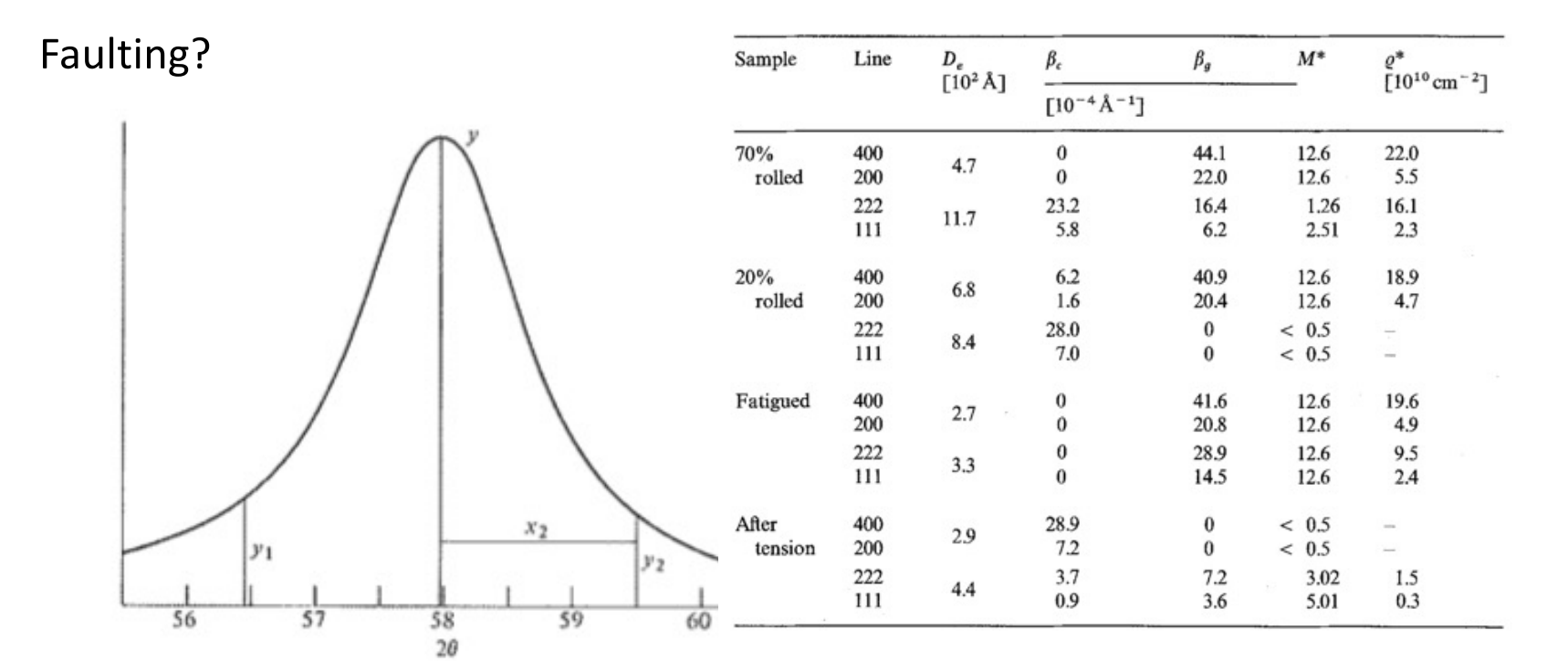
Plastically deformed Cu



Origin of strong peak asymmetry?

H. Mughrabi, Acta Metall. 31 (1983) 1367



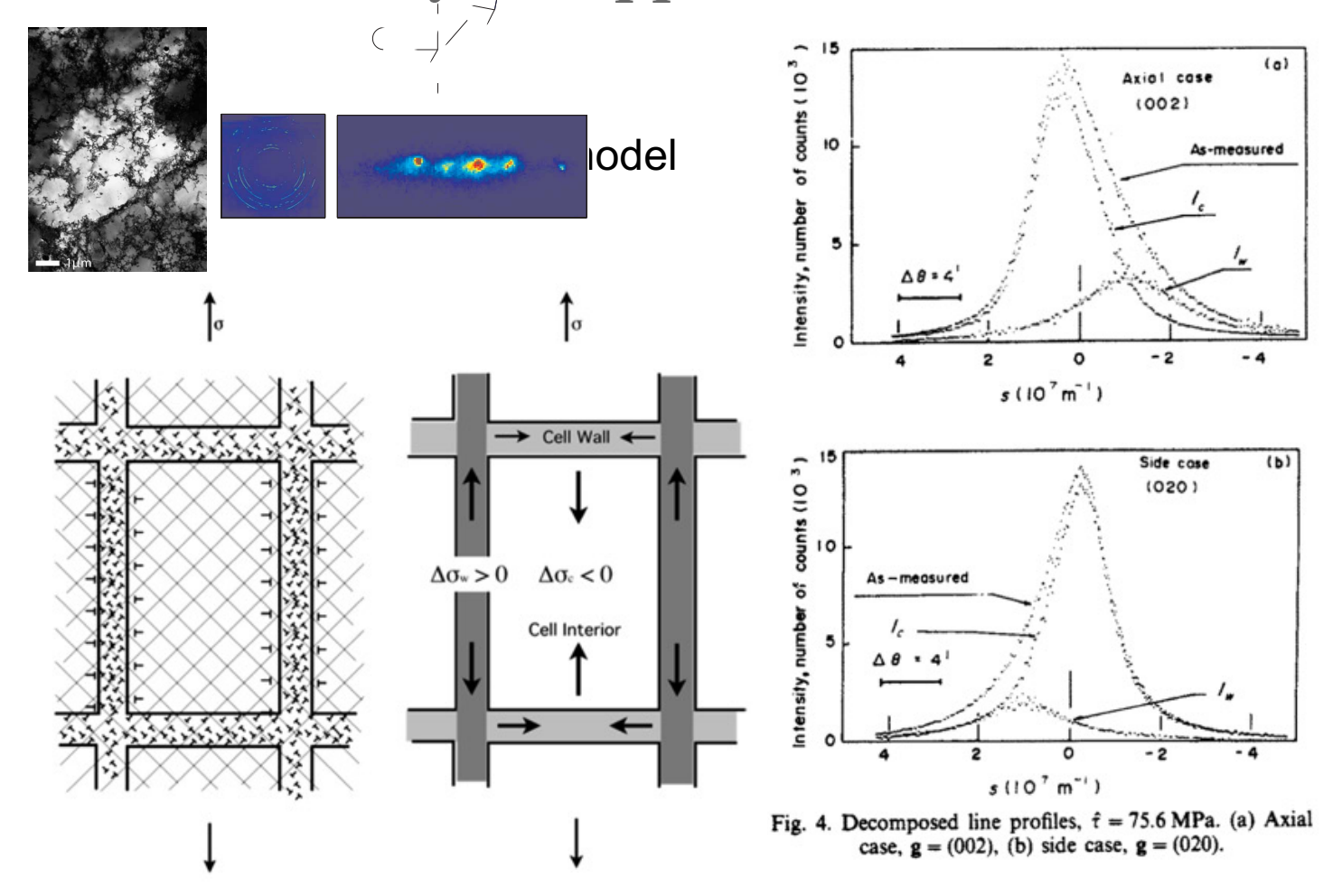


$$\beta = \frac{\sqrt{3} \pi x_2 (y_1 - y_2)}{2A} \left\{ 1 + \left[\frac{\lambda}{4\pi D(\text{eff. 200})(\sin \theta_2 - \sin \theta_0)} \right]^2 \right\}. \quad (13.76)$$

B.E. Warren X-ray diffraction (1969)

EPFL PAUL SCHERRER INSTITUT

The story of copper



H. Mughrabi, Acta Metall. 31 (1983) 1367

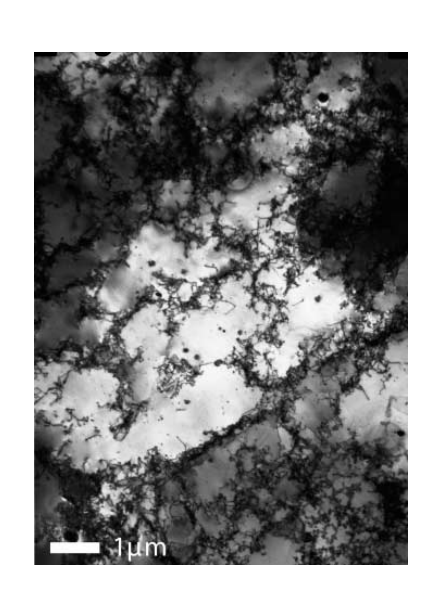


Advantage or disadvantage?

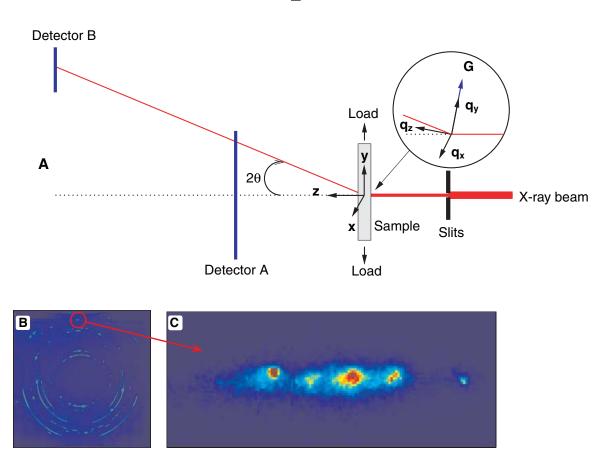
- One of the big advantages of x-ray powder diffraction: provides statistical relevant information (compared to, for instance, electron microscopy)
- One of the big disadvantages of x-ray powder diffraction: provides only averaged information, sometimes obscuring the source of changes in peak shape.
- Solution: move away from conventional powder diffraction and use local x-ray probes





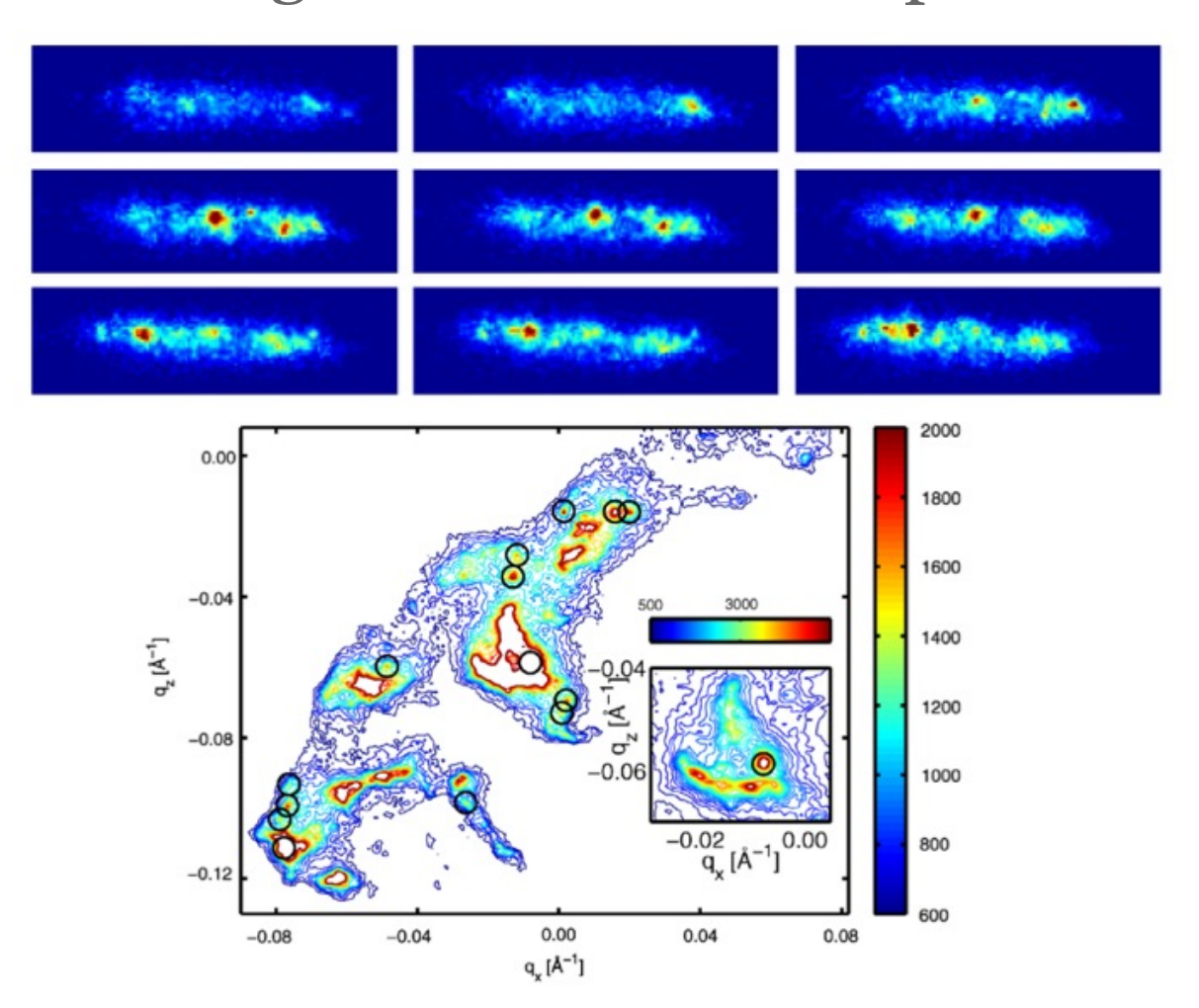


Plastically deformed Cu

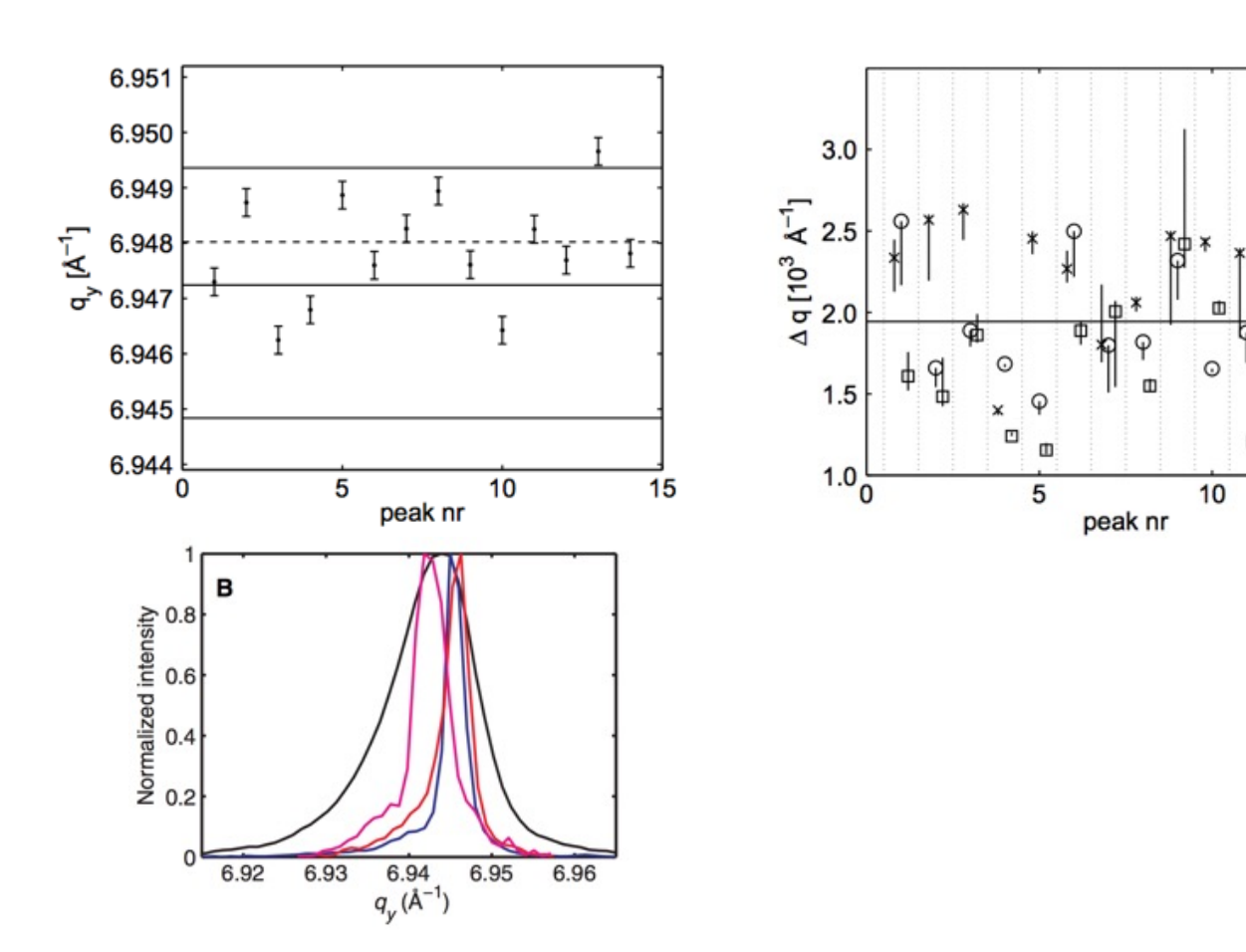


Jacobsen et al. Science 312 (2006) 889





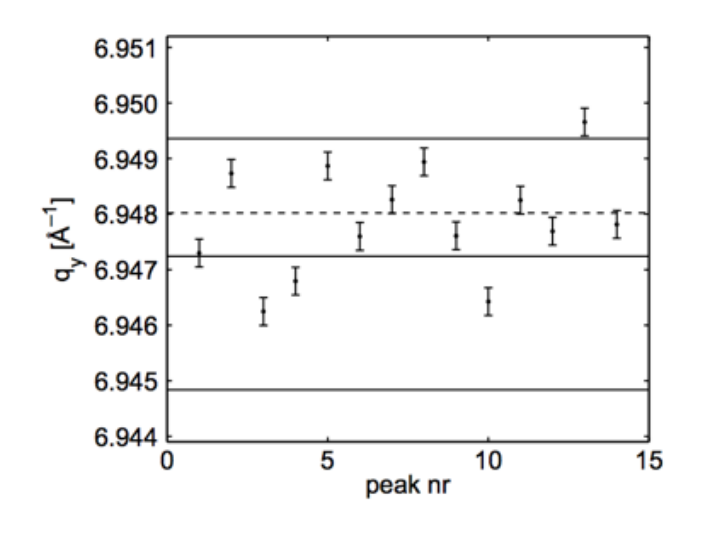


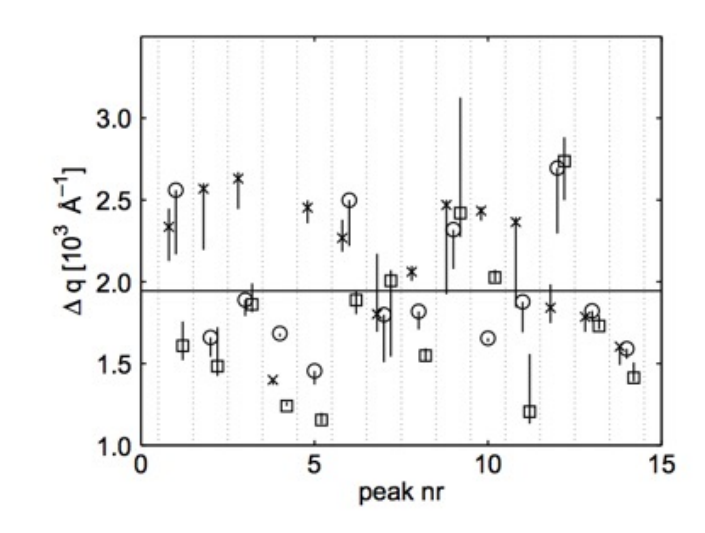


15

Jacobsen et al. Science 312 (2006) 889







Sub-grains are dislocation-poor (<10¹³ m⁻²)

,Bulk' diffraction peaks are composed of diffuse background (dislocation walls) + sum of sharp peaks from the sub-grains, each with a different stress level, leading to broad diffraction peaks

Jacobsen et al. Science 312 (2006) 889



Take home messages

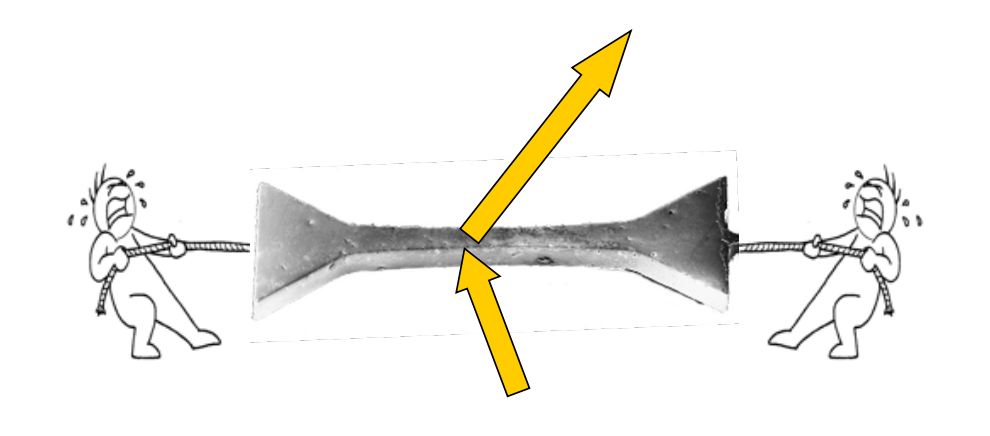
Critically assess all possible causes for peak broadening

Each method will give you a number

Use multiple analysis techniques



In situ diffraction





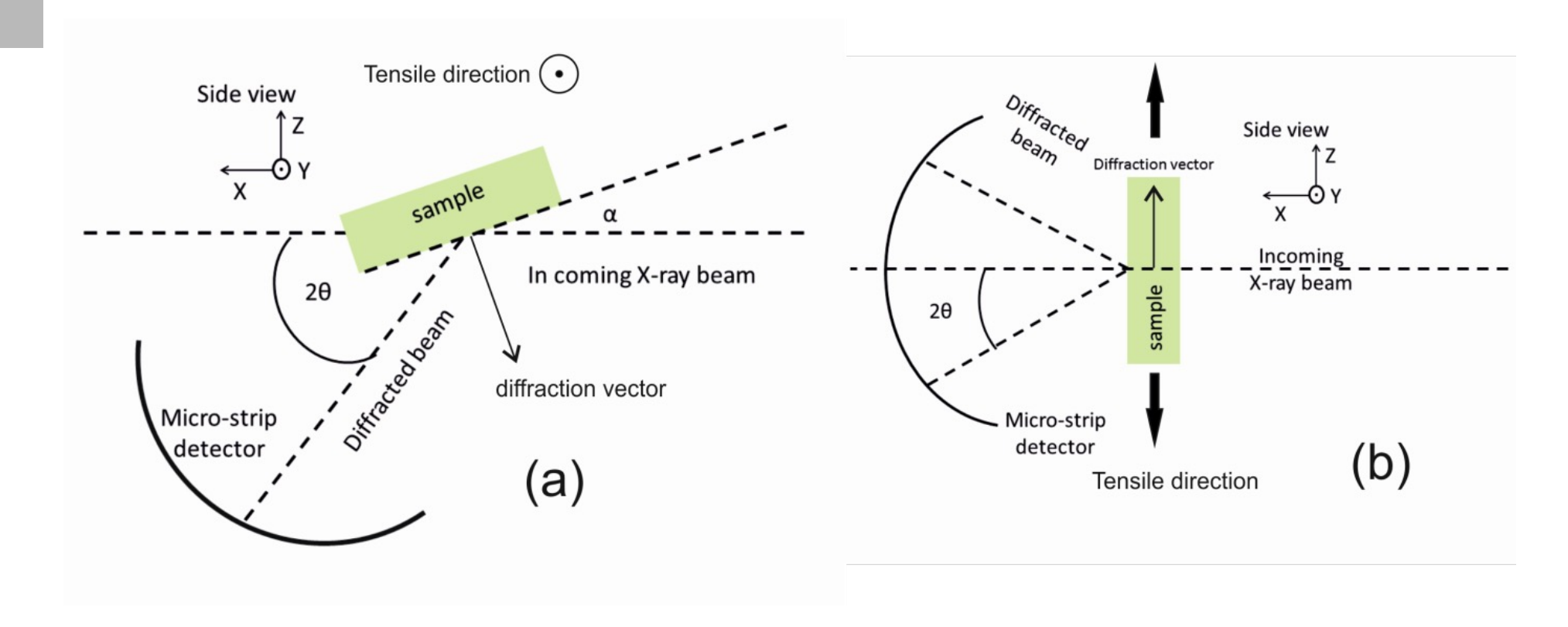
In-situ deformation

In-situ annealing/cooling/quenching



In situ powder diffraction

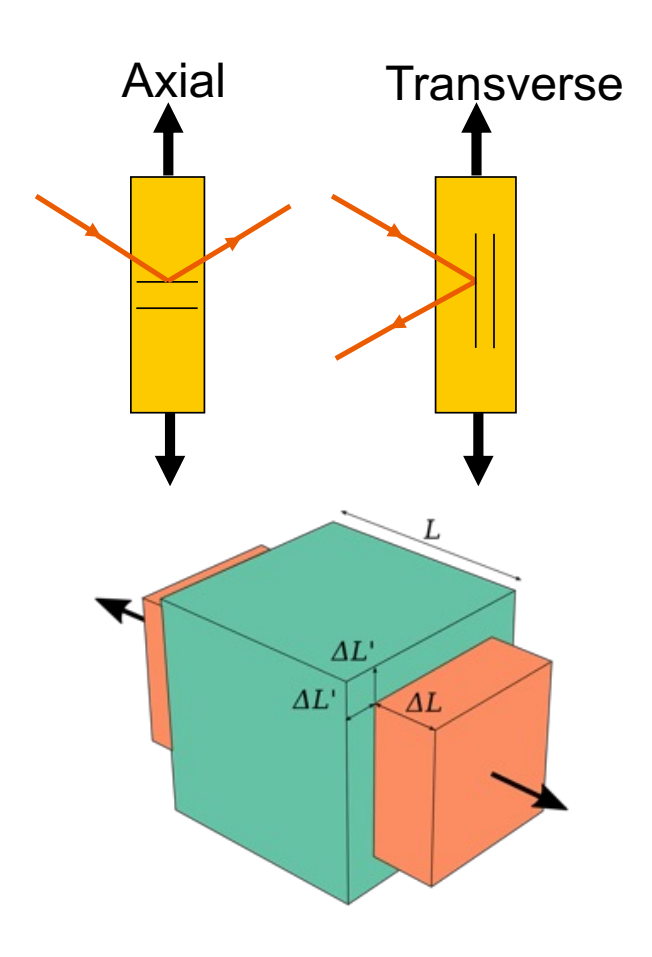
• Usually sample and detector are fixed





Axial versus Transverse





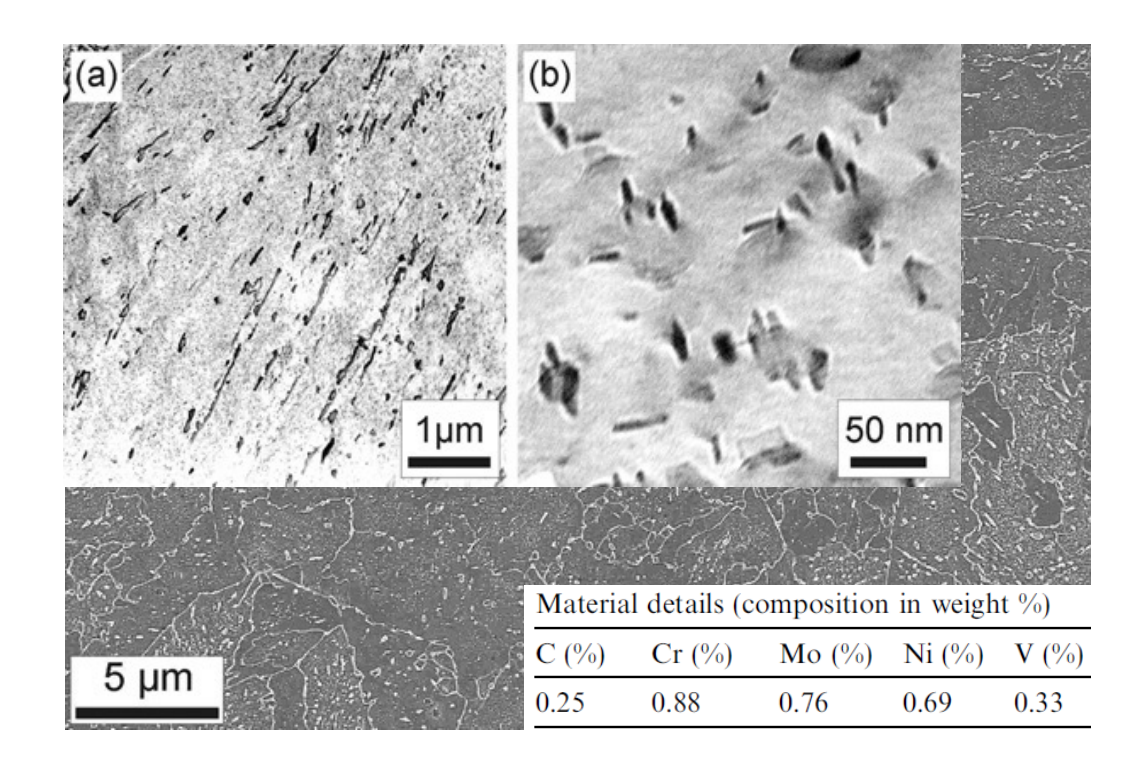


The story of cementite



The story of cementite

- Matrix precipitates
- Ferrite cementite (very heterogeneous)



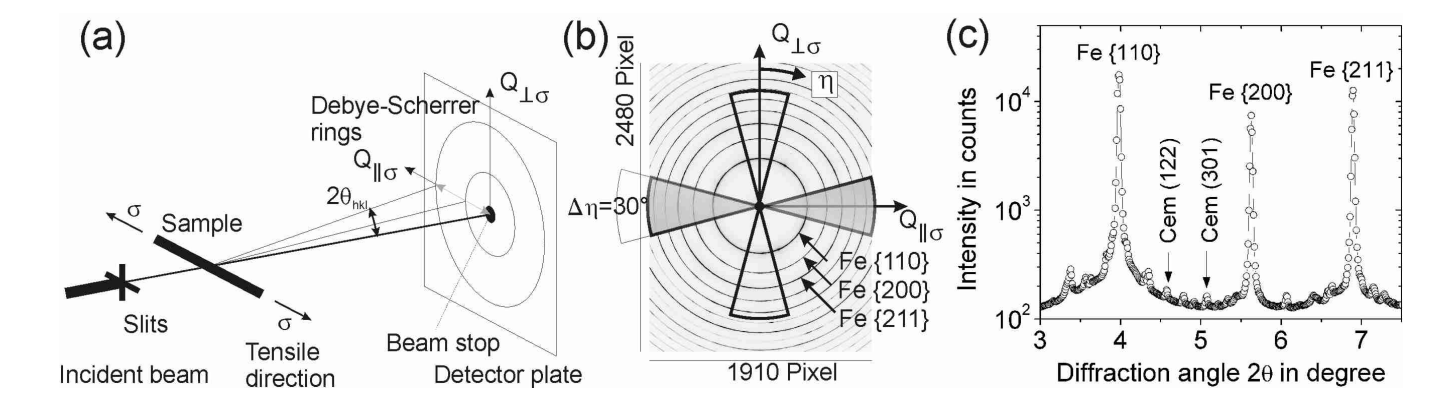


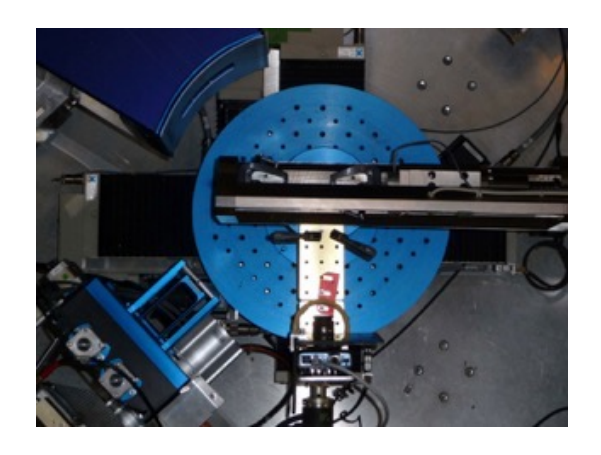
Issue with statistics

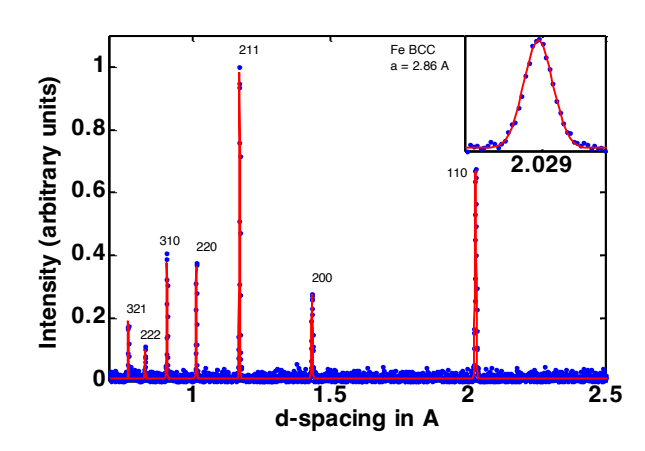
- When the sample cannot be rotated
 - ➤ Issue with large-grained materials
 - ➤ Issue with texture
- Solutions:
 - ➤ Small oscillations during acquisition of one spectrum
 - ➤ Time-of-Flight neutron diffraction
 - > But, neutron diffraction doesn't pick up phases with low volume fraction



Combine X-Rays and Neutrons

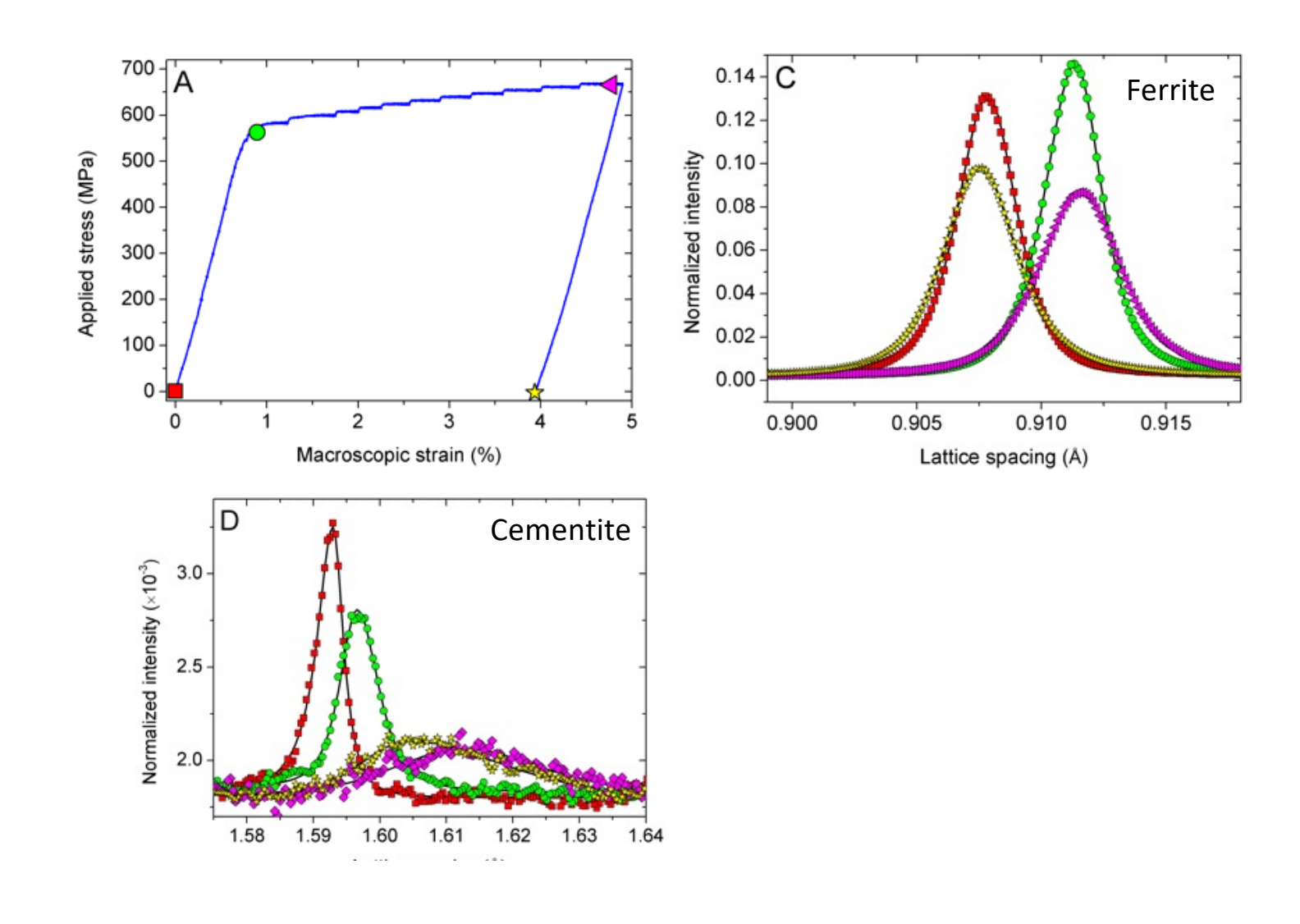






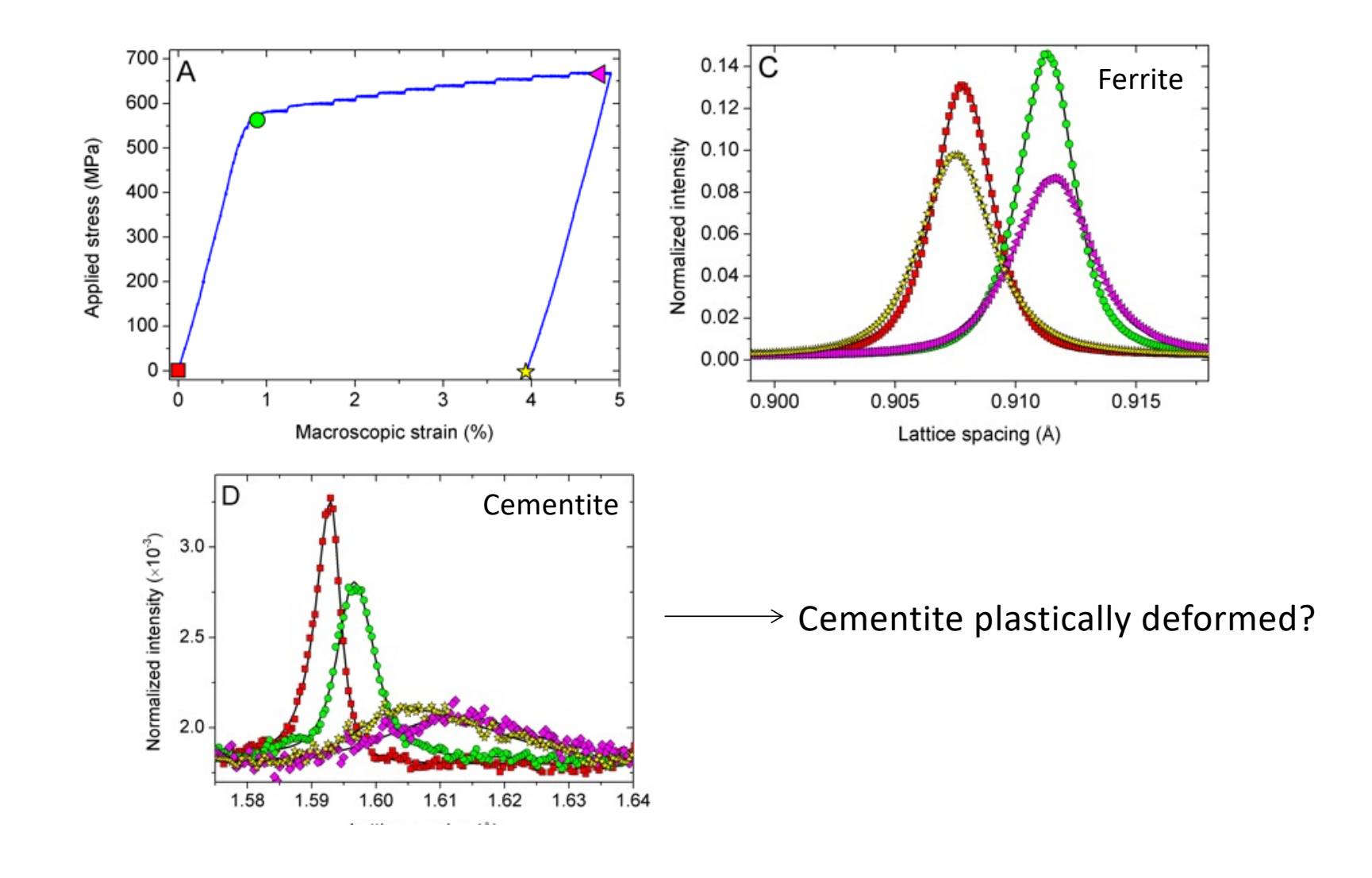


Evolution peak profiles



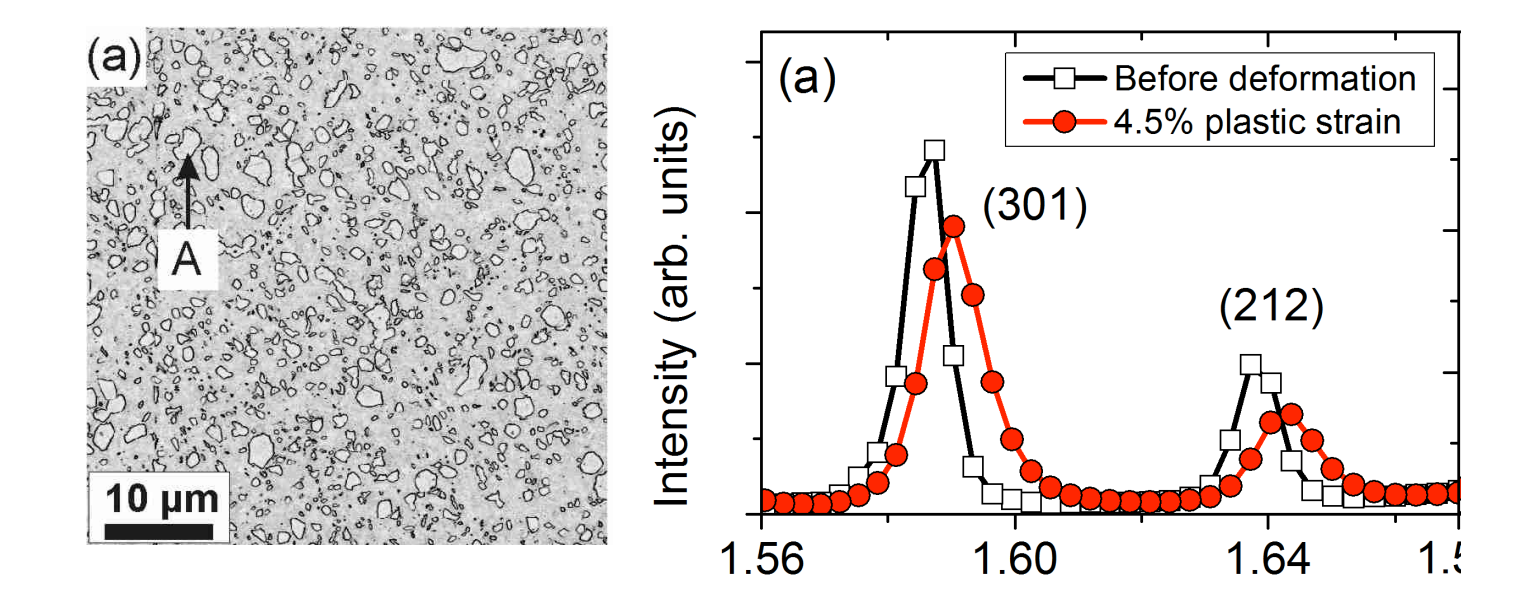


Evolution peak profiles





Homogeneous ferrite – cementite structure



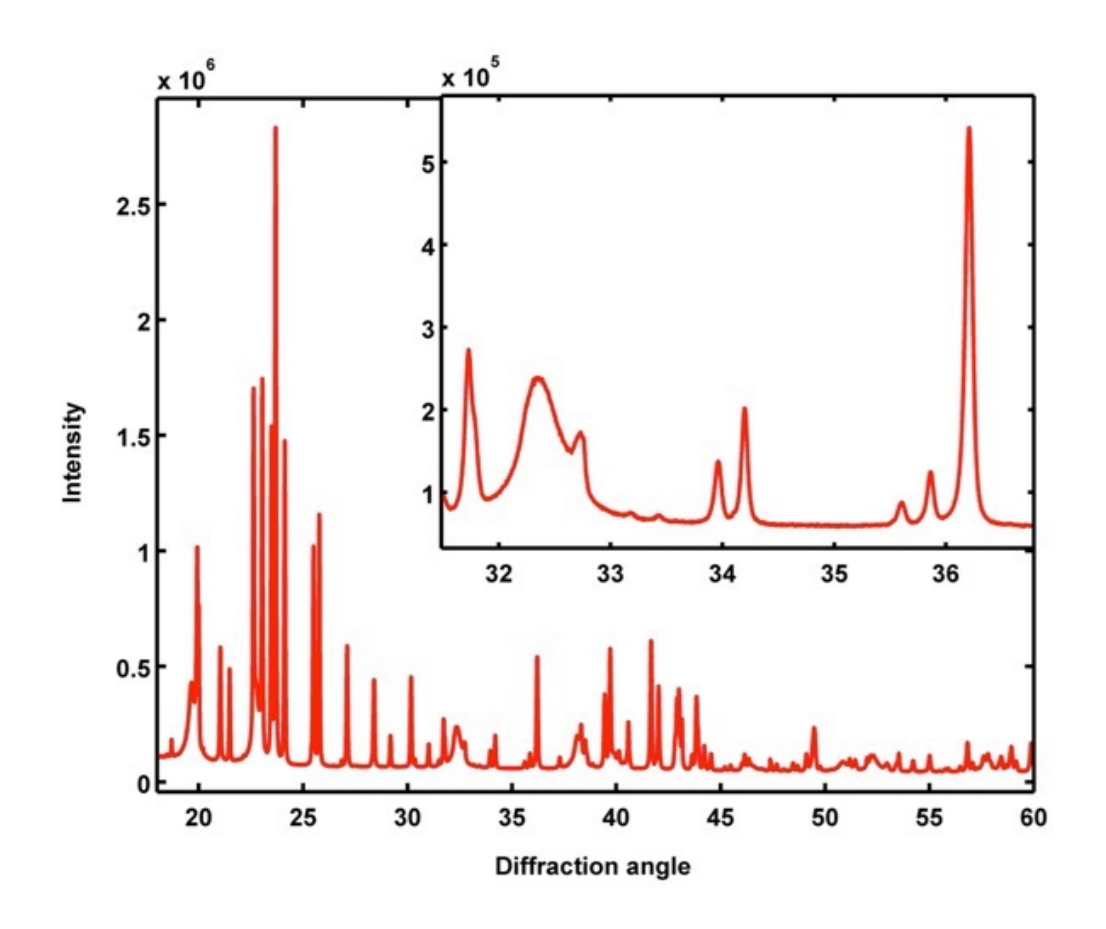
Much less cementite peak broadening in homogeneous structure ...



Broadening in cementite?



- Separate carbide powder from the matrix: ca. 3wt.%
- Record diffraction pattern (Cementite & Vanadium Carbide)
- Compare before and after deformation





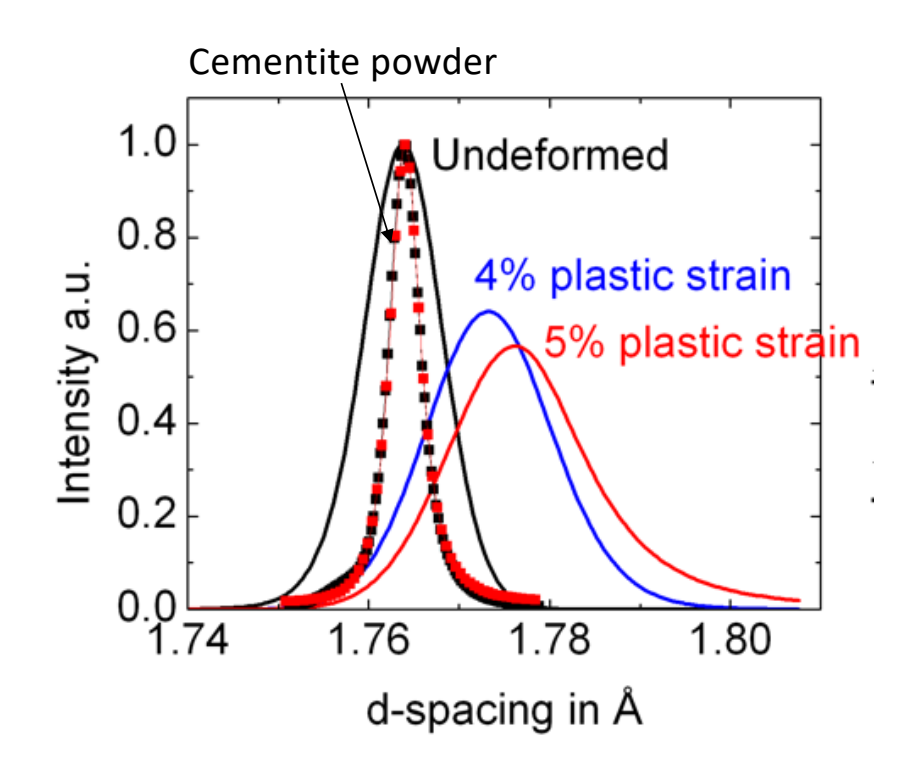
Broadening in cementite?



Not broadening because of size

Not broadening because of dislocations

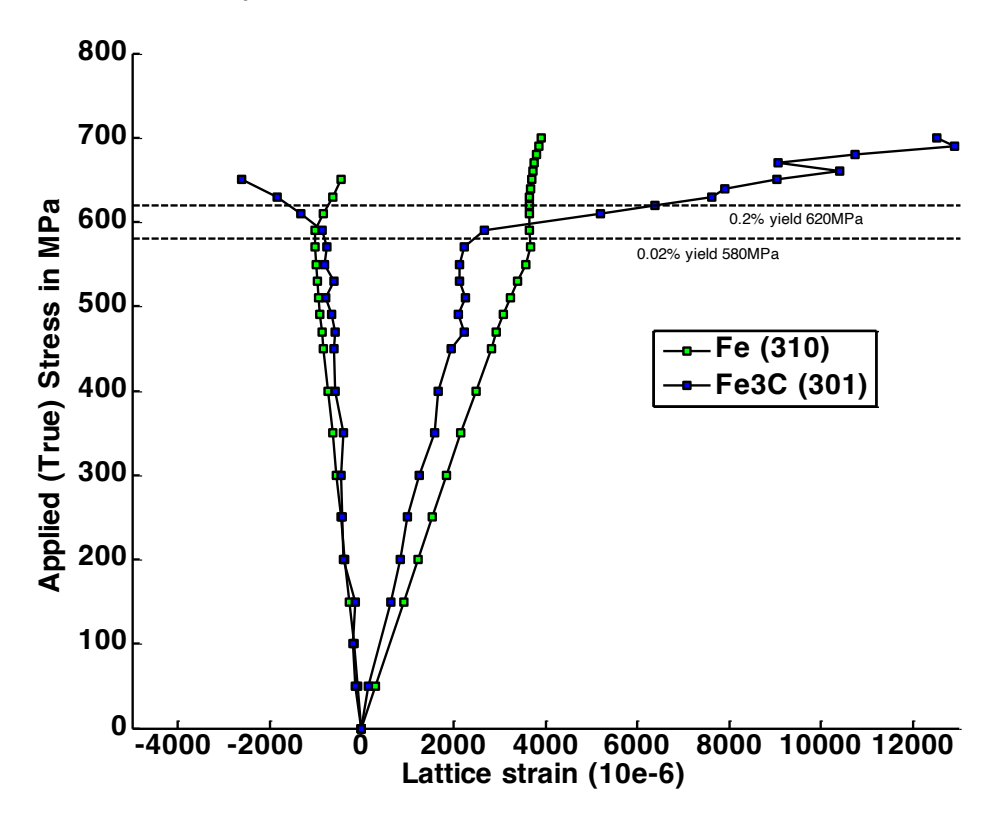
So what is it?





Cementite broadening comes from ...

Different stress levels in the precipitates (diffraction peaks consist of many narrower peaks, slightly shifted compared to each other)



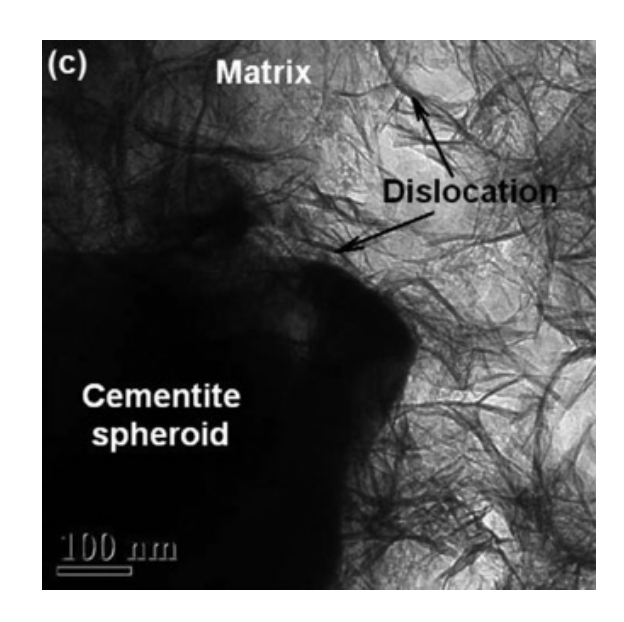


Cementite broadening comes from ...

Different stress levels in the precipitates (diffraction peaks consist of many narrower peaks, slightly shifted compared to each other)

or ...

Pile-up of dislocations at the precipitate – matrix interface causing strong strain gradients inside the precipitates





Take home messages:

Heterogeneous microstructure can lead to significant peak broadening

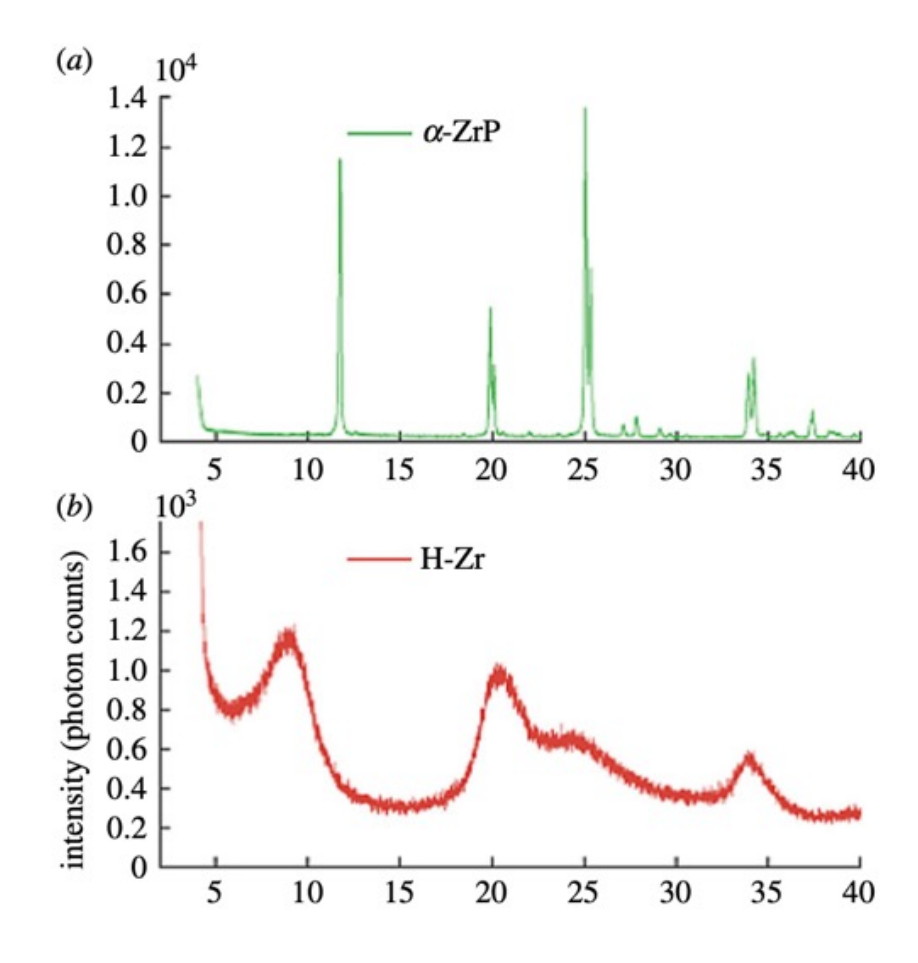
Peak broadening not necessarily an indication for plasticity





Pair distribution function

- X-ray powder diffraction ideal for materials with sufficiently large grain size
- For nanocrystalline materials with grain sizes in the range of a few nm or for amorphous materials, the diffraction peaks become very broad and diffuse.
- Peak profile analysis does not work, as several assumptions do not hold up at very small grain sizes.
- In the pair distribution function a wide range of reciprocal space is probed.

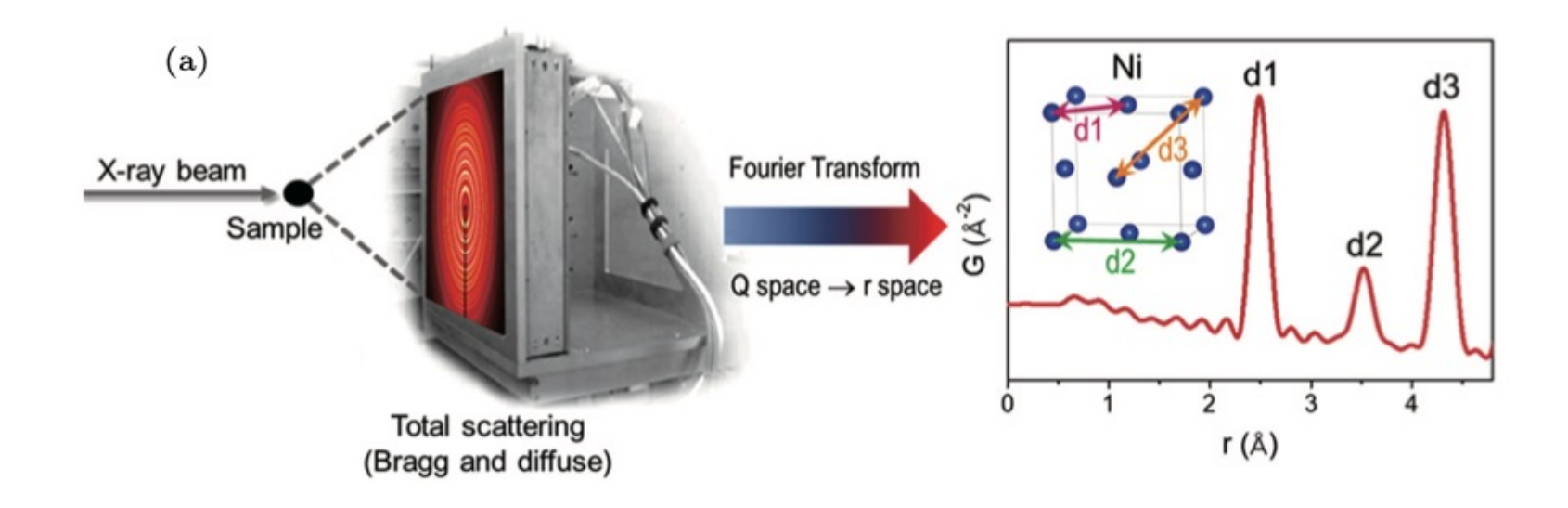




Pair distribution function

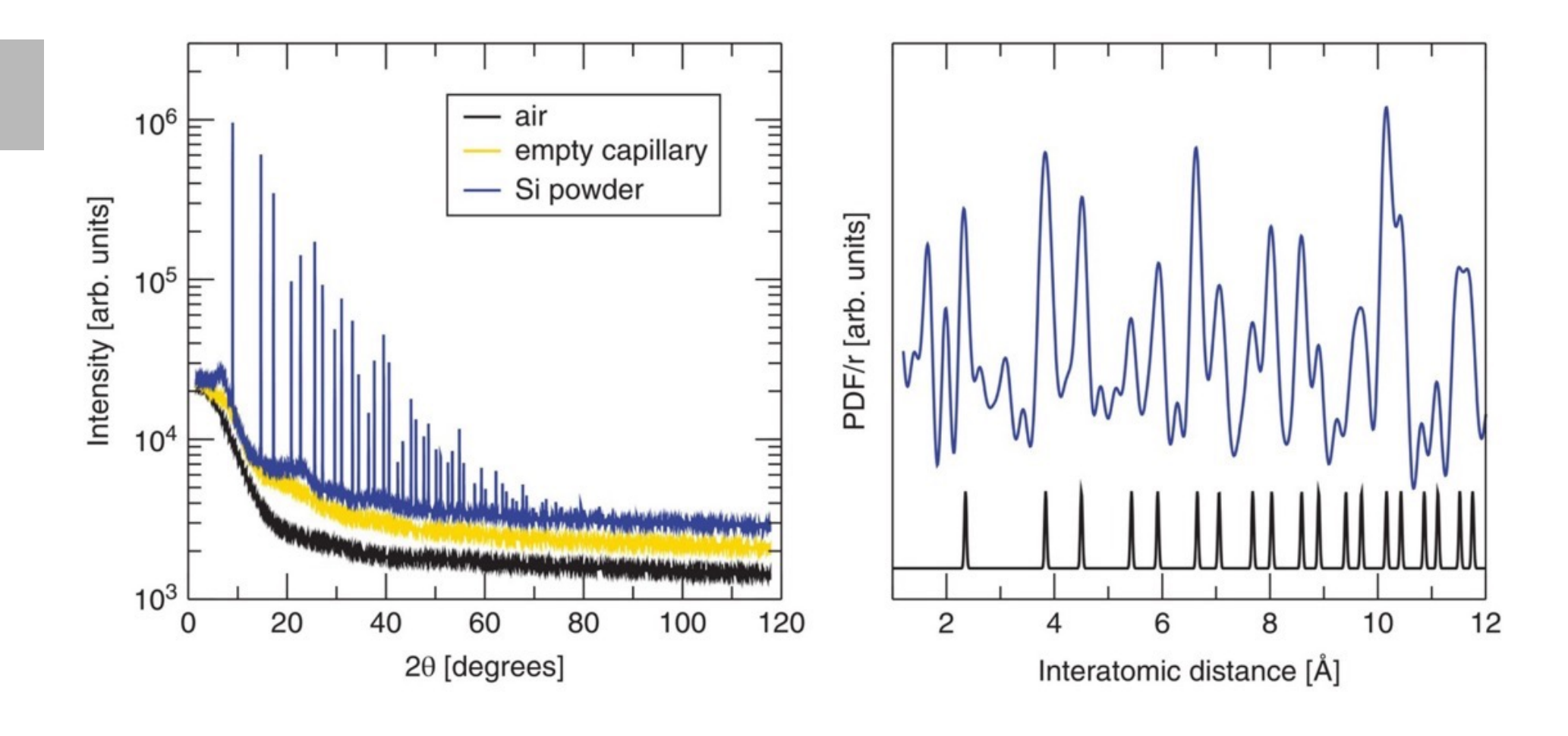
PDF:
$$g(r) = \frac{1}{4\pi\rho_0 r^2 N} \sum_{i} \sum_{j \neq i} \delta(r - r_{ij})$$

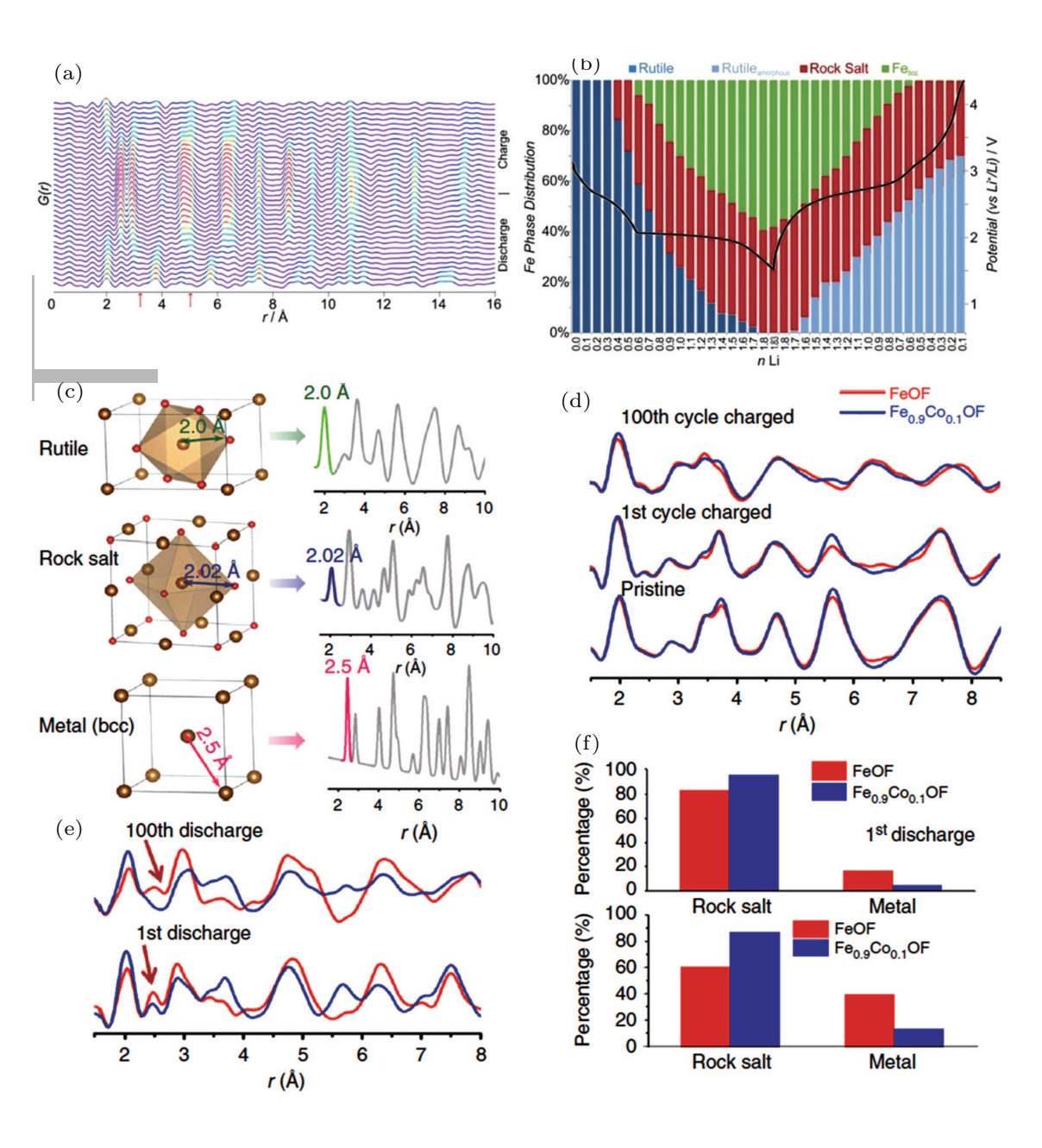
With ρ_0 the average number density of atoms, N the total number of atoms and r_{ij} the distance between atoms i and atom j. The PDF gives the scaled probability of finding two atoms in a material a distance r apart





Pair distribution function





- (a) The *in situ* PDF data of iron oxyfluoride $(Fe^{II}_{(1-x)}Fe^{III}_{x}O_{x}F_{2-x}, x = 0.6)$ during the first discharge—charge cycle. Characteristic peaks
- (b) Evolution of phase composition during cycling.
- (c) Characteristic atomic pairs in rutile, rocksalt, and body-centered-cubic metal and their corresponding PDF peaks.
- (d) PDF patterns of Fe_{0.9}Co_{0.1}OF and FeOF at pristine state, charged state after the 1st cycle, and charged state after the 100th cycle.
- (e) PDF patterns of Fe_{0.9}Co_{0.1}OF and FeOF at discharged state after the 1st cycle and discharged state after the 100th cycle.
- (f) Percentages of metal and rocksalt phases in Fe_{0.9}Co_{0.1}OF and FeOF obtained by fitting PDF results

Wiaderek et al J. Am. Chem. Soc. 135, 4070 (2013)

Fan et al Nat. Commun. 9, 2324 (2018)





Energy dispersive X-ray diffraction

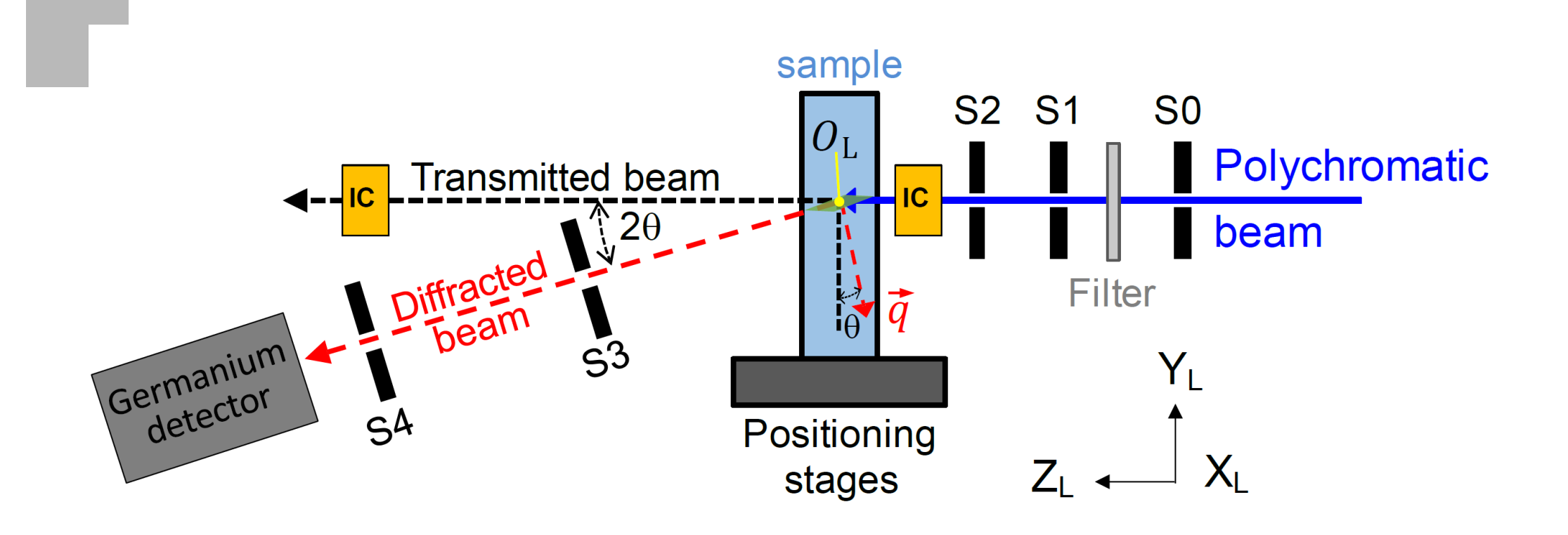
• In EDXRD the diffraction angle θ is kept constant and the lattice spacing d is obtained experimentally by determining the energy E of the diffracted beams of the originally polychromatic beam:

$$d = \frac{hc}{2E \sin \theta}$$

- Usually used in combination with high X-ray energies to allow for large penetration depths.
- No need for a goniometer, can even be made portable.
- When using a wide energy range, depth-dependent measurements are possible.

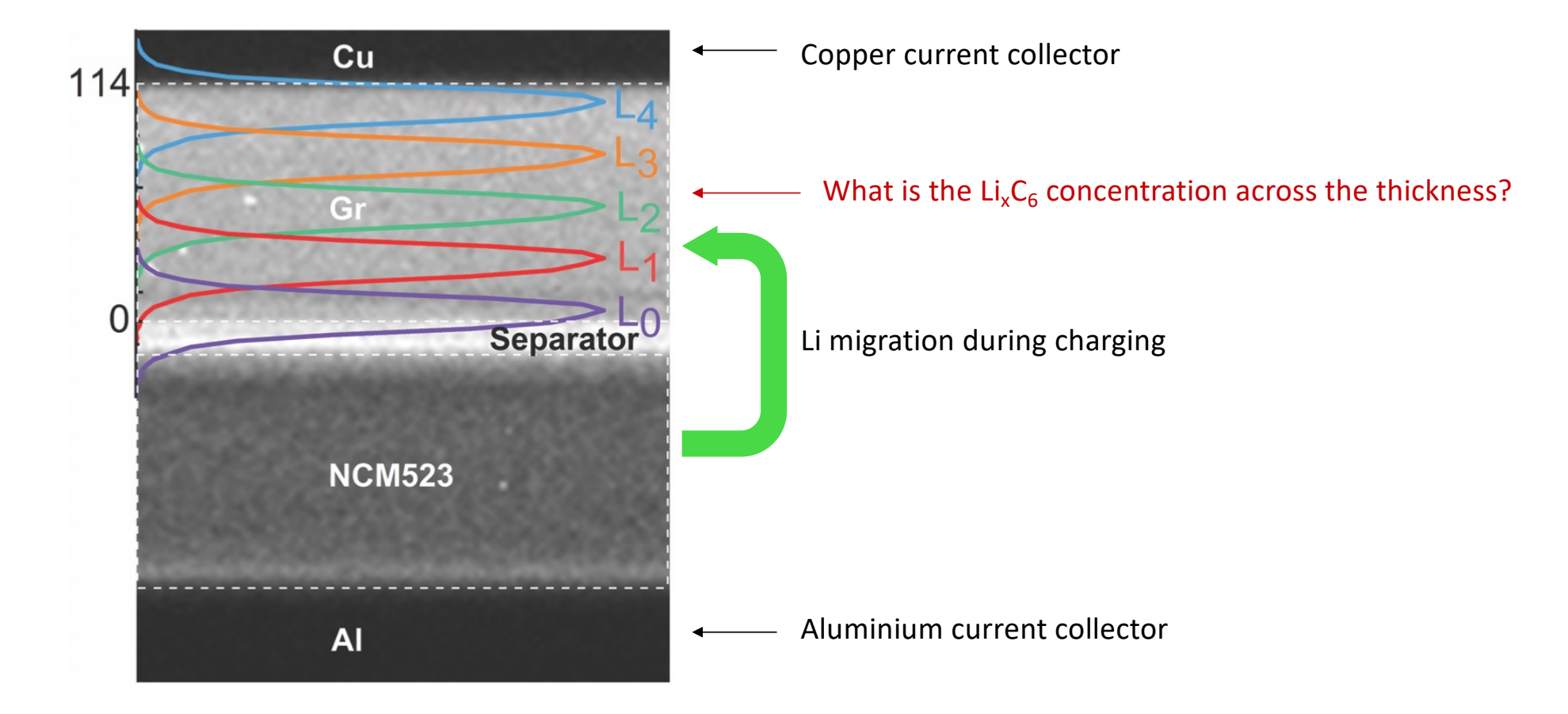


Energy dispersive X-ray diffraction





Application – Battery research



Quantifying lithium concentration gradients in the graphite electrode of Li-ion cells using operando energy dispersive X-ray diffraction. Koffi P. C. Yao et al, Energy & Environmental Science 12 (2019) 656



Application – Battery research

Experiment:

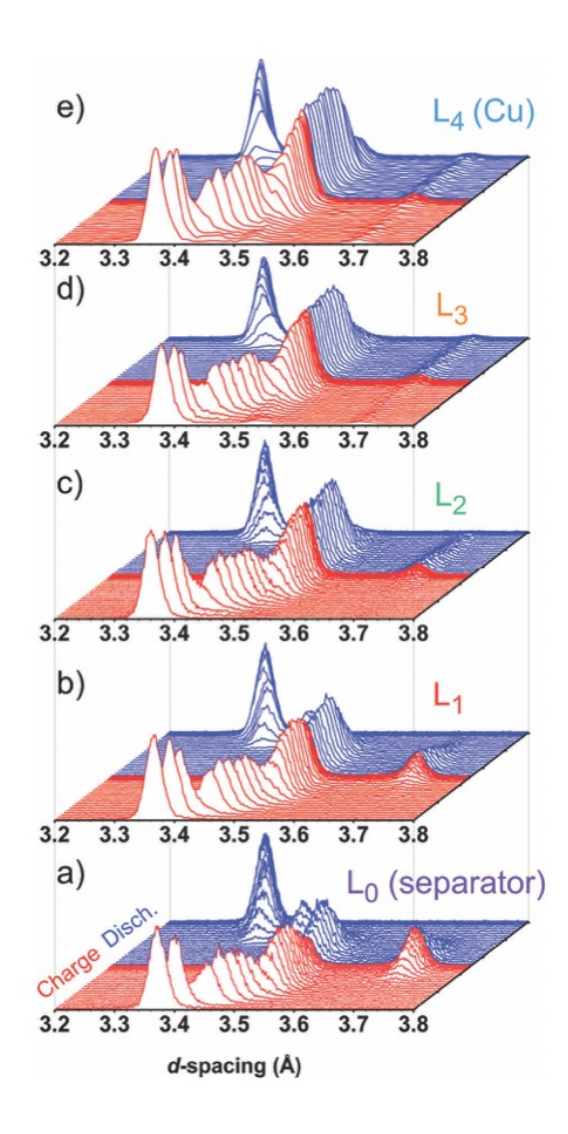
- X-ray photons with energies between 5 and 250 keV
- Ge detector placed at a fixed angle $\theta \approx 3^{\circ}$
- X-ray beam was 18.3 μm x 1045 μm
- 1 min per acquisition for a total period of 3 h per charge/ discharge cycle

Analysis

- The Li–Gr intercalation system exhibits several phases (commonly referred to as stages)
- The Li content x is found by:

$$x = \sum_{i} x_{i} = \sum_{i} \Gamma_{i} / \sum_{j} f_{j}^{-1} \Gamma_{j} \qquad \Gamma_{j} = I_{j}^{hkl} / (m_{j}^{hkl} | F_{j}^{hkl} |^{2})$$

with fj is the fractional Li content of the corresponding Li_xC_6 phase j, I^{hkl} is the relative integrated flux of scattered X-ray photons from phase j, m_{hkl} is the multiplicity of the Bragg reflection with the Miller indices (hkl) originating from phase j in the peak region of interest, and F_{hkl} is the corresponding scattering factor





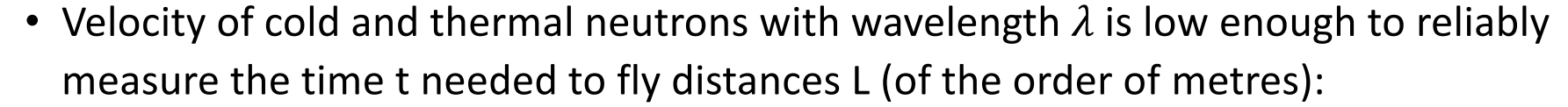
Application – Battery research

Species	Strongest Bragg peak, (hkl)	Multiplicity m _{hkl}	Estimated F _{hkl}	Value of f _i
graphite	(002)	2	16.8	0
LiC ₃₀	(004)	2	49.72	1/5
LiC ₁₈	(004)	2	33.85	1/3
LiC ₁₂	(002)	2	50.2	1/2
LiC ₆	(001)	2	25.3	1



EPFL PAUL SCHERRER INSTITUT

Neutron time-of-flight

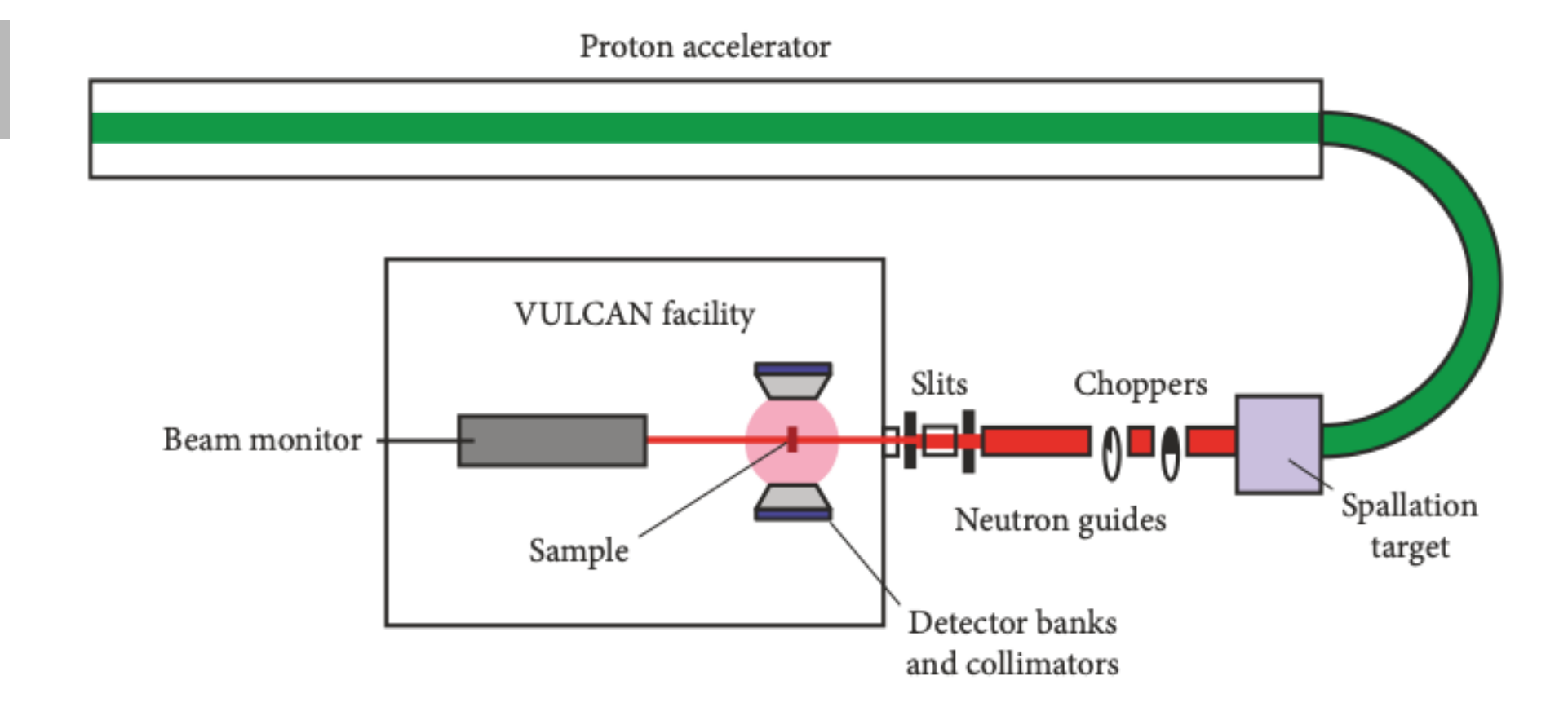


$$t = \frac{\lambda m_n}{2\pi\hbar} L$$

- Start signal is provided by:
 - Timing signal of the pulsed source
 - Signal from a chopper
- Stop signal is provided by the neutron detector
- ToF allows to
 - determine the wave length of a detected neutron
 - work with a pink neutron beam
 - work at fixed diffraction angles

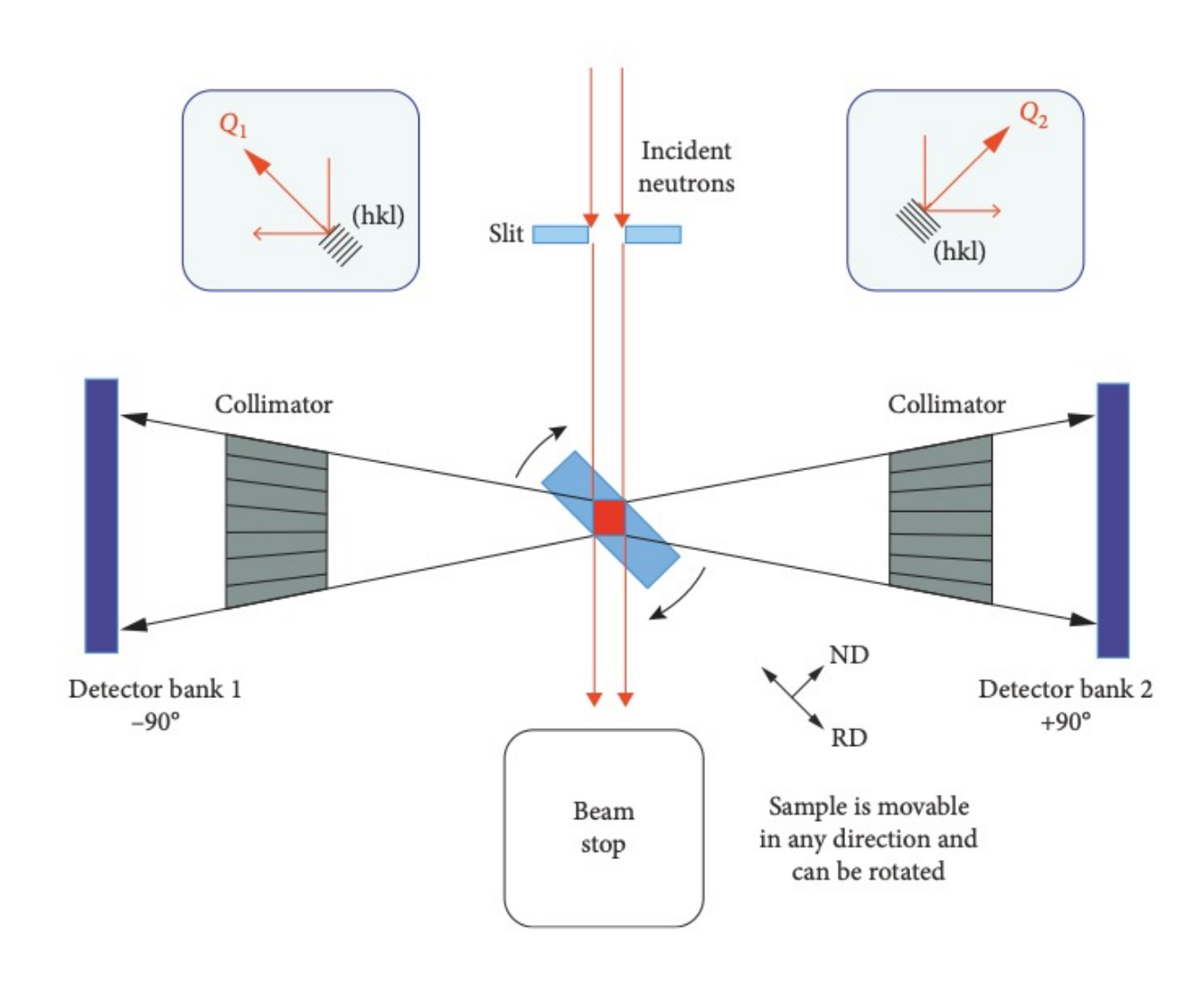


Neutron time-of-flight





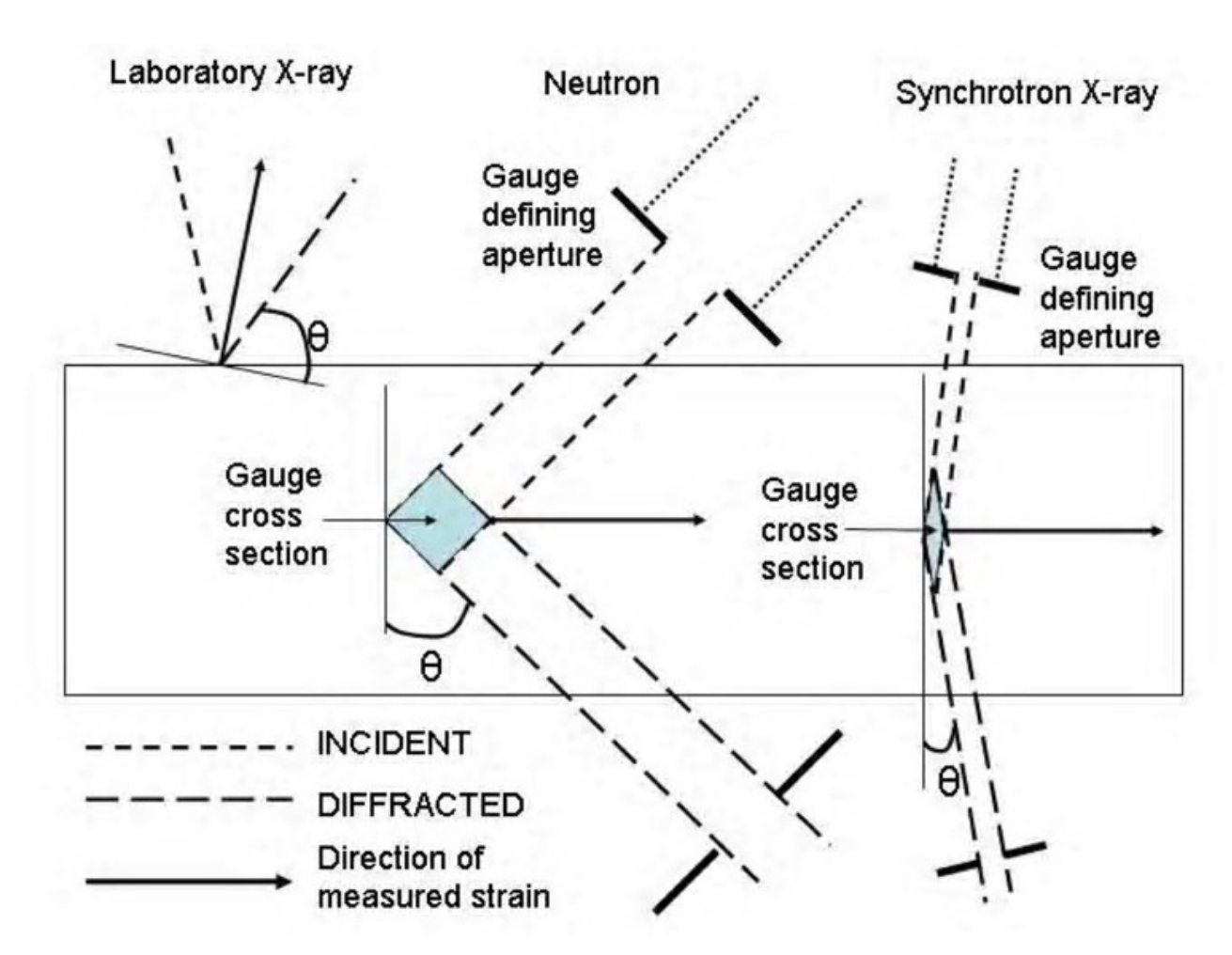
Neutron time-of-flight





Factors to consider:

- Penetration depth
- Flux
- Activation
- Sample environment
- Grain statistics
- Gauge volume
- ...



A square gauge volume has important advantages for residual stress measurements. Elastic strain is defined as the relative change of the lattice spacing d_{hkl} from the stress-free lattice spacing d_{hkl}^0

$$\varepsilon_{hkl} = \frac{d_{hkl} - d_{0,hkl}}{d_{0,hkl}} = \frac{\Delta d_{hkl}}{d_{0,hkl}} = \frac{\sin \theta_{0,hkl}}{\sin \theta_{hkl}} - 1$$

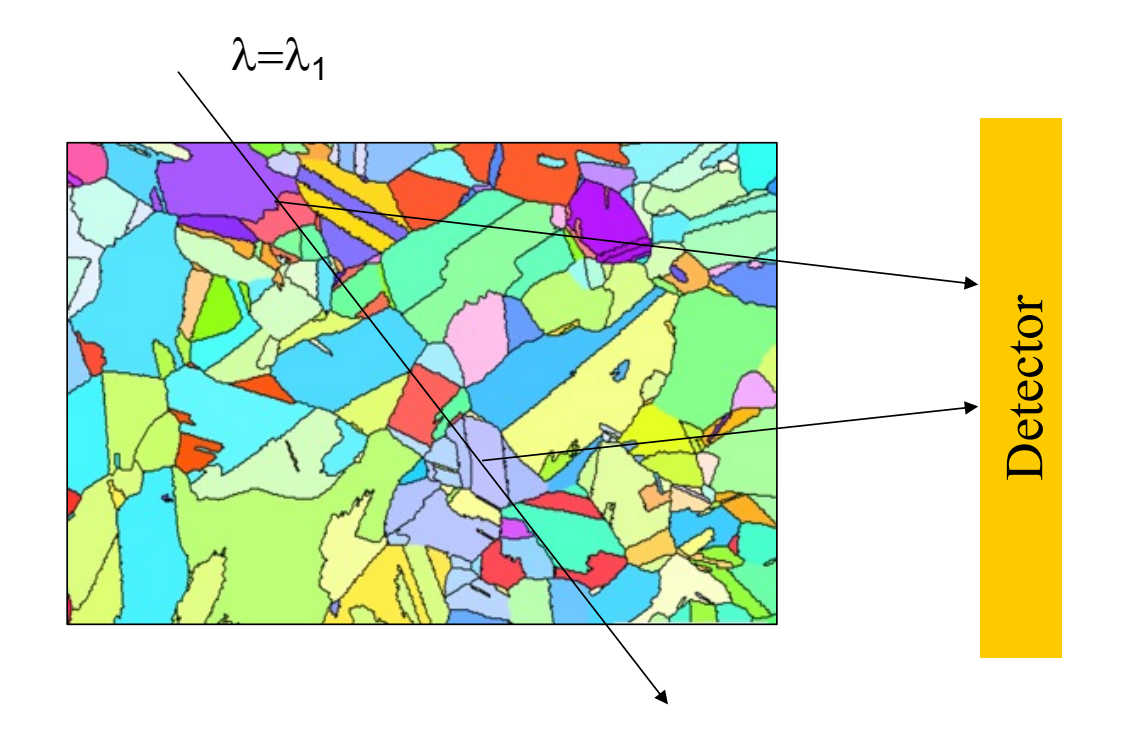
Stress σ_{ij} and elastic strain ε_{kl} are second rank tensors and are related through elastic constants C_{ijkl} :

$$\sigma_{ij} = \underline{C}_{ijkl} \, \mathcal{E}_{kl}$$

Full determination of the strain tensor requires measurements of the elastic strain in at least six independent directions. If the principal strain directions within the specimen are known, measurements along these three directions are sufficient.

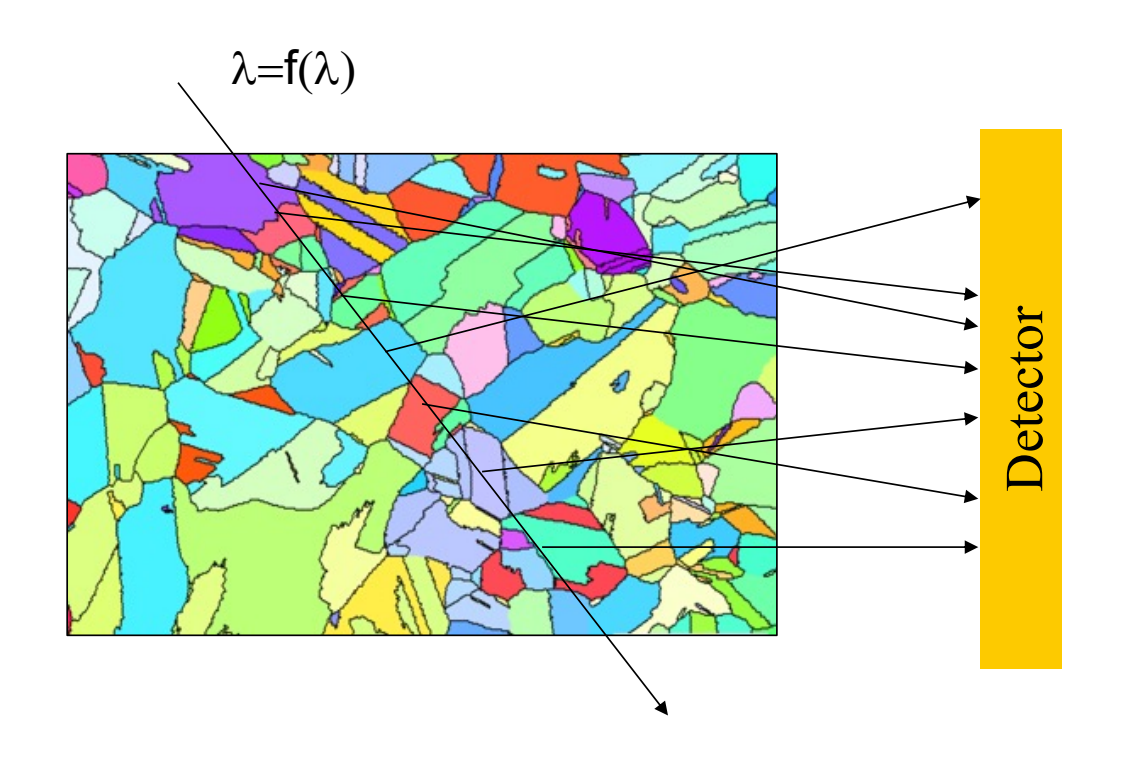


• In order to obtain statistical relevant information, sufficient grains need to be in the gauge volume. In ToF, a pink beam is combined with a large neutron detector.





• In order to obtain statistical relevant information, sufficient grains need to be in the gauge volume. In ToF, a pink beam is combined with a large neutron detector.





• AA7449: Al-Zn-Mg-Cu

Complex processing route with thermal treatments

Residual stresses in large components because of different cooling rates during

quenching



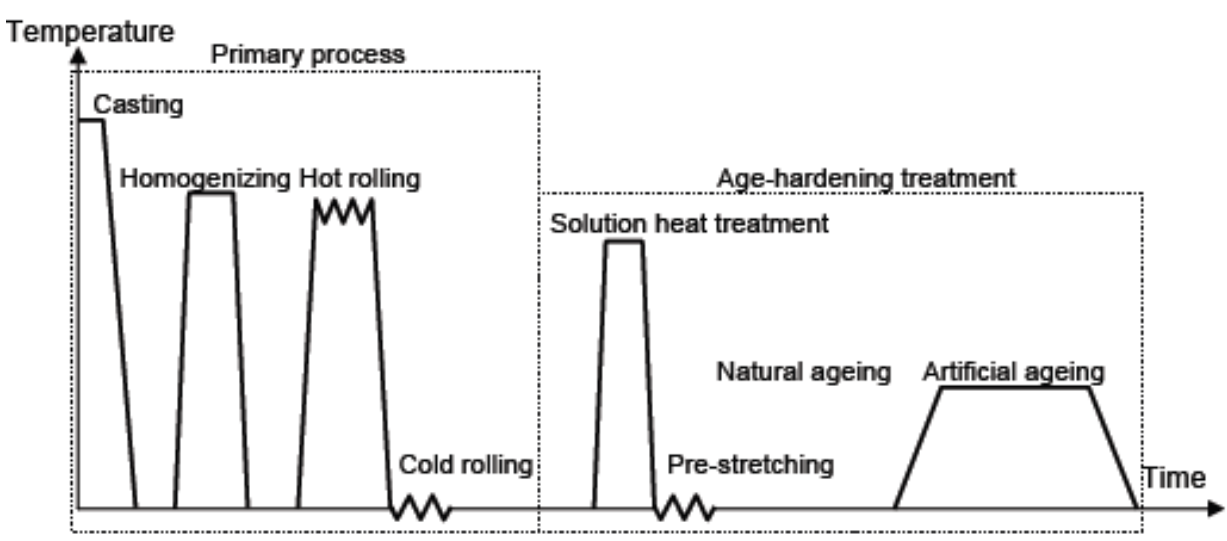
Fig. I-6. Schematics of the processing steps for AA7xxx

Understanding quenching:

https://www.youtube.com/watch?v=gNrT-G2Zo9w

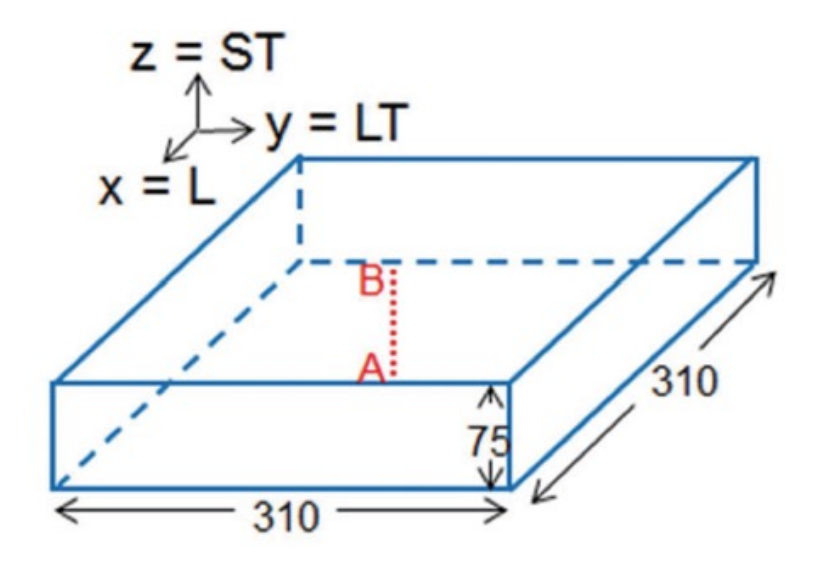
Prince Rupert's Drops:

https://www.youtube.com/watch?v=xe-f4gokRBs



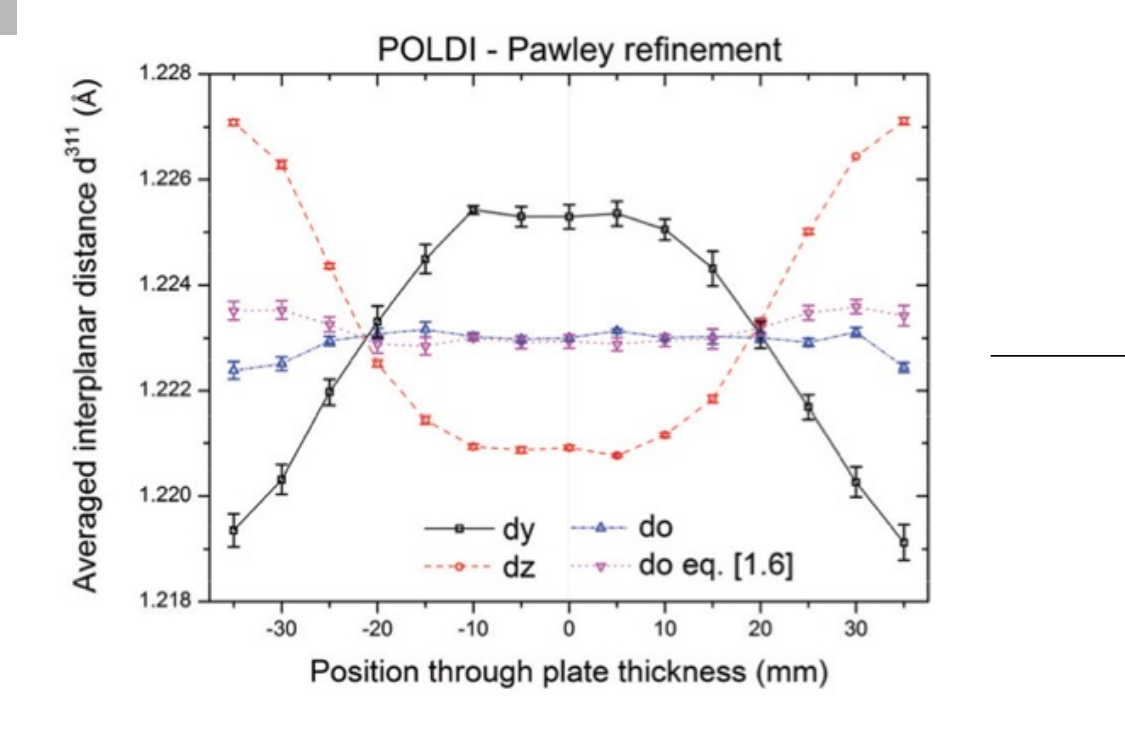


- ToF neutron diffraction ideal:
 - Large penetration depth in aluminium
 - Large grain sizes
 - No need for high spatial resolution
- Residual stresses are measured along A-B





• Line profile through the plate thickness

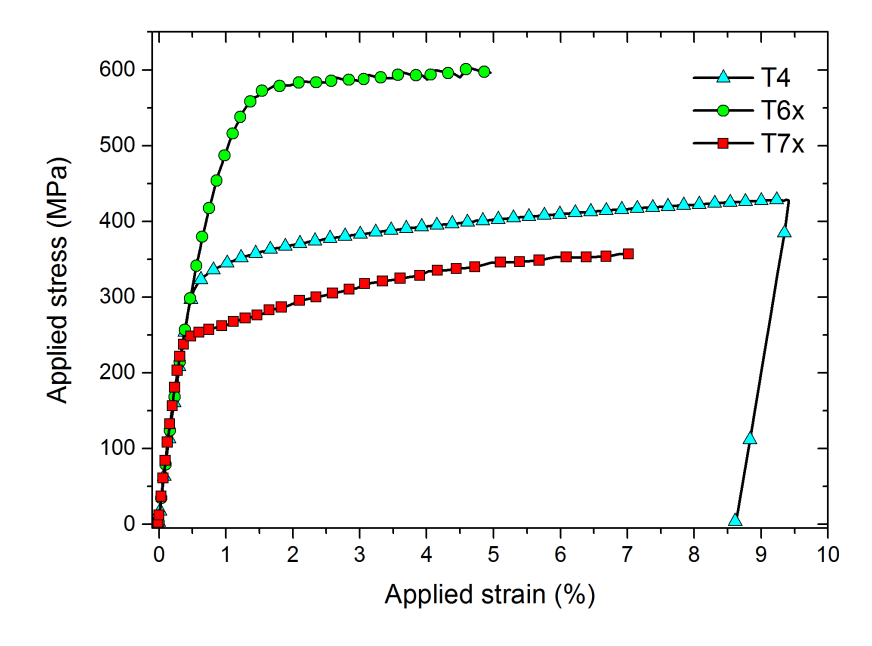


In order to convert to stress we need the diffraction elastic constants. How to measure this?



• Cut dogbone samples out of thick block and perform tensile tests

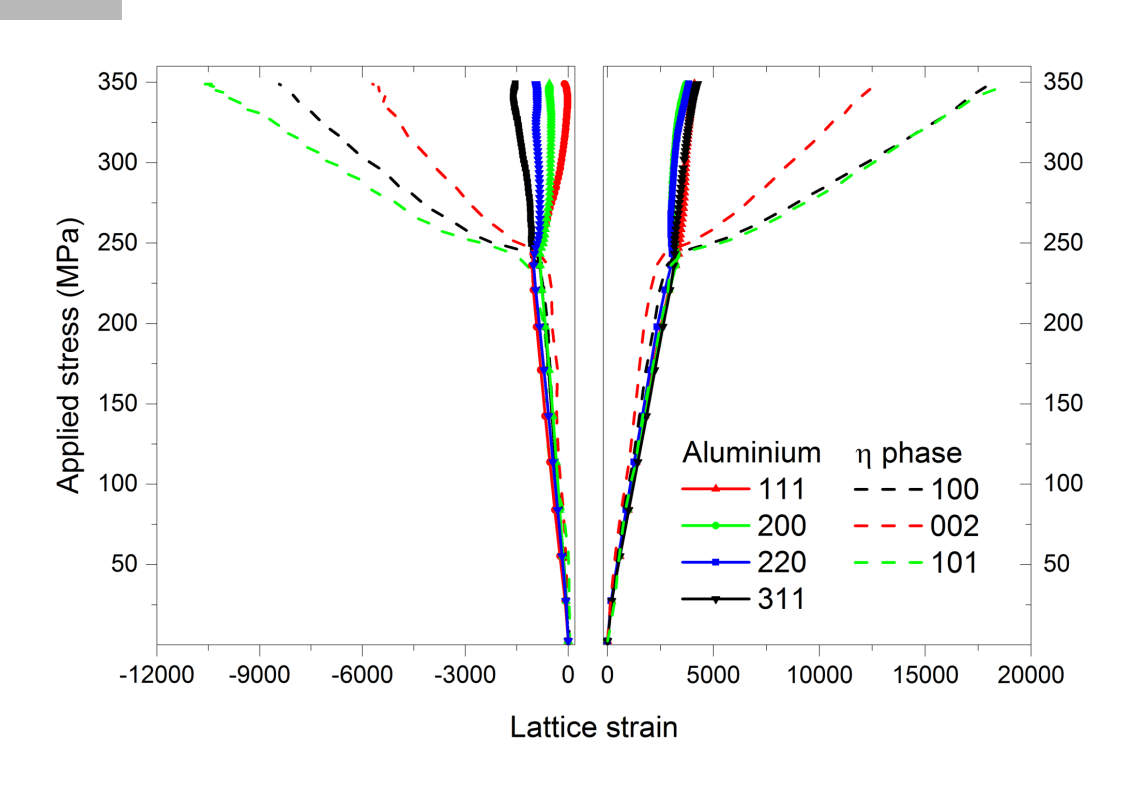








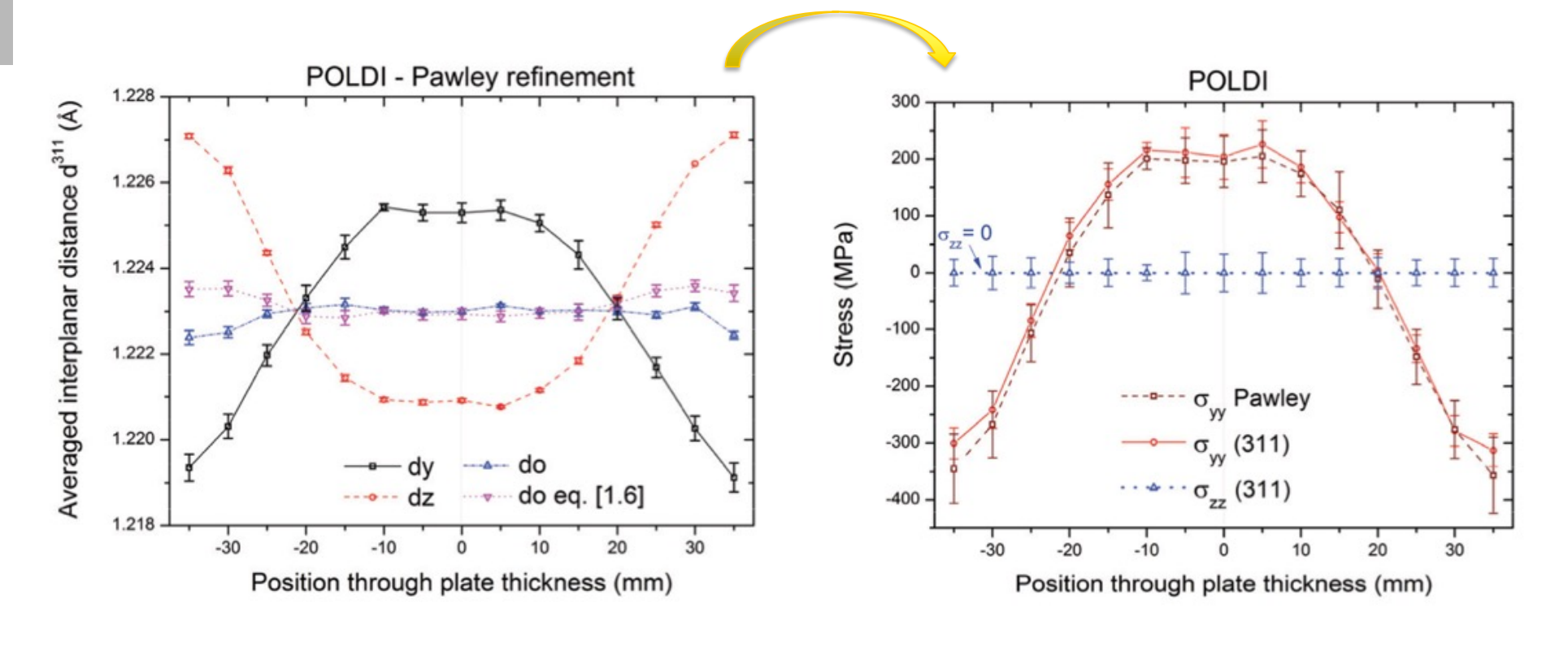
- Measure lattice strain as a function of applied stress.
- Slope in the elastic regime provides the diffraction elastic constants



Reflection	T4	T6x	T7x
Al {111}	73.8 ± 1.7	67.8 ± 2.6	69.8 ± 1.3
Al {200}	67.0 ± 3.2	69.3 ± 2.4	70.5 ± 1.2
Al {220}	72.5 ± 4.2	74.4 ± 3.6	73.3 ± 1.4
Al {311}	69.7 ± 3.1	70.7 ± 3.4	71.9 ± 1.2
η (100)			84.9 ± 1.5
η (002)			96.5 ± 2.4
η (101)			82.7 ± 2.6



• Line profile through the plate thickness



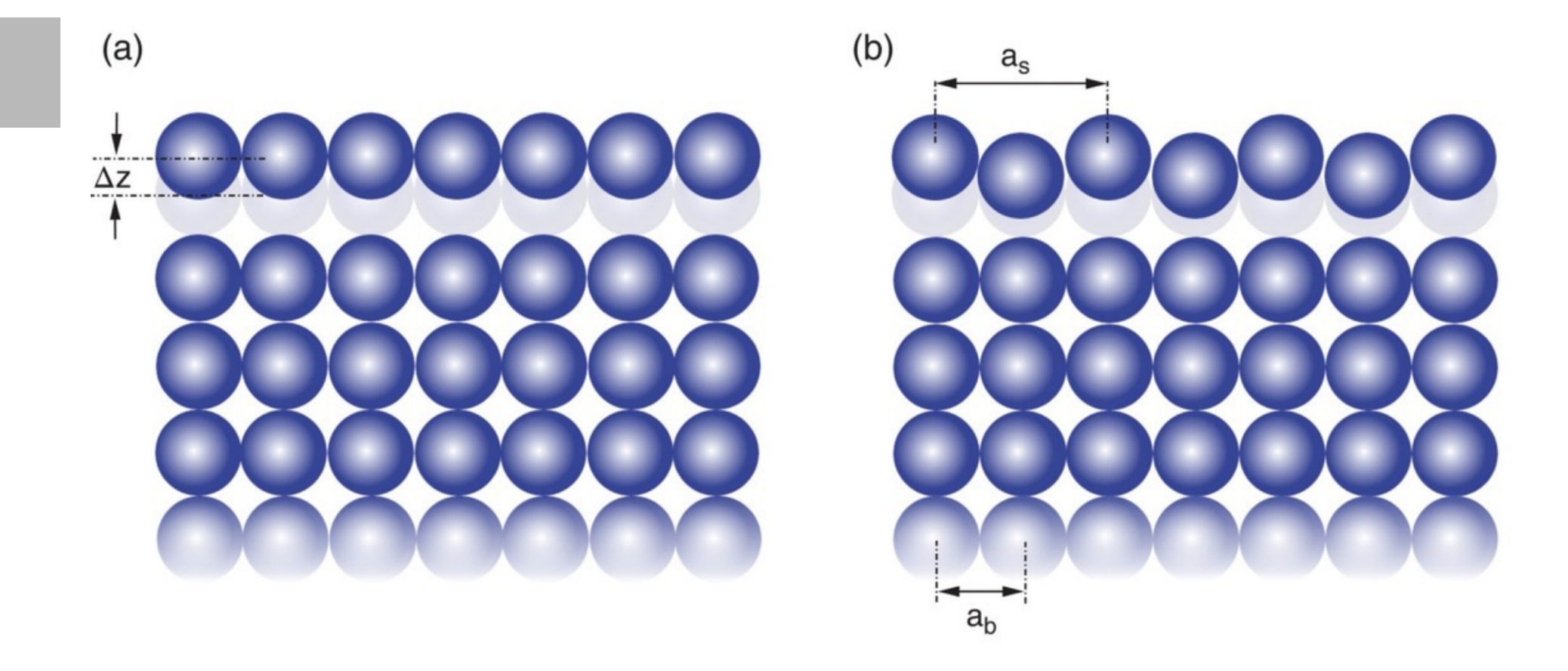


What is Pawley refinement?

- Similar to Rietveld refinement
- Intensities are not calculated based on structure factor (bound to the structure) but are a fitting parameter
- Does not take into account texture
- Robust method for refinement of unit cell and less stringent than Rietveld
- Another alternative to Rietveld: Le Bai refinement
 - Can be used when there is no initial structural model.
 - Presume that all the integrated intensities are initially equal
 - After one iteration, isolated peaks will have an observed intensity equal to the observed area under the Bragg peak. For overlapping reflections, the procedure has to be tackled iteratively







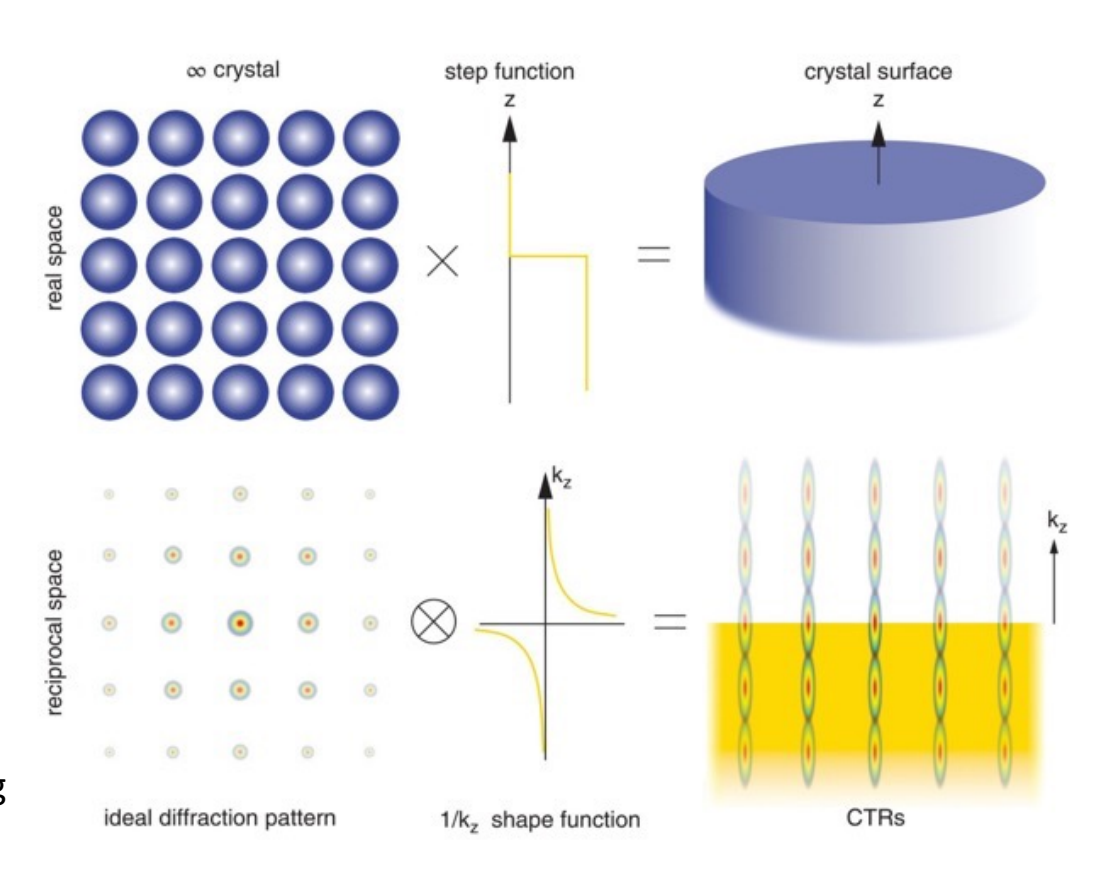


- In the simplest derivation of diffraction patterns, two assumptions are made firstly, that one is operating in the kinematical limit (that is, single-scattering), and secondly, that the crystal is infinitely large. This results in the diffraction peaks being infinitely narrow (known as 'delta functions'). In reality, of course, all diffraction spectra are smeared out to a certain degree because there is partial absorption and extinction.
- Crystals are finite in extent and one therefore measures a finite sample volume. The
 diffraction pattern of a finite crystal can be generated by convolving the Fourier
 transform of an infinitely large crystal structure (i.e. its 'ideal' diffraction pattern) with
 the Fourier transform of the function describing the boundary of the real crystal
 (called the 'shape function').



A single crystal terminated with an atomically flat surface has a step function as the boundary function. This has an FT showing a 1/kz relationship that extends significantly in reciprocal space. The convolution of this with the 'ideal' diffraction pattern results in the latter being smeared out to produce a continuous signal in the direction perpendicular to the sample surface. These are crystal truncation rods (CTRs).

Any shifts in the atomic positions of the upper layers from their bulk positions, due to surface reconstructions and/or relaxations, will have a marked effect on the form and magnitude of the scattered amplitudes in portions of the CTRs away from the Bragg maxima. Recording CTRs therefore provides an exceptionally sensitive method for unravelling the structure of crystalline surfaces and interfaces.

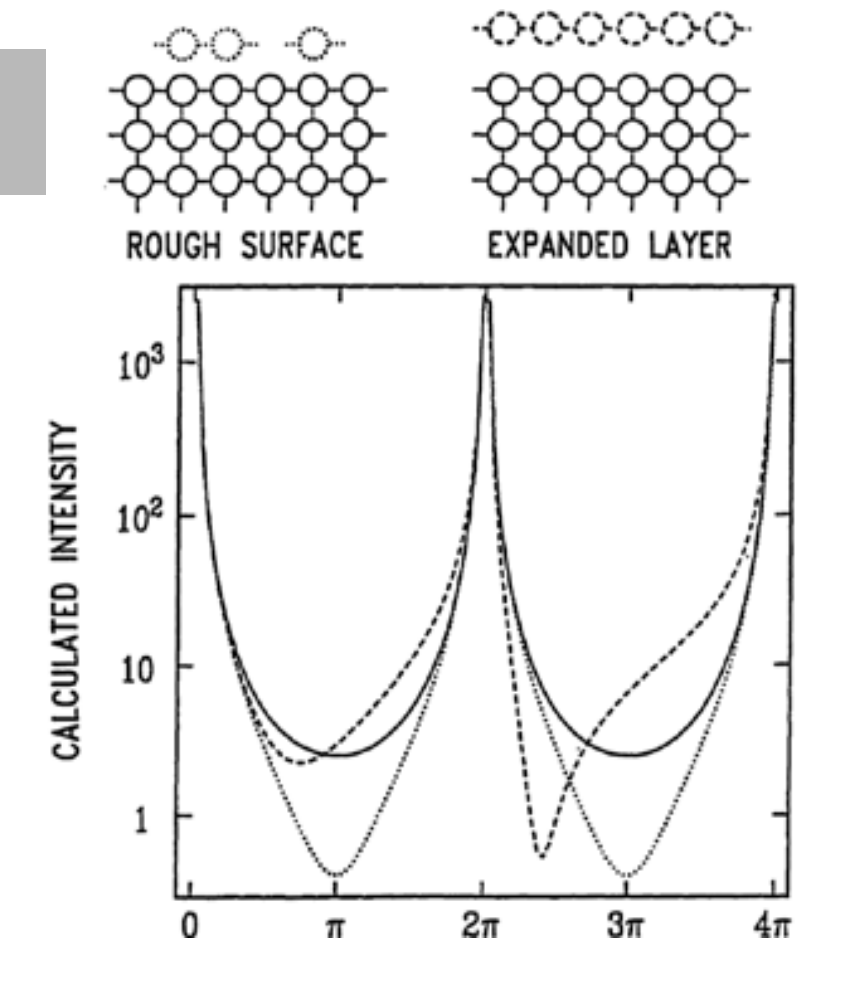




- SXRD measurements are carried out using a grazing incident angle α , with respect to the sample surface. The choice of α depends on the experiment, sample quality, and scattering strength.
- For incident angles close to the critical angle α_c , the surface sensitivity increases rapidly. Exactly at α_c , the reflected wave is perfectly in phase with the incident wave, and the evanescent wave amplitude is approximately twice that of the incident wave. The evanescent intensity therefore approaches four times that of the incident beam. The penetration depth is low, and so the bulk contribution is suppressed. Hence, at α_c , the surface sensitivity is highest
- Disadvantage: large footprint on the sample and very sensitive to small changes (0.01 degrees) of the incoming angle.



Application



- The full curve is for an ideally terminated simple-cubic lattice of atoms; its functional form is just $1/(\sin q_z)^2$, whose divergence at Bragg points $q = 2n\pi$ is clearly visible.
- The dashed curve corresponds to an outward displacement of a single layer of atoms at the surface; the intensity curve near the Bragg peaks, where there is little surface sensitivity, is barely changed, but the intensity at the CTR minimum is strongly modified.
- The dotted curve is for a rough surface, modeled by random omission of a fraction of the atoms in the top layer. The biggest effect is at the CTR minimum, this time with a symmetric drop of the intensity curve.